NBS

Technical Note 260

RESEARCH ON CRYSTAL GROWTH AND CHARACTERIZATION AT THE NATIONAL BUREAU OF STANDARDS JULY TO DECEMBER 1964

U. S. DEPARTMENT OF COMMERCE
NATIONAL BUREAU OF STANDARDS

THE NATIONAL BUREAU OF STANDARDS

The National Bureau of Standards is a principal focal point in the Federal Government for assuring maximum application of the physical and engineering sciences to the advancement of technology in industry and commerce. Its responsibilities include development and maintenance of the national standards of measurement, and the provisions of means for making measurements consistent with those standards; determination of physical constants and properties of materials; development of methods for testing materials, mechanisms, and structures, and making such tests as may be necessary, particularly for government agencies; cooperation in the establishment of standard practices for incorporation in codes and specifications; advisory service to government agencies on scientific and technical problems; invention and development of devices to serve special needs of the Government; assistance to industry, business, and consumers in the development and acceptance of commercial standards and simplified trade practice recommendations; administration of programs in cooperation with United States business groups and standards organizations for the development of international standards of practice; and maintenance of a clearinghouse for the collection and dissemination of scientific, technical, and engineering information. The scope of the Bureau's activities is suggested in the following listing of its four Institutes and their organizational units.

Institute for Basic Standards. Electricity. Metrology. Heat. Radiation Physics. Mechanics. Applied Mathematics. Atomic Physics. Physical Chemistry. Laboratory Astrophysics.* Radio Standards Laboratory: Radio Standards Physics; Radio Standards Engineering.** Office of Standard Reference Data.

Institute for Materials Research. Analytical Chemistry. Polymers. Metallurgy. Inorganic Materials. Reactor Radiations. Cryogenics.** Office of Standard Reference Materials.

Central Radio Propagation Laboratory.** Ionosphere Research and Propagation. Troposphere and Space Telecommunications. Radio Systems. Upper Atmosphere and Space Physics.

Institute for Applied Technology. Textile and Apparel Technology Center. Building Research. Industrial Equipment. Information Technology. Performance Test Development. Instrumentation. Transport Systems. Office of Technical Services. Office of Weights and Measures. Office of Engineering Standards. Office of Industrial Services.

---

* NBS Group, Joint Institute for Laboratory Astrophysics of the University of Colorado.
** Located at Boulder, Colorado.

NATIONAL BUREAU OF STANDARDS

Technical Note 260

ISSUED MAY 8, 1965

RESEARCH ON CRYSTAL GROWTH AND CHARACTERIZATION AT THE NATIONAL BUREAU OF STANDARDS JULY TO DECEMBER 1964

Edited by Howard F. McMurdie
National Bureau of Standards

For sale by the Superintendent of Documents, Government Printing Office
Washington, D.C., 20402 - Price 50 cents

Contents

RESEARCH ON CRYSTAL GROWTH AND CHARACTERIZATION

AT THE NATIONAL BUREAU OF STANDARDS

JULY THROUGH DECEMBER 1964

Edited by

H. F. McMurdie

ABSTRACT

The National Bureau of Standards with partial support from the Advanced Research Projects Agency of the Department of Defense is continuing a wide program of studies involving crystalline materials. These include investigation of methods and theory of growth, study of detection and effects of defects, determination of physical properties, refinement of chemical analysis, and determination of stability relations and atomic structure. The types of materials range from organic compounds, through metals, and inorganic salts to refractory oxides. This Technical Note, the fifth in the series, summarizes the progress of these various projects from July through December, 1964, and lists the related publications and participating scientists.

1. INTRODUCTION

The National Bureau of Standards continues a wide and active program in many aspects of material research. This publication, the fifth in a series, indicates current activity for the period July through December 1964 in the area of crystallography, crystal growth, investigations on properties of crystals, and on methods of study. The National Bureau of Standards has been encouraged by the Advanced Research Projects Agency of the Department of Defense to extend the study of crystals, particularly in the field of crystal growth and has aided with financial support. This Note describes briefly the current state of the many projects here in the general field of crystal studies and no effort has been made to identify the specific projects supported by ARPA. Only in the few instances in which financial support from other agencies contributed to the program has an acknowledgement been given. These items should be considered as progress reports, not in the nature of finished studies. The formal papers resulting from the work are listed in these pages.

To aid in integrating the crystal program here and to encourage cross linking between participants in the program, a number of meetings, discussions and lectures have been arranged. In many cases these report and discuss our current work, in other scientists from outisde material science centers appear.

The program as a whole at the National Bureau of Standards is under the direction of Dr. Harry C. Allen, Jr.

We wish to acknowledge the editorial assistance of Mrs. Pat Smallwood of the Inorganic Material Division and the help given by the assistant editors who have represented the Bureau Divisions as follows:

Heat	J. F. Schooley
Analytical Chemistry	A. R. Glasgow, Jr.
Mechanics	R. S. Marvin
Polymers	E. Passaglia
Metallurgy	R. L. Parker
Solid State Physics	A. H. Kahn
Inorganic Materials	F. A. Mauer
	E. N. Farabaugh
Physical Chemistry	D. E. Mann
Radio Standards Physics	J. L. Dalke

The four previous semiannual reports in this series were published as NBS Technical Notes 174, 197, 236, and 251.

2. CRYSTAL GROWTH

This chapter is concerned with mechanisms and techniques of crystal growth and dissolution.

2.1 Growth of Dislocation-Free Metal Crystals from the Melt

T. H. Orem
R. L. Parker

Crystallization of Metals Section

For background, see NBS Technical Notes 174, Sect. 4.3; 197, 2.3; 236, 2.1; and 251, 2.1.

Since our last report we have grown 12 aluminum crystals by the Czochralski method. All were grown in new crucibles of special purity graphite, using Al starting material of 99.9999% initial purity. We have taken about 200 Lang topographs of eight crystals during the period.

Chemical analysis of the aluminum before melting in our conventional (~99.9%) purity graphite crucibles, and then after melting, showed that we had been picking up considerable impurity from the graphite. It was enough to reduce 5-9's and better purity aluminum to around 3-9's. We then acquired and used some ultra-high purity graphite crucibles (about5-9's pure) and found that 5-9's and 6-9's aluminum now did not pick up significant impurity. The cone of defects often seen in earlier Lang topographs was no longer present.

Figure 1 shows a positive print of a Lang topograph of our specimen 134, which is the best Al crystal we have yet grown. It is free of dislocation lines in the region near the tip. In addition, fringes following the outline of the crystal are seen in this region. They are called Pendellösung fringes [Kato and Lang Acta Cryst. 12, 787 (1959)] and are an indication of extremely high crystal perfection; they require the dynamical theory of diffraction for an interpretation. So far as we are aware, there is no prior published evidence of any observations of Pendellösung fringes in metal crystals. They have been observed in Si, quartz, and LiF.

2.2 Kinetics of Growth of Crystals from the Melt

J. G. Early
R. L. Parker

Crystallization of Metals Section

The background of this project may be found in NBS technical Notes 174, Section 4.4; 197, Section 2.4; 236, Section 2.2 and 251, Section 2.2.

A commercial zone-refining apparatus was purchased and installed. Several preliminary attempts were made to zone refine tin in order to check the operation of the zone refiner. Even though no attempt was made to insure optimum conditions for purification, chemical analysis of the samples indicated that purification was occurring and that probably tin of sufficient purity for these experiments could be prepared.

Figure 1. Lang Topograph of the best Al crystal so far produced.

With the aid of Dr. S. R. Coriell, of the Crystallization of Metals Section, considerable time has been spent reviewing the theoretical basis for this experiment as outlined by Kramer and Tiller [J. Chem. Phys. 37, 841 (1962)], and Kramer and Tiller [Westinghouse Report 64-924-118-P4 (1964)]. Emphasis has been placed on correlation and interpretation of the type of data obtained from an experiment in light of assumptions used to develop the theory. This work is currently underway.

Finally, preparations are almost complete for an experiment using purchased tin of 99.9999% purity.

2.3 Theory of Dendritic Crystallization

S. R. Coriell
R. L. Parker

Crystallization of Metals Section

The stability of the shape of a particle growing by diffusion (or heat flow) in a supersaturated solution (or supercooled liquid) is being studied. We have previously considered the case of the growth of perturbations on a cylinder (See NBS Tech. Note 251, Section 2.3 and Coriell and Parker 1965). It was found that when the radius of the cylinder was larger than a certain radius, R_c, the cylinder was not stable with respect to certain infinitesimal perturbations of shape.

One of the assumptions in the previous treatment was that there was no diffusion in the solid-liquid interface, i.e., the surface diffusion coefficient, D_s, was assumed equal to zero. Since surface diffusion will cause the transport of matter from places of high curvature to places of low curvature, the effect of surface diffusion will be to make the cylindrical shape more stable. The stability of the cylinder and of the sphere with a non-vanishing surface diffusion coefficient has been treated. When the quantity $(D_s C/Dc_0)$ is large, the critical radius R_c is appreciably increased by surface diffusion. In the above ratio C is the concentration of solute in the growing particle, c_0 is the equilibrium concentration of solute at the solid-liquid interface, and D is the diffusion coefficient for solute in the solution. Estimates of this ratio have been made for typical experiments for growth of crystals from supersaturated solution and for growth of crystals from the vapor phase in the presence of an inert gas. It appears that the ratio can be very large for the case of solid-vapor growth and can increase the critical radius R_c by one or two orders of magnitude.

2.4 Crystal Growth Studies by Electron Field Emission Techniques

S. C. Hardy
R. L. Parker

Crystallization of Metals Section

The heterogeneous nucleation of Hg on W is being studied in an electron field emission microscope (see NBS Technical Note 251, Section 2.4).

The time required to form nuclei has been measured over a narrow range of vapor pressures as a function of emitter temperature. Figure 2 shows a number of nucleation time versus substrate temperature curves, each curve being taken at constant vapor pressure. The pressures given on the figure are relative values. The sharp breaks in the curves are interpreted as critical supersaturations below which nuclei will not form. The observation of such critical supersaturations is in agreement with nucleation theory.

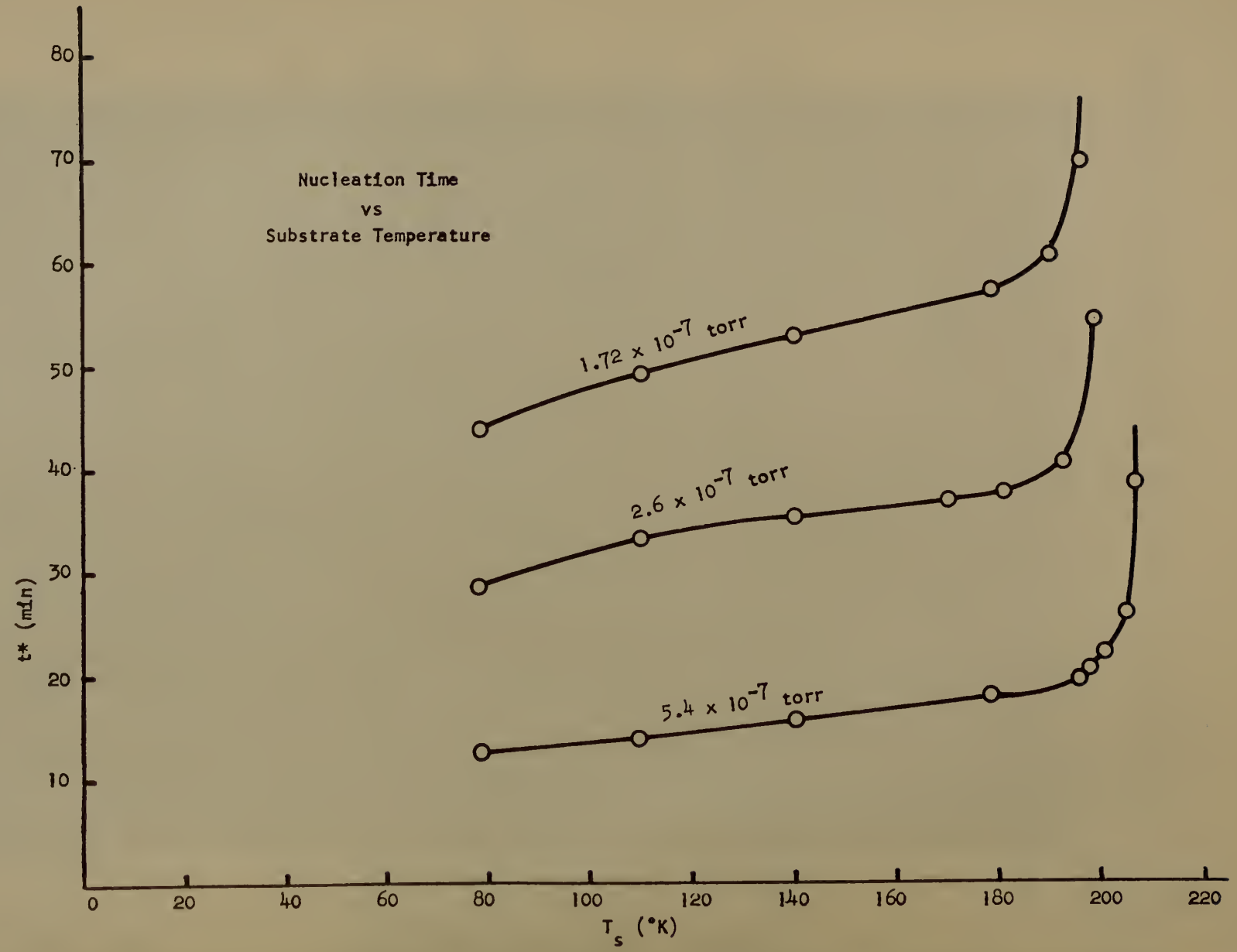

Figure 2. Nucleation Timer Versus Substrate Temperature Curves.

2.5 Field-Emission Microscopy of Crystal Growth Processes

A. J. Melmed

Corrosion Section

The method of preparing clean single-crystal field emitters by epitaxial growth on tungsten field emitters offers some real advantages over other techniques for studying metals which are normally difficult or impossible to study by field-emission microscopy. Therefore attempts were made to use this method for preparing clean iron surfaces for subsequent oxidation studies. Moreover these attempts were successful, but some questions still remain to be answered.

The field-electron emission microscopes used for this work were essentially conventional tubes with the addition of an iron vapor source. The nucleation and growth processes proved to be extremely sensitive to small amounts of impurities; the use of impure starting material or inadequate outgassing of the finally assembled source caused excessive multiple nucleation and highly defective crystalline growths. Therefore, floating zone refined iron of the highest available purity was used and source assemblies were thoroughly degassed. Ambient pressures in the tube were usually $< 5 \times 10^{-10}$ torr.

Experiments were done over the temperature range $\sim 350^{\circ}C$ - $1000^{\circ}C$. The iron crystals nucleated at the edge of tungsten [011] planes, grew out into the [111] regions, and then extended over the rest of the tungsten field-emitter surface and thickened. The iron crystal plane nucleated was an [001] plane and the crystal grew superposed on the tungsten substrate with like planes parallel to each other. Large crystals could be grown, but the useful temperatures for producing high purity iron crystals seem to be limited to a smaller range due to diffusion of tungsten from the substrate into the growing crystal. It was calculated that in order to have essentially no tungsten diffusion the growth temperature must be about $420^{\circ}C$ or lower, if growth times of about 5 minutes are used. For shorter growth times higher temperatures may be used. Crystals were grown over the temperature range $350^{\circ}C$ - $750^{\circ}C$. Field-ion microscope experiments are planned to examine the actual impurity content of the crystals, but until these experiments are done, the crystals grown at lower temperatures will be used for further work, i.e., oxidation studies.

2.6 Electrodeposition of Single Crystals

J. P. Young
F. Ogburn

Electrolysis and Metal Deposition Section

Silver was electrodeposited from solutions of silver ammonium nitrate under a variety of conditions. Depending primarily on the solution concentration we were able to get crystals and dendrites in several different forms. These included approximately equiaxed crystals several millimeters across and with many well defined facets, dendrites several millimeters wide and one to two centimeters long, extremely thin platelets covering an area of 10 to 100 square millimeters, and whiskers or needles centimeters long and a fraction of a millimeter in diameter. We have examined the structure of only the one dendrite and that only partially. It gives an x-ray diffraction pattern of a well formed single crystal and its facets are of high index planes. Our plans are to examine the structure of a number of these growths.

2.7 Theoretical Studies in Crystal-Whisker Growth

J. A. Simmons
R. E. Howard

Metal Physics Section

R. L. Parker

Crystallization of Metals Section

and

H. Oser

Applied Mathematics Division

The object of this work is to obtain accurate solutions of the equations describing the rate of growth of metal whiskers from the vapor and the rate of build-up of the concentrations of adsorbed atoms on the sides of growing whiskers. These equations and methods for determining their solution were described in NBS Technical Notes 236, Section 2.2 and 251, Section 2.20.

The computer program described in NBS Technical Note 251 was found to be stable and growth curves were computed for small times, $t \leq 1$ sec. Due to excessive computing times the program was rewritten to thin out the integration mesh as the whisker grows, thereby cutting the computation time by a factor of 10. Other difficulties associated with restarting the integration procedure of Subroutine 1 after computing the concentration profile by Subroutine 2 have yet to be resolved although considerable progress has been achieved.

2.8 The Effect of Light on the Oxidation of Copper Single Crystal Surfaces in Water

Jerome Kruger
Joan P. Calvert

Corrosion Section

Studies of the effect of illumination on the growth of oxide films on copper single crystal surfaces immersed in water containing different amounts of dissolved oxygen reveal that, while illumination has little effect on the oxidation progess when the water is in equilibrium with a 100% oxygen atmosphere it does lower the rate of film formation when the water is in equilibrium with 1% oxygen. For both the (111) and (100) planes white light causes a departure from the rate law observed for oxidation in the dark. At intensities of 290 $\mu w/cm^2$ or higher the film formed on the (111) plane never grows beyond a limiting thickness of 100 Å, (Figure 3). The behavior observed can be explained on the basis of a competition between growth and dissolution reactions, the dissolution reaction being promoted by illumination. A paper on this work has been published (Kruger and Calvert 1964).

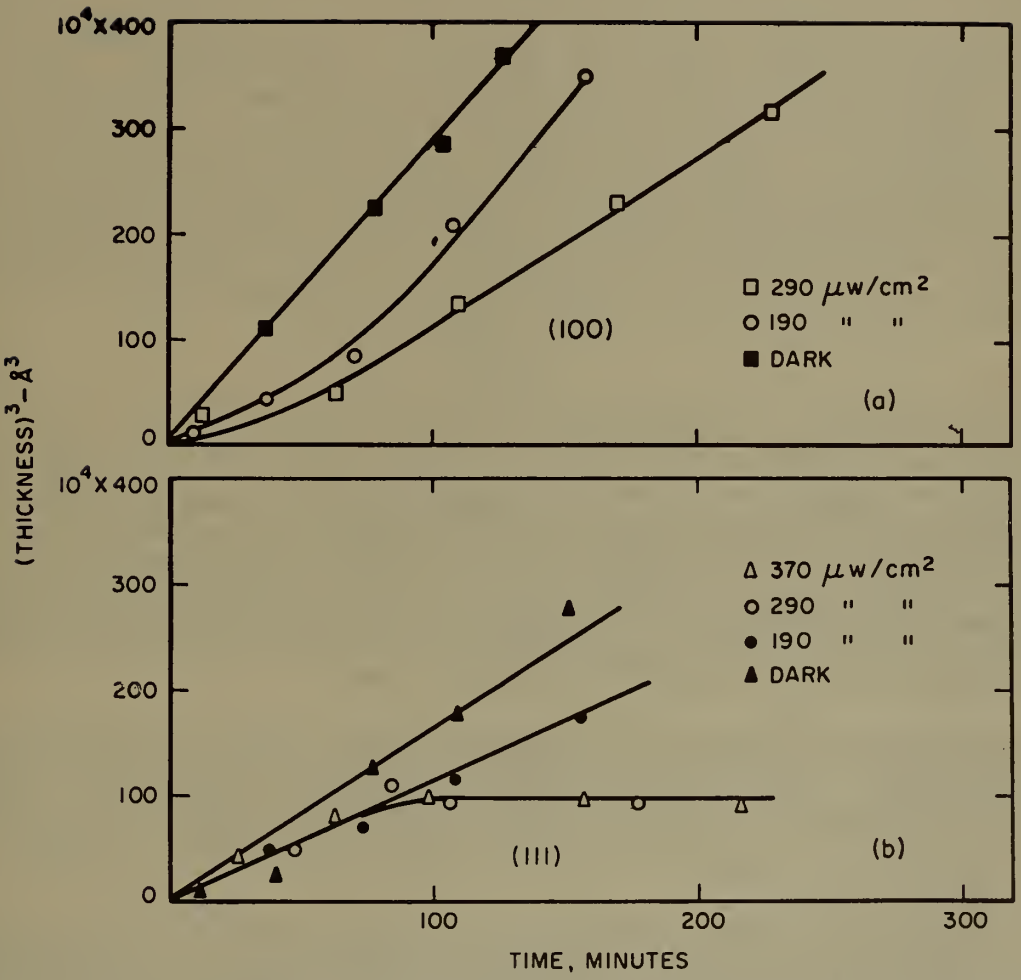

Figure 3. Cubic plot showing the effect of illumination of different intensities on the growth of oxide films on copper single crystals immersed in water in equilibrium with 99% He 1% O_2 gas mixture. (a) (100) Surface, (b) (111) surface.

2.9 Crystal Growth of Refractory Phases from Solvents

H. S. Parker

Crystal Chemistry Section

The purpose of this investigation is to develop and evaluate methods of growth of highly perfect crystals at temperatures below the melting point of the crystal. The preliminary work has been described in NBS Technical Note 251, Section 2.11.

Briefly, the techniques [originally proposed by Pfann, Trans. AIME 203, 961-4 (1955), see also: Tiller, J. Appl. Phys. 34, 2757-62 (1963); Mlavsky and Weinstein, J. Appl. Phys. 34, 2885-92 (1963) and J. Appl. Phys. 35, 1892-4 (1964); Griffiths and Mlavsky, J. Electrochem. Soc. 111, 805-10 (1964)] currently under investigation involves the movement of a thin (0.1 to 1.0 mm) solvent zone in a "sandwish" composed of the seed crystal, the solvent zone, and the polycrystalline source material. Movement of the solvent zone results when the assemblage is placed in a suitable temperature gradient such that solution is occurring at the hotter solvent-solute interface and epitaxial growth is occurring at the cooler interface. Thus this method differs from the usual zone melting technique in which operating temperatures are generally at or above the melting point of the crystal involved and zone movement results from relative motion of the cyrstal and heat source.

One of the major problems associated with the successful use of the traveling solution zone technique is the selection of a suitable solvent for the desired crystal growth. Among the important properties of the solvent are a low melting point or formation of a low-melting eutecic with the desired crystal, sufficient solubility of the crystal in the solvent (this solubility need not be high, since there is essentially an infinite amount of source material compared to the dimensions of the zone and the amount of solvent present), a liquidus slope ($\Delta C/\Delta T$) such that attainable temperature gradients will result in formation of a stable and steadily moving zone and consequent supersaturation at the cooler interface, lack of solid solubility with the crystal of interest, and low vapor pressure. In addition, the diffusion rates of the solute species should be high in the solution zone.

As reported in NBS Technical Note 251, Section 2.11, ZnO has been chosen as the initial experimental material and minor amounts of growth have been obtained using $PbMoO_4$ as a solvent. Other possible solvents have been investigated but no evidence of growth has been obtained. The major drawback to the use of $PbMoO_4$ is its relatively high vapor pressure at the necessary operating temperatures which, in a typical growth run, range from 1050° - 1500°C.

The investigation of other fused salts as possible solvents has been continued. At the present time, the $BaO-B_2O_3$ system appears to have promise. By the programmed cooling from 1350°C of mixtures containing approximately 44 percent by weight ZnO, 12 percent B_2O_3 and 44 percent BaO, it has been possible to crystallize ZnO over a limited portion of the temperature range. Compositions in the ternary system $ZnO-BaO-B_2O_3$ are being investigated to establish the compositional region wherein ZnO is the primary phase, and to determine the approximate shape of the liquidus surface in this region in order that suitable compositions and operating temperatures be selected for growth experiments.

Results obtained so far indicate the presence of a ternary eutectic or peritectic melting at less than 800°C and containing between 10 and 15 percent by weight of ZnO, with the remainder composed of BaO and B_2O_3 in the weight ratio 3.54/1. This BaO/B_2O_3 ratio corresponds to the eutectic melting at 905°C in the binary system $BaO-B_2O_3$ (Phase Diagrams for Ceramists, p. 97, the American Ceramic Society, Inc., Columbus, Ohio 1964). As ZnO is added, keeping the ratio of BaO/B_2O_3 constant at 3.54/1, the liquidus increases to a temperature of approximately 1175°C in compositions containing 25 percent by weight of ZnO. The compositional region between 25 and 50 percent by weight ZnO is currently being investigated. Since it has already been established that ZnO will crystallize at temperatures below 1350°C in this compositional range, it appears that this system holds considerable promise both from the standpoint of vapor pressure of the solvent and operating temperatures low enough to minimize problems associated with the volatility of ZnO. Due to the apparent high solubility of ZnO in this solvent, preliminary growth experiments using this 3.54/1 BaO/B_2O_3 eutectic mixture as the solvent have not been successful. In order for the solvent zone to reach a saturated condition, such large quantities of ZnO must be dissolved as to prevent the formation of a narrow zone, even when the over all temperature gradient in the system is of the order of 400°C/cm. In future experiments we will attempt to use a solvent composition initially containing ZnO in an amount which is nearly enough to produce saturation at the operating temperature.

2.10 Kinetics of Crystal Growth from Solution

J. L. Torgesen
R. W. Jackson

Crystal Growth Section

The experimental technique of Albon and Dunning [Acta. Cryst. 12, 219 (1959)] has been used to observe microscopically the growth layer morphology and growth kinetics of ammonium dihydrogen phosphate as its crystals grow from aqueous solution (see NBS Technical Note 251, Section 2.12). Small crystals of ADP have been grown by feeding with supersaturated solution in a special cell, mounted and temperature-controlled on the rotating stage of a microscope. With reflected light and at a magnification of 50X the surface features of the {100} and {101} faces were examined.

Growth on the {100} face of ADP crystals proceeds by a screw dislocation mechanism. The growth spirals are roughly elliptical in shape and oriented with the short axis of the ellipse parallel to the [001] axis of the crystal. Neighboring screw dislocations of opposite hand (Frank-Read source) are most frequently observed. The step velocity is of the order of 10^{-3} cm/min.

Growth on the {101} face proceeds by the movement of layers from the edges towards the center of the face, with the step height from all edges often of the same order of magnitude within the ability to observe. The stepped pit onto which the layers converge is often annihilated, leaving momentarily a face without observable steps. In accordance with the observations and conclusions of Bunn and Emmett [Disc. Faraday Soc. No. 5, 119 (1949)] it is believed that these layers have their origin in the spiral growth on the {100} face. It is conceivable that the layers distribute themselves along the edges of the {101} face and then proceed to build up layers on that face. A similar, even more striking example of this growth step morphology has been observed in {10$\bar{1}$1} faces of sodium nitrate.

When chromic ion impurity is added to the ADP solution, the growth spirals on {100} assume an almost rectangular shape, again with the short dimension of the rectangle parallel with the [001] axis of the crystal. This suggests that the habit modification caused by the chromic ion [J. Jaffe and B.R.F. Kjellgren, Disc. Faraday Soc. No. 5, 319 (1949)] proceeds by selective adsorption along the one-dimensional growth fronts rather than by adsorption on certain crystal planes, and further, that the changes in crystal habit are secondary to the changes in the morphology of the growth spirals.

2.11 Crystal Growth and Thermal Etching of Argon

G. L. Pollack
E. N. Farabaugh

Crystal Chemistry Section

This work was described in NBS Technical Note 197, Section 2.13.

A paper of the above title describing the experiments and the result has been accepted for publication (Pollack and Farabaugh 1965).

2.12 Crystal Growth in Silica-Gel Medium

J. L. Torgesen
A. J. Sober

Crystal Chemistry Section

Salts which are sparingly soluble in water can be grown in single crystal form in silica-gel medium [Holmes, J. Franklin Inst., 184, 743 (1917)] by the slow inter-diffusion of the component ions (see Technical Notes 197, Section 2.5, 236, Section 2.8, and 251, Section 2.13). Most applicable to materials having solubilities of the order of 0.01 to 0.1 percent, the method has been used to produce single crystals of a variety of materials up to several millimeters in size. These include copper tartrate, calcium tartrate, lead mono- and di-iodide, calcium sulfate dihydrate, and mercuric iodide.

Oxidation-reduction reactions which produce slightly soluble products may be conducted in the silica-gel medium to give single crystals of acceptable size. Cuprous chloride crystals, as optically clear, well-developed tetrahedra up to 3 mm on edge, have been grown by the inderdiffusion of cupric chloride and hydroxylamine hydrochloride.

Recent studies have explored ways and means to inhibit excessive nucleation which leads to large numbers of small crystals. It has been found that ultra-filtration (filter pore sizes down to 0.1 micron) of the component solutions does not significantly effect the number of nuclei and crystals which form. More effective in reducing nucleation has been the interposition of a "neutral" gel zone (containing initially no reacting ions) between the ion-source regions of the system. In some cases, e.g. copper tartrate, the number of nuclei decreases by two to three orders of magnitude to give three or four crystals per cc of gel medium.

As crystals grow to appreciable size (~ 2 cm), it is evident that the gel is split near the crystal corners and edges. The crystals are obviously growing under stress. In addition, the supply of nutrient material is enhanced in these localized regions of crystal surface, resulting in irregular growth. Arrangements are presently being studied whereby these limitations of the method can be eliminated.

2.13 High Temperature Crystal Growth

W. S. Brower

Crystal Chemistry Section

The use of direct electromagnetic heating, using high frequency RF power, for floating zone crystallization (see NBS Technical Note 251, Section 2.6) has been continued. A chamber has been constructed for the floating zone apparatus which will permit the control of atmosphere for floating zone crystallization of NiO and $MnFe_2O_4$.

Large single crystals of Cr_2O_3 (0.75 cm.dia. x 8 cm) have been grown by the verneuil technique and etching techniques have been developed for revealing dislocation arrays on the (10$\bar{1}$1) cleavage surfaces and on (0001) surfaces prepared by mechanical polishing (Brower and Farabaugh, 1964).

2.14 Crystal Growth from Solution

J. L. Torgesen
A. T. Horton

Crystal Chemistry Section

Large single-crystal specimens of ammonium dihydrogen phosphate and sodium chlorate continue to be produced by growth from solution using temperature-program techniques (see NBS Technical Notes 174, Section 4.5, 197, Section 2.5, 236, Section 2.8, and 251, Section 2.7). Only limited success has been realized in the growth of large single crystals of potassium acid phthalate (KAP). Excessive growth of crystallites in the solution surface, particularly in regions of contact with the grwth jar, heaters, thermometer, etc., contribute to volunteer growth which impedes the growth of the single crystals. Measurements to reduce this interference, a new dome-shaped lid by which condensing solvent is directed to wash more effectively the sides of the growth jar and using polyethylene sleeves on the upper sections of the heaters and thermometers, have been worthwhile.

Characterization of ADP crystals (see also Section 3.19) by x-ray diffraction topography and etch pit techniques has been continued with the latter corroborating the results which have been obtained on crystal perfection by x-ray methods. The two characterization methods have been shown to be in approximate one-to-one correspondence in the identification of dislocations in crystal sections prepared by sawing with abrasive wheels. The absence of both etch pits and topographic images in sections carefully prepared by string-sawing and solution polishing is taken to indicate that the material, as grown from aqueous solution, is dislocation-free. A preliminary report on characterization studies on ADP was orally presented in August, 1964 (Deslattes, et al, 1964).

Preliminary observations of the slip systems in ADP indicate a dominant slip along the equivalent pair of tetragonal axes and a minor, though significant slip along the unique tetragonal axis.

Attempts are presently in progress to produce large single crystal specimens of disodium pentacyanonitrosyl ferrate dihydrate. The material is to be used as a standard in the measurement of Mössbauer chemical isotope shift.

Work on the growth of oxalic acid single crystals from solution in glacial acetic acid and in acetone-water mixtures has been concluded. The details of this investigation are reported in a paper recently published (Torgesen and Strassburger, 1964).

2.15 Transitions in Vapor-Deposited Alumina

J. J. Diamond
A. L. Dragoo

High Temperature Chemistry Section

A transport film was formed on the interior of a pyrex flask when the end of an enclosed alumina rod was melted in vacuum (5×10^{-6} mm of Hg) with an arc image furnace. Infrared adsorption by the film showed a water band at 2.9μ and several adsorption fringes because the film was the same order of thickness as the wavelength of the incident radiation. The material lost about 4% in weight when ignited to 1200°C. The film did not give any pattern when subjected to either x-ray or electron diffraction analysis. The film thus is a slightly hygroscopic alumina and is "amorphous" to the limits of detectability (grain size < ~500Å).

The transition of the film to α-alumina was studied as a function of time and temperature. Representative d-spacings and intensities are illustrated in Fig. 4 for x-ray diffractometer results from annealed samples of the powdered film. A diffraction line corresponding to d=1.39Å (the strongest line of most transition aluminas) appeared after annealing the film in air for one-half hour at 570°C. All lines obtained from samples annealed at 570°C (maximum time, 16 hours) were very weak, and the certainty of these lines was determined by their presence in more than one pattern. A transition form (Fig. 4b), approximating a mixture of δ- and θ-aluminas identified by Stumpf [J. W. Newsome, H. W. Heiser, A. S. Russell and H. C. Stumpf, Aluminum Company of America, Alcoa Research Laboratories, Tech. Paper No. 10 (revised, 1960), p. 12] was presented after 32 hours at 670°C and for all heating times and temperatures investigated up to 16 hours at 870°C. Anneals at 870°C for 32 hours (Fig. 4c) and 920°C for 16 hours resulted in the abrupt appearance of α-alumina lines along with those of the transition form. Disappearance of the transition form was very nearly completed by 1070°C (16-1/2 hours), leaving α-alumina pattern as illustrated in Figure 4e.

The influence of the substrate on the formation of the vapor-deposited film was investigated by depositing the film both on a single-crystal sapphire disk and on a glass microscope slide. The films were stripped from the substrates and examined by electron microscopy and diffraction. The Al_2O_3 film deposited on the sapphire disk was polycrystalline, with a grain size of about 2200Å, and showed one faint diffraction ring at d=1.25Å (δ- or θ-alumina); whereas the film deposited on the glass slide showed no crystallinity (grain size was not determined). The film did not grow epitaxially on the sapphire as evidenced by the small grain size. Although the crystallinity of the substrate appears to have induced some crystallization of the

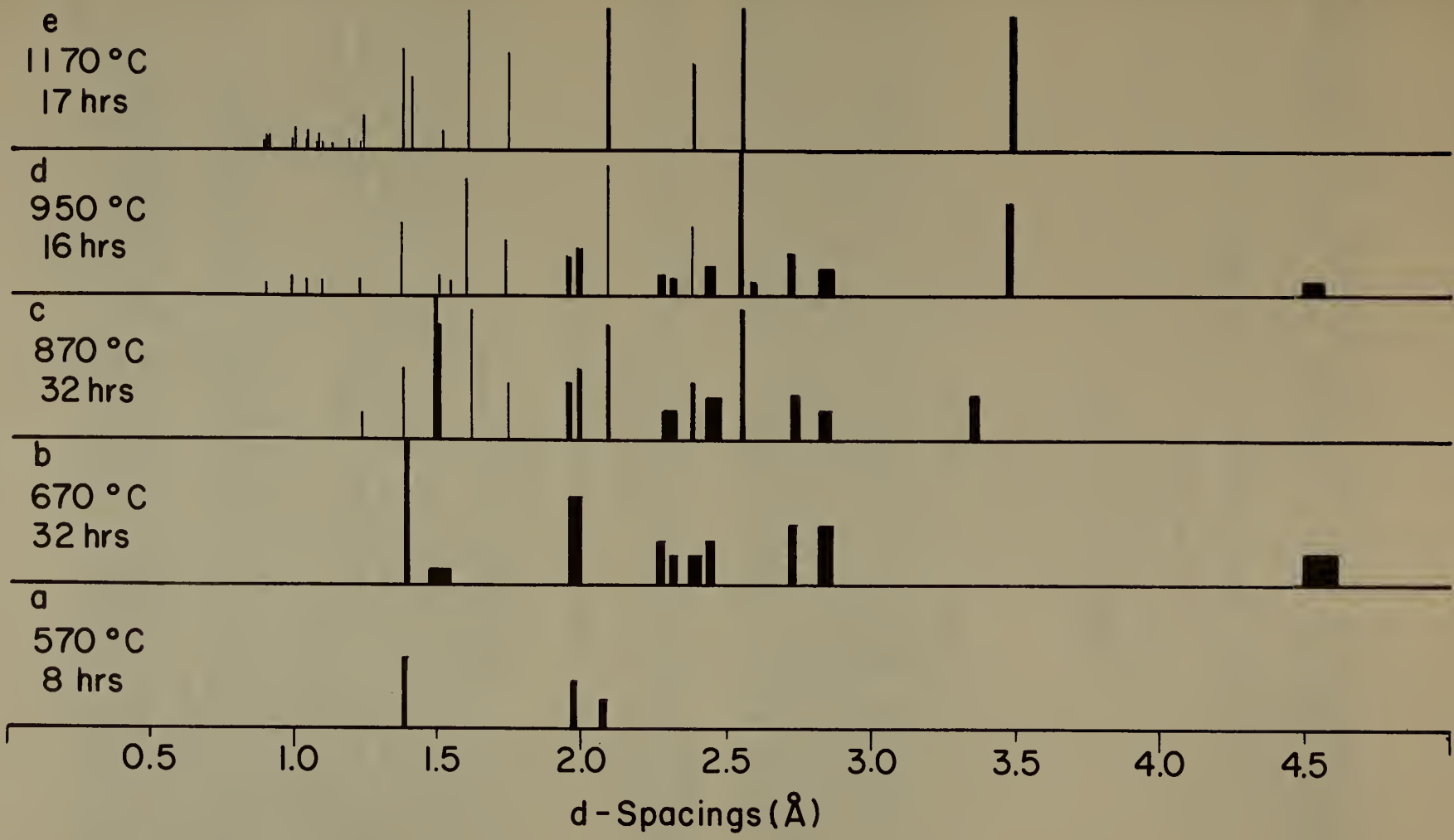

Figure 4. Transitions of Amorphous Al_2O_3 Films.

film, the single faint ring of the transition form suggests that the impinging vapor species, primarily Al and O [J. Drowart, G. DeMaria, R. P. Burns and M. G. Inghram, J. Chem. Phys. 32, 1366 (1960)], cool too rapidly to form the ordered α-alumina structure.

2.16 Crystal Growth from the Melt of Substances With a Low Melting Point

A. T. Horton

Crystal Chemistry Section

and

A. R. Glasgow

Analysis and Purification Section

Glass apparatus is used for the purification and growth of crystals with melting points up to about 130°C by a modified Bridgman technique. The temperatures of the melt and the solid are maintained by two immiscible liquids at whose interface a sharp temperature drop exists. A sealed pyrex tube containing the specimen is slowly lowered through the interface. The specimen is maintained under its own vapor pressure in contact only with the glass container. Provision is made for the removal of the last portions of the specimen to solidify in several successive recrystallizations.

The equipment has been found effective for the purification of trans-stilbene, dimethyl oxalate, benzoid acid and benzene. It could also be used for careful studies of thermal and radiation stability of pure substances.

2.17 Crystal Growth and Structure Studies

D. E. Roberts

Solid State Physics Section

Single crystals of MgF_2 have been pulled from the melt. The greatest difficulty has been the reaction of the charges with oxygen or water vapor. This liberates HF, which is destructive to the crystal puller, and MgO, which is soluble in the melt. The problem may be solved by construction of a system resistant to HF and operation in an HF atmosphere. Boules of good quality have been prepared in an existing apparatus by following a few precaustions:

1. The use of high purity MgF_2 as starting material.
2. Maintenance of a dry, oxygen-free atmosphere in the crystal puller.
3. Limitation of boule size to about 1/2" diameter and pulling speed to under 1/4" per hours.

Molybdenum oxide has been prepared from both the liquid and vapor phases. Crystals grown from the melt show many striations and are of little value. Vapor grown crystals form thin plates large enough for useful samples. At least nine phases of oxide are known to exist. Except for MoO_3 and possibly MoO_2, it is difficult

to isolate a specific oxide. The present effort is in the preparation of samples of a single phase.

$PbCl_2$ has been prepared from the melt. Crystals grow readily but fracture badly on cooling. Annealing does not prevent fractures. Growth from the vapor phase and from solution are being tried.

Single crystals of rutile (TiO_2) are being grown by the flame fusion method. $SrTiO_3$ has also been grown but boules are not single crystals.

2.18 Melting Temperature of Copolymers

J. P. Colson and R. K. Eby

Polymer Physics Section

Samples of a copolymer series have been crystallized with different lamella thicknesses as measured by small angle x-ray diffraction. Rapid heating on a microscope hot stage has been used to measure the melting temperature of the samples which have independently varied comonomer concentration and lamella thickness. Analysis of the initial results shows that variation of the melting temperature with these variables can be fitted to an equation derived with a model of inclusion of the comonomer units in the lattice as defects. This work has been reported in two papers (Eby 1963 and Eby 1964). The constants of fitting, which are related to the equilibrium melting temperature, the fold surface energy and the energy of the lattice defects, yield suitable values with these intial results.

2.19 Non-planar Solution Grown Crystals of Poly (4-methylpentene-1)

F. Khoury
J. D. Barnes

Polymer Physics Section

An optical and electron microscopic study has been made of the habits and morphology of chain folded crystals of poly (4-methylpentene-1) (P4MP1) precipitated from diluted solutions of the polymer in mixed solvents (50% xylene: 50% amyl acetate) at temperatures in the range 50°C-90°C. The outcome of this investigation has been to establish the existence of P4MP1 crystals which exhibit, to varying degrees distinctly curved growth habits.

It has been previously established [F. C. Frank et al. Phil. Mag. 4, 200 (1959)] [D. C. Bassett, Phil. Mag. 10, 595 (1964)] that P4MP1 can be crystallized from solution in the form of thin planar (or almost planar [D. C. Bassett, Phil. Mag. 10, 595 (1964)]) crystals consisting of a single or several superimposed square shaped lamellae which are of the order of 100 Å in thickness. It has also been established [F. C. Frank et al, Phil. Mag. 4, 200 (1959)][D. C. Bassett, Phil. Mag. 10, 595 (1964)] that the chain molecules are regularly folded within the constituent lamellae of such crystals and that the chain segments are oriented normal to the plane of lamellae. Furthermore, the lamellae are bounded laterally by (100),(010) growth faces (P4MP1)has tetragonal unit cell, a=b=18.66Å c 13.80 Å, containing four chains in a 7_2 helical conformation oriented with their axes parallel to the c-axis of the unit cell.).

Our present study has revealed that whereas crystals exhibiting the same habit as the described above are formed at 90°C (Fig. 5), at lower temperatures (80°C, 70°C, 60°C, 50°C) multilayer crystals are formed which exhibit distinct departures from the planar habit of the crystal shown in Fig. 4. It has been found that although the crystals formed at these lower temperatures consist of chain folded lamellae bounded laterally by (100), (010) growth faces, the crystals exhibit a distinctly curved overall shape resulting essentially as a consequence of the progressive curling which occurs during growth at the crystal corners where (100) and (010) growth faces meet. This latter feature has been found to become more pronounced the lower the temperature of crystallization.

Examples are shown in Fig. 6 (a, b) of crystals grown at 70°C as seen in different perspectives under the phase contrast microscope while still in suspension in liquid. At that temperature the corners ofthe crystals have curled back through 180° or more and are close to meeting one another the crystals have roughly the overall appearance of a hollow bowl.

It should be pointed out that the curved crystals observed during the course of the present study are not peculiar to the solvent system used. We have grown similar curved crystals from solutions of the polymer in xylene alone. Indeed, the similarity between certain types of curved crystals grown from xylene: amyl acetate as they appear in the collapsed state (they collapse very readily on drying) under the electron microscope, and some recently published electron micrographs of xylene grown crystals [A. E. Woodward, Polymer 5, 293 (1964)] is striking. On the basis of our complementary studies of the corresponding xylene: amyl acetate grown crystals while they were still in suspension in solvent, it appears that the crystals described by Woodward possess curved growth habits, and are not hollow pyramids with steep sides as has been proposed.

2.20 Isothermal Thickening of Polyethylene Crystals

James J. Weeks
John D. Hoffman

Polymers Division

Low-angle x-ray studies have been carried out on polyethylene while it was in the act of crystallization at 128°C. The objective was to determine whether the crystal lamellae thickened on storage. Studies were made on both Marlex 50, and a fraction of 240,000 molecular weight. Marlex 50 thickened at an initial rate of 105 Å/decade, and the fraction thickened at 75 Å/decade. The thickening process thus behaves in its first stages as was predicted. Both specimens showed an abrupt falling off in the rate at long times.

A note (Weeks and Hoffman, 1965) has been submitted.

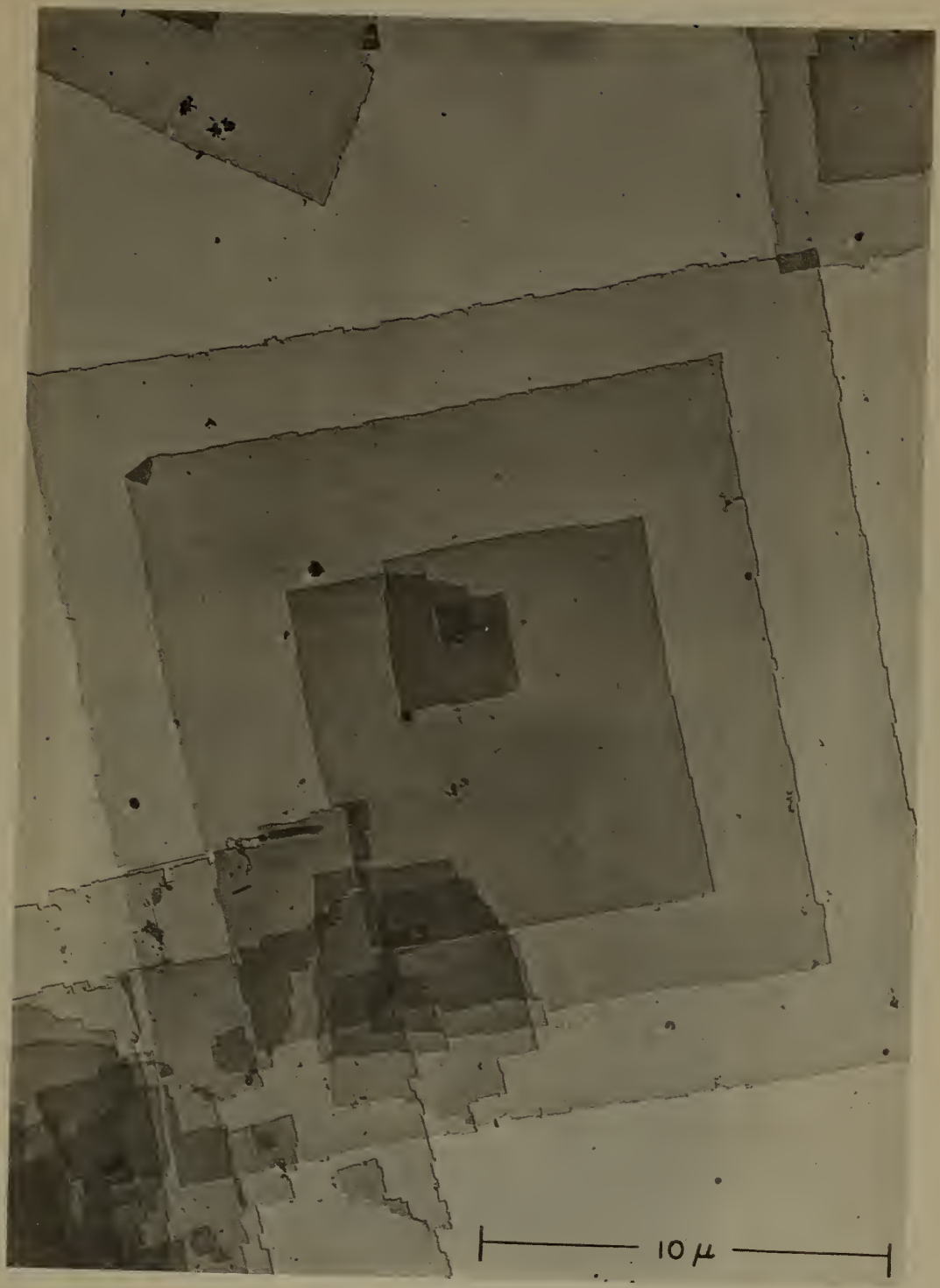

Figure 5. Crystals of Poly (4 methylpentene-1) grown at 90°C.

Figure 6 a.

Figure 6b

Figure 6. (a & b) Crystals of Poly (4 methylpentene-1) grown at 70°C under phase contrast microscope.

2.21 Single Crystals of n-Paraffins

John M. Crissman
Elio Passaglia

Polymer Physics Section

Several almost-single crystals of n-eicosane ($C_{20}H_{42}$) several centimeters long and 0.4 cm in diameter have been grown by the Bridgeman technique. X-ray investigation indicates that the crystals grow with the long-axis of the molecules orienting essentially normal to the growth direction. The structure is triclinic, and some disorder exists. The exact nature of this is being determined. Although the material was zone refined it is felt that purification was not complete, and a sample of more rigorously zone-refined material is now available.

2.22 Fractionation in Polymer Crystallization

E. A. DiMarzio
J. I. Lauritzen, Jr.
E. Passaglia

Polymers Division

A theoretical treatment of the problem of fractionation in polymer crystals whose formation is kinetically controlled has been developed. With each of the various types of fractionation problems one can associate a diagram on the basis of which the general rate equations can be detived. These equations have not been solved in general but the pure flux determined solution can be obtained by the techniques of linear algebra. With certain restrictions on the rate constants, the equations may be cast into the form of an eigenvalue problem: $[A-B]P = \lambda P$ where A is a matrix containing the forward and B one containing the backward reaction rates at the growth front of the crystal and P is a vector whose components, Pij, are the number of crystals with species j in the last position and species i in the next to last position. Sij represents the number of chains per second which grow by adding species j to a crystal with species i in the last position, and this is related to Pij by the equation

$$Sij = \lambda_j P_{ij}$$

which is a type of eigenvalue equation with λ_j the eigenvalue. The consequences of this formalism are being investigated. It is found that the same formalism can be used to solve the problem of fluctuations in step height and this problem is being programmed for the 7094 computer. Equilibrium is the special case of the general treatment.

2.23 Homogeneous Nucleation Studies

F. Gornick
G. S. Ross
L. J. Forlen

Polymers Division

During the current report period, the experimental techniques for studying the homogeneous nucleation frequency in linear polyethylene have continued to be developed and improved. It is now possible to prepare droplets of the bulk material in a size range from two to five microns. Suitable cells have been developed for containing the samples. Suspending materials and transferring techniques are now considered to be adequate for these studies. Reducing the amount of heterogeneous nucleation which occurs in any sample continues to be the most difficult problem but considerable headway has been made in this area.

Several isothermal studies have been completed using cinephotomicrographic techniques. Various techniques for analyzing the photographic results have been examined and statistically evaluated to determine the most efficient and accurate method for extracting meaningful data from each experiment. A machine technique developed by the Data Processing Systems Division for processing pictorial information has been used for one picture and appears to be a most promising technique. Dr. George Moore of the Metallurgy Division has developed a program which may be used for tabulating numbers of frozen droplets at any given time and temperature as well as their size and shape factors. This program is currently being rewritten for 'PILOT' and is expected to be in operation by May. The use of this method is expected to reduce greatly the time required to analyze the photographic results as well as increase the reproductibility of the counts.

During the next reporting period the studies on the unfractionated samples of polyethylene are expected to be completed. Investigations on other samples of this polymer will also be started.

2.24 Radio Materials Synthesis

P. M. Gruzensky

Radio and Microwave Materials Section

As indicated in Technical Note 174, Section 4.21, the purpose of this project is to synthesize ultra-pure or known composition materials which are not available readily elsewhere, and which are of particular interest for fundamental investigations of various solid state properties.

During this report period, efforts have been concentrated on the growth of sodium chloride single crystals from pure aqueous solutions. Alkali halide crystals in general are grown readily from a melt, however, optical and electrical properties are so sensitive to trace impurities and slight imperfections, that reproducible results often difficult to obtain (see for example, Butler, et al., J. Chem. Phys. 39, 242 (1963)). Essentially isothermal evaporation of chemically purified sodium chloride solutions has yielded several single crystals, one with edge dimensions of 2.5 cm. Conductivity measurements by a dc pulse technique indicate that the conductivity in the extrinsic temperature region is two orders of magnitude lower than that of commercially available melt grown crystals.

2.25 Hydrogluorothermal Growth of Crystalline BeF_2 under HF Pressure

A. R. Glasgow, Jr.

Analysis and Purification Section

In the development of a "hydrofluorothermal" process for the growth of BeF_2 crystals in a platinum-lined steel bomb under pressure of 30-50 atmospheres of HF, anhydrous addition of HF to a closed bomb is required. The technique for this addition from a rupture-disc ampoule (Fig. 7) was perfected whereby gaseous HF was transferred from a cylinder to an evacuated manifold of Monel, degassed in a trap by alternate freezing and melting under a vacuum, condensed in the ampoule and then sealed (E, Fig. 6), weighed at room temperature, added to the bomb, and finally released to the closed bomb by rupturing the platinum-disc (D, Fig. 7) by its increase in internal pressure when the bomb was heated to 150°C.

3. STUDIES OF DEFECT CRYSTALS

This chapter is concerned with studies of defect-sensitive properties of single crystals.

3.1 Optical Properties of "Pure" and Impure Crystals

R. F. Blunt

Solid State Physics Section

Principal attention was devoted to continuing the investigation of irradiation induced color centers in MgF_2 (see report by M. I. Cohen, Section 3.2 of this report). The work reported in Section 3.1, Technical Note 251, has been extended to include the use of polarized light on oriented crystals. The initial strong band has $E_{\perp}c$ and $E_{\parallel}c$ components at 255 and 265 nm, respectively. As reported earlier, optical bleaching of this band produces a strong hand at 370 nm with $E_{\perp}c$. Additional weak bands at 300 and 320 nm (with $E_{\perp}c$) have now been observed along with the 370 nm band, as seen in Fig. 8. Detailed bleaching experiments, in the course of which the 300 nm band is permanently removed, show that the 320 nm band arises from a center lying along a [110] direction. The 260 and 370 nm bands are cylindrically symmetric about the c-axis. None of the bands seem to have symmetry appropriate to an F-center, but the 320 nm could arise from a hole trapped at the two adjacent anions lying along [110] directions forming V_k centers. The 260 nm band could be a cation vacancy, but the 300 and 370 nm bands would remain unexplained.

This work has resulted in two papers: Blunt and Cohen, 1964a and Blunt and Cohen, 1964b.

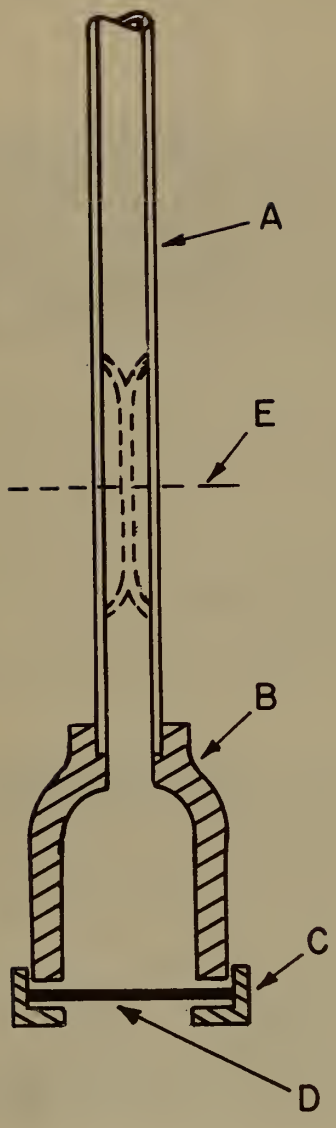

A. Platinum tube 1/8 inch O.D. .010 inch wall

B. Platinum-iridium body 90% Pt and 10% Ir alloy

C. Platinum-iridium ring 90% Pt and 10% and Ir alloy

D. Platinum disc, foil .001 inch thick soldered to B and C

E. Position where tube is cut off after filling with HF and closing tube with pliers

Figure 7. Rupture-Disc-Ampoule.

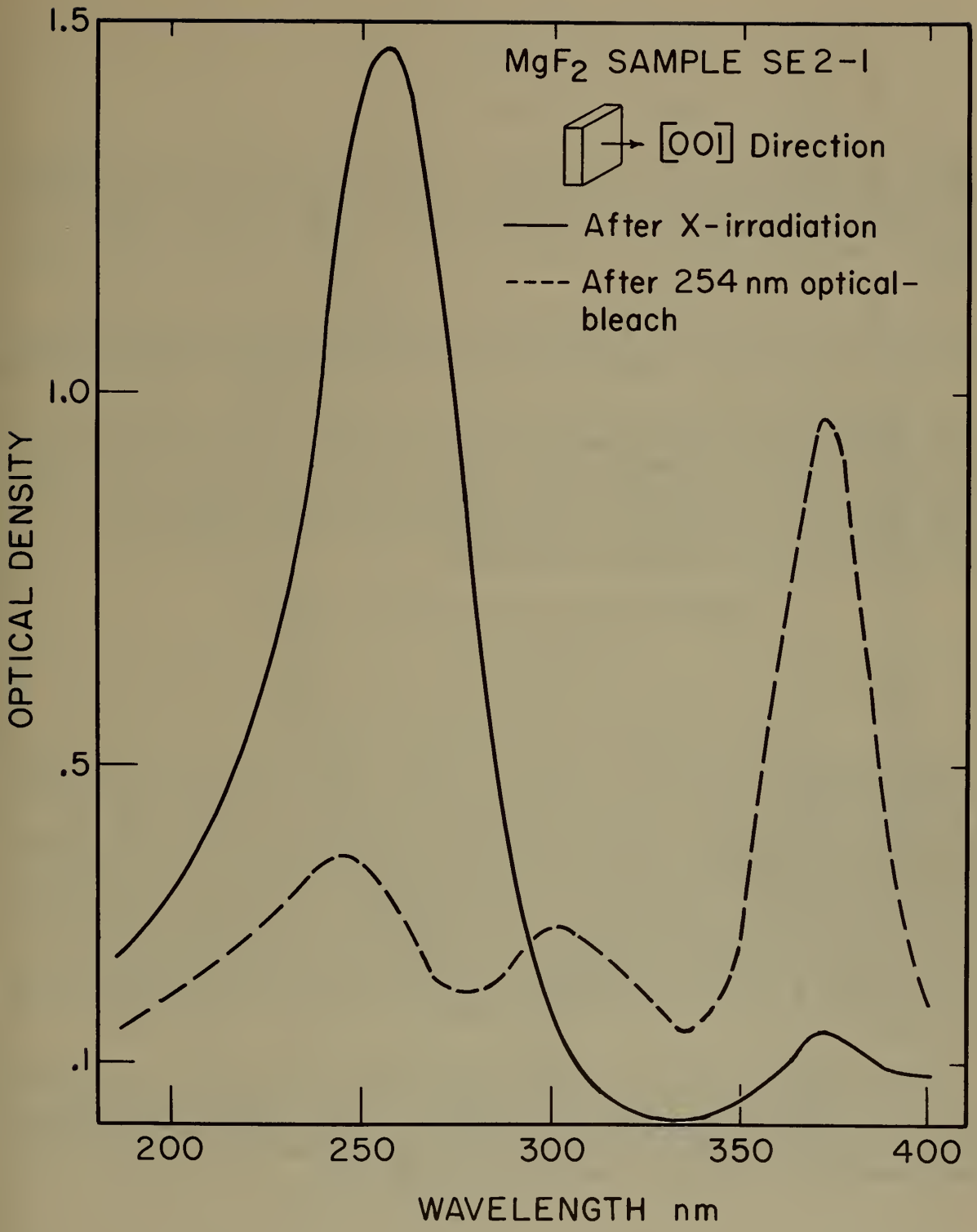

Figure 8. The optical absorption spectra of an MgF_2 crystal (0.05 cm thick) just after irradiation and just after a subsequent 254 nm optical bleach.

3.2 Irradiation Studies

M. I. Cohen

Solid State Physics Section

Work on irradiation induced color centers in magnesium fluoride has continued. The output of the tungsten target, high-output X-ray source has been measured by means of silver-activated phosphate glass dosimeters [Schulman, Klick, and Radin, Nucleonics 13, 30 (1955)] calibrated by V. H. Ritz of the Naval Research Laboratory. This measurement indicates a dosage rate on the order of 11 x 10^{19} eV/cm^2/hr at the sample position.

Measurements of the number of 250 nm centers produced (assuming an oscillator strength of 1) as a function of the absorbed dose were made using the method described by Ritz, and his form of the Smakula equation [V. H. Ritz, Phys. Rev. 133, A1452 (1964)].

The resulting curve (Fig. 9) shows an initial, fast-rising region which is commonly attributed to defects already present in the crystal. The "linear" portion of the curve which follows is usually taken to be the result of damage to the crystal by the absorbed radiation. Extrapolation of the "linear" region back to zero absorbed energy, indicates an initial concentration of defects of the order of 3 x 10^{16} centers/ cm^2. The slope of the region indicates that the absorption of 90,000 eV is necessary to form one 250 nm center.

3.3 Stacking Fault Energy in Silver-Tin Alloys

A. W. Ruff, Jr.
L. K. Ives

Lattice Defects and Microstructures Section

Measurements are being made on isolated extended dislocation nodes in thin foils of silver-tin alloys. The tin content varies from 0-8 atomic percent over the solid solution range. The radius of the circle inscribed within each extended node is measured (bisectrix method). Since the node plane is generally inclined at some angle to the plane of projection in the electron microscope, the inscribed circle becomes distorted and corrections are required. The node plane and orientation in the sample are determined from suitable electron diffraction patterns. The Burgers vectors of the nodal dislocations are determined from the dislocation contrast behavior in different Bragg reflections. The samples are mounted in a two-axis microgoniometer which can produce a tilt up to 16 degrees in any direction. Bright-field studies are then conducted on the nodes by tilting the samples into different single Bragg reflections.

Several different theories exist which relate measured node radii to the material stacking fault energy, differing in the complexity assumed for the problem. Two theories have recently been reported (one analytical, one numerical) which treat the problem in a realistic fashion. They require as input information the node radii and Burgers vectors, along with other constants of the material.

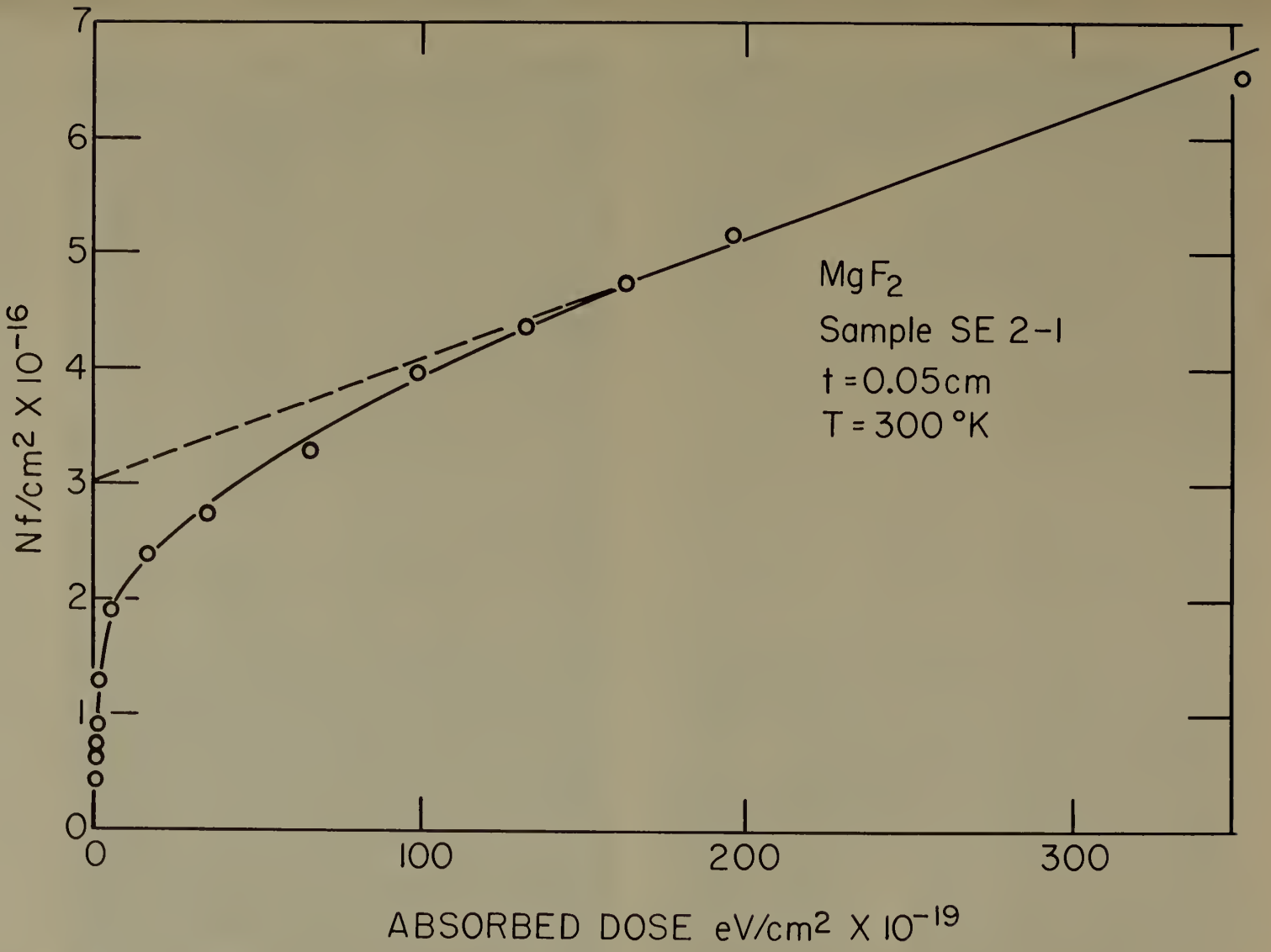

Figure 9. X-ray saturation curve for an MgF_2 crystal. Nf/cm^2 is plotted as a function of absorbed dosage in ev per cm^2. The sample was 0.05 cm thick.

Preliminary results have been obtained for the alloy compositions 4, 6, and 8 atomic percent tin. The full significance of the data must wait for the results of all compositions, and for a comparison with x-ray faulting probability measurements on the samples. First indications are that the fault energy decreases with increasing tin concentration from an extrapolated value of about 40 ergs/cm^2 for pure silver, to a value of about 4 ergs/cm^2 at the solid solubility limit. This low value would explain the profuse twinning and faulting observed in this and other similar alloys. Figure 10 illustrates a node in a sample of 8% tin, the transmission micrographs taken in two different reflections. In the lower micrograph, the nodal stacking fault is not visible due to its orientation with respect to the operating reflection. Two of the three nodal dislocations are visible, however, leading to the Burgers vectors assignments shown.

3.4 Stacking Fault Probabilities in Metals

C. J. Newton
A. W. Ruff, Jr.

Lattice Defects and Microstructure Section

A study of stacking fault probability by means of X-ray diffraction effects has been undertaken in a series of silver alloys. Small relative changes in the separation of the diffraction peaks in the x-ray powder pattern are observed when one compares the pattern from the cold-worked material with that from annealed material of the same composition. This relative peak shift, as well as certain other diffraction effects, enables one to calculate the probability of faulting in the cold-worked material.

The specimens currently under examination are a series of uniformly prepared filings of ingots of silver-tin with the tin content ranging from zero to about ten atomic percent. The angles of diffraction of the first two diffraction lines are being determined by point counting intensities in a diffractometer and employing a parabola-fitting procedure at the peak. This yields the relative peak position with a precision of about $\pm$ 0.005° in 2θ. The relative peak shift is then found with a precision of about $\pm$ 0.01°. The relative peak shift, and the stacking fault probability computed from it are found to increase quasi-parabolically with the increase of tin content in silver. Figure 11 shows the peak separation $\Delta 2\theta = 2\theta_{200}-2\theta_{111}$, in the annealed and cold-worked material as a function of tin content; and Figure 12 shows the relative peak shift, $\Delta\Delta 2\theta = \Delta 2\theta_{CW}-\Delta 2\theta_{Ann}$, which is proportional to minus the stacking fault probability.

Consideration is being given to extending the measurements to solid alloy specimens and to other solutes in silver. It is hoped to correlate the observed stacking fault probabilities with stacking fault energies measured in the same material by an electron microscopic technique in another project in this section.

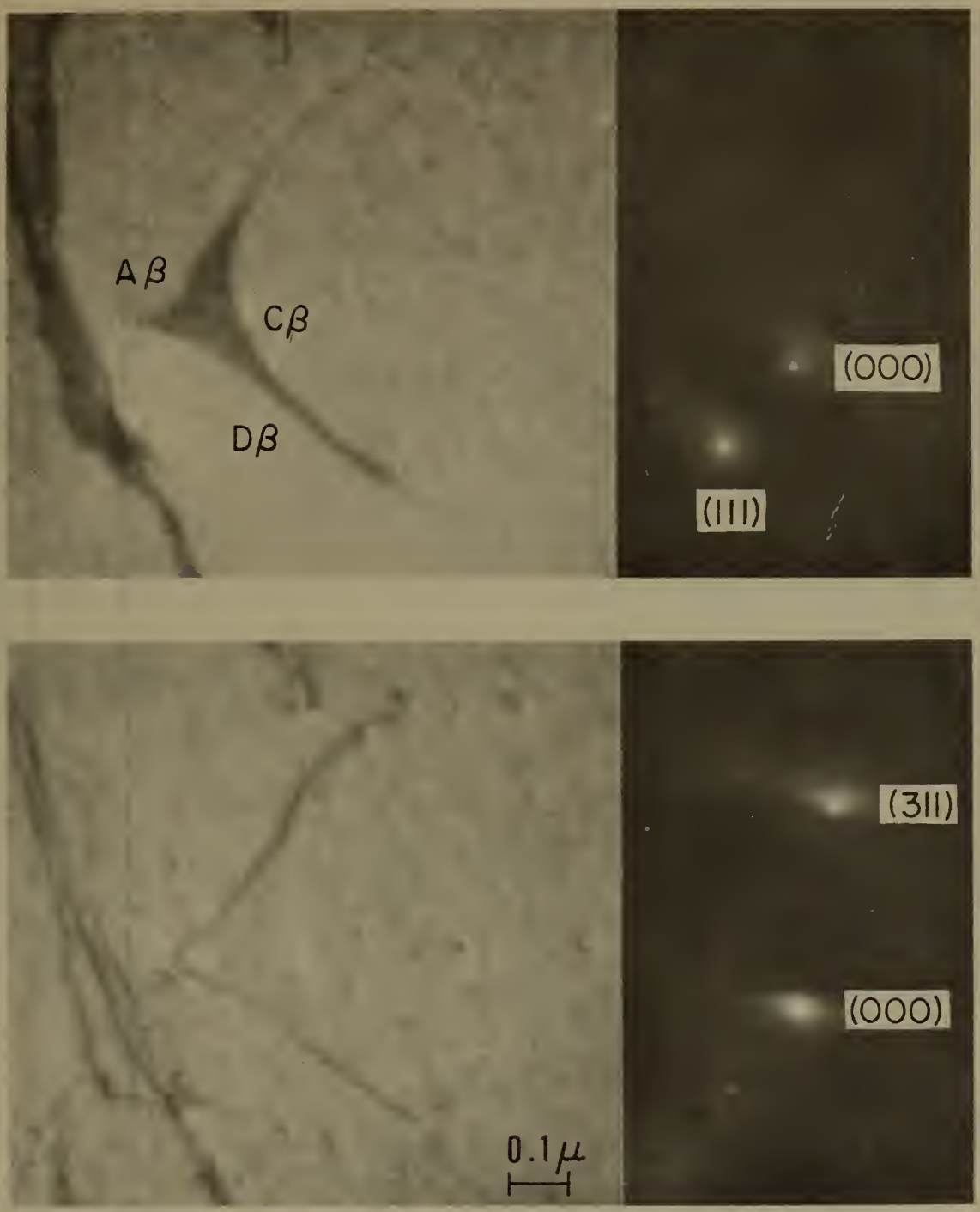

Figure 10. Transmission electron micrograph from a sample of silver - 8 atomic percent tin. The dislocation node is shown in two different Bragg reflections, (111) and (311). The nodal stacking fault is visible in the first case but not in the second, due to an orthogonal relation between the stacking fault shear and the (311) reflection. The observed contrast differences lead to the assignment of Burgers vectors shown. The node distortion is attributed to surface effects and to its inclination with respect to the viewing direction.

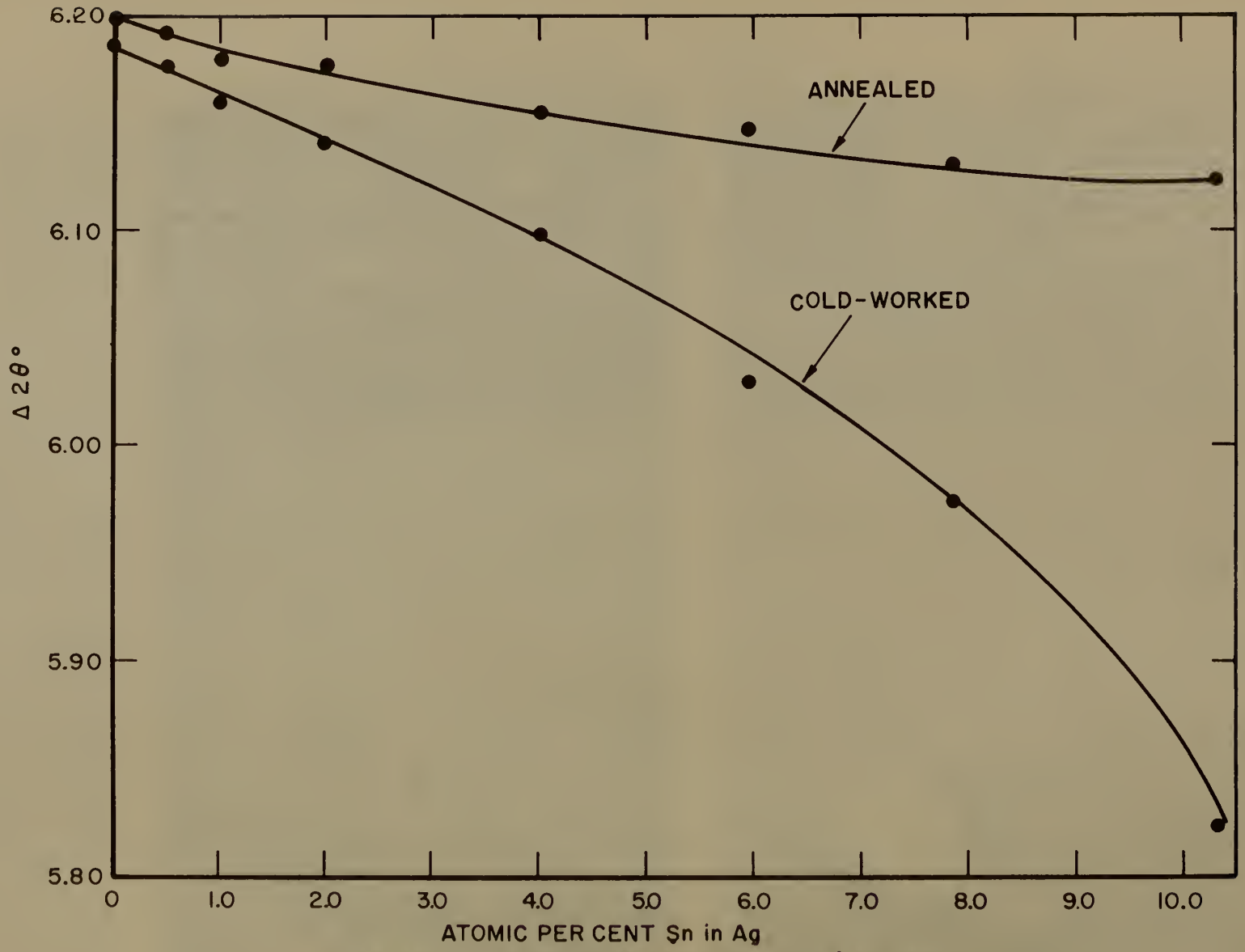

Figure 11. Relative separation of first two diffraction lines, $\Delta 2\theta = 2\theta_{200} - 2\theta_{111}$, in some Ag-Sn alloys as a function of Sn in Ag.

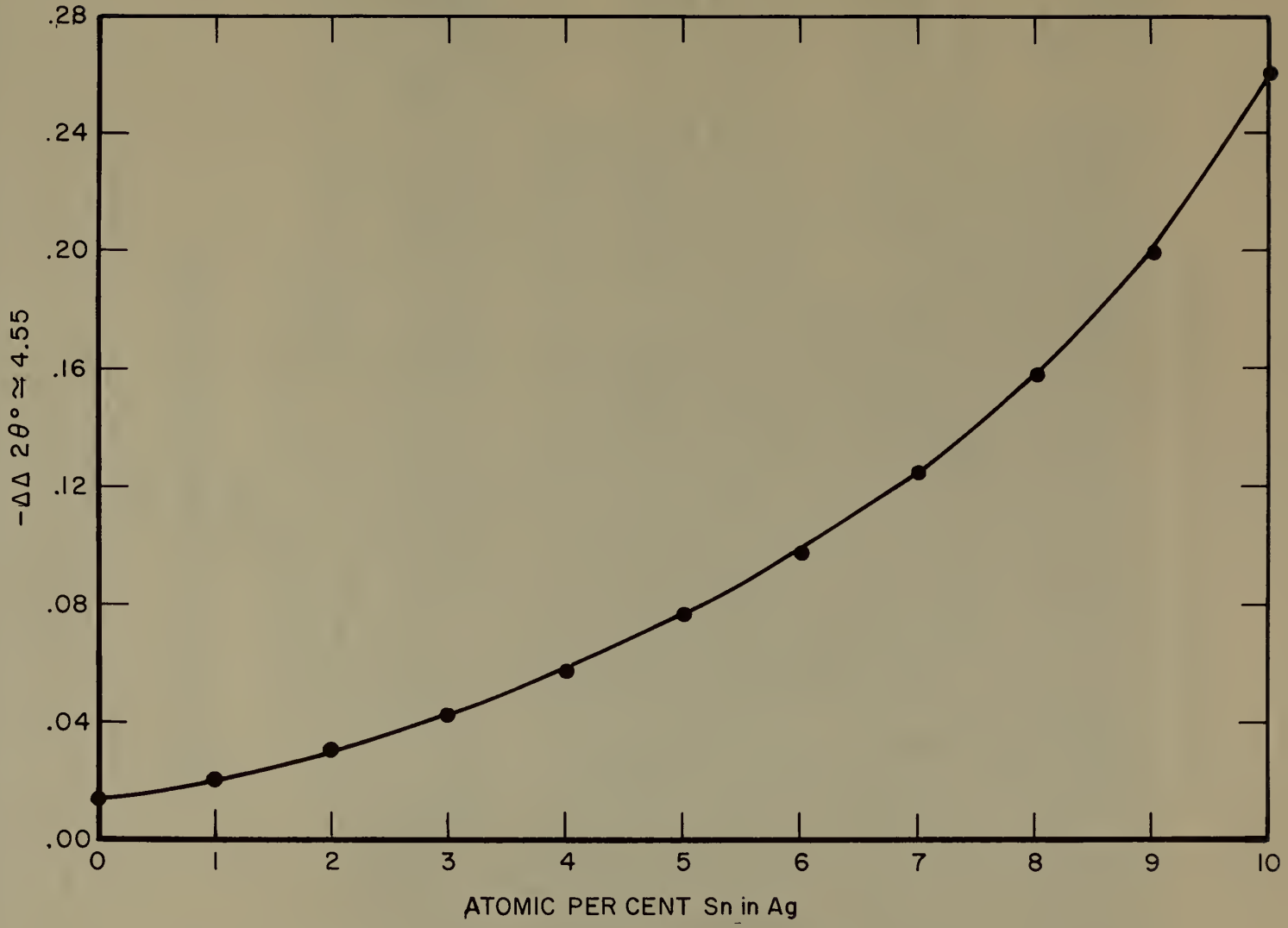

Figure 12. Relative shift of first two diffraction lines, $-\Delta\Delta 2\theta = -[\Delta 2\theta_{cw} - \Delta 2\theta_{Ann}]$ in some Ag-Sn alloys as a function of Sn in Ag.

3.5 Extrinsic Stacking Faults in Silver-Tin Alloys

L. K. Ives
A. W. Ruff, Jr.

Lattice Defects and Microstructures Section

Three-fold dislocation nodes which form a planar network in FCC materials must satisfy certain rules of continuity. In particular the two possible nodes, called P and K-nodes, must alternate in a stable network. The K-nodes are themselves stable when extended, due to mutual repulsion of the partial dislocations across the node. The P-nodes will, conversely, contract to a point at the node center. The simple network therefore consists of alternate extended and contracted nodes.

A different conclusion is reached, however, if both types of stacking faults possible in the FCC structure are included. The normal intrinsic fault, which corresponds to a single slip process, exists at the extended K-nodes. The contracted P-nodes can now also extend, containing an extrinsic fault. This type of fault is predicted to have a greater energy than the intrinsic fault, since it is crystallographically equivalent to two adjacent intrinsic faults.

Previously only intrinsic faults had been reported in FCC alloys. We have observed recently both types of faults in alloys of silver-8 atomic percent tin, using transmission electron microscopy techniques. Figure 13 shows a typical example of adjacent intrinsic-extrinsic dislocation nodes. A similar and independent result was recently reported in an alloy of gold-tin, and this phenomena may be generally true of very low stacking fault energy materials. While no theory exists yet by which the extrinsic P-node shape parameters can be translated into fault energy, it seems clear that the extrinsic fault energy is several times greater than the intrinsic fault energy.

Many questions remain, however, including those concerning segregation at the different faults, and the temperature dependence of the fault energy. The exact mechanism by which the extended P-nodes form is not clear, nor are the conditions which determine the balance where the two faults meet. Observations show that the extended P-nodes are glissile; this may explain why only intrinsic faults are found to intersect the sample surfaces. So far, this has precluded a more direct contrast study of the fault character.

3.6 Thermodynamics of Segregation of Solute Atoms to Stacking Faults in FCC Binary Alloys

R. deWit

Lattice Defects and Microstructures Section

and

R. E. Howard

Metal Physics Section

As described in NBS Technical Note 251, Section 3.5, the object of this work was to calculate on the basis of a certain model of the stacking-fault (1) the equilibrium concentration of impurity atoms which segregates there, (2) effects of such segregation

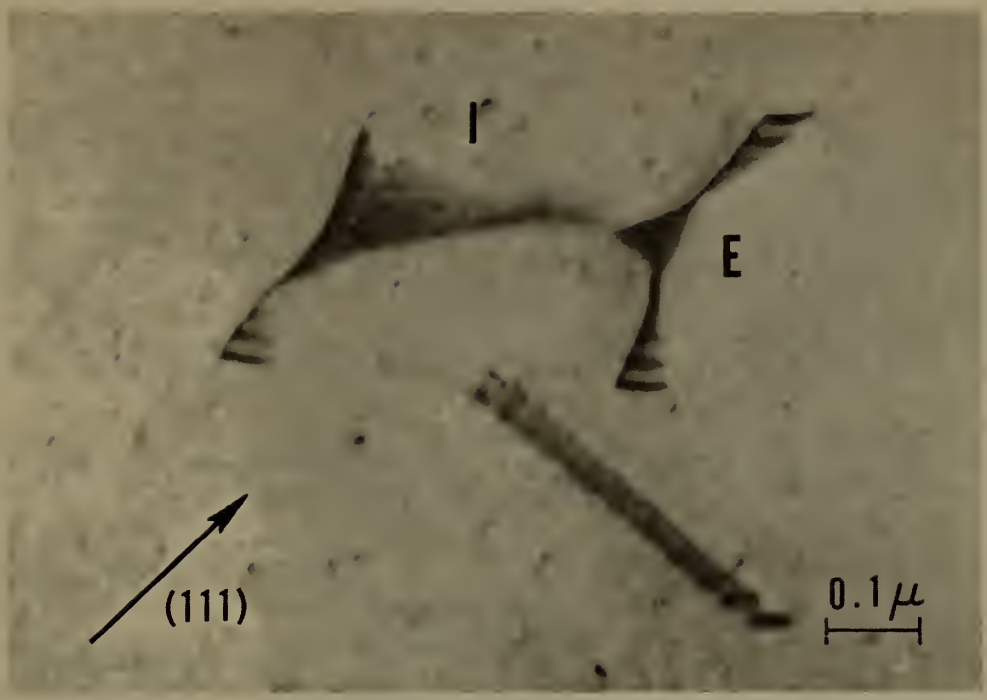

Figure 13. Transmission electron micrograph of adjacent three-fold dislocation nodes in a sample of silver - 8 atomic percent tin. Both nodes are extended in contrast to the usual alternation of extended-contracted nodes in the FCC structure. The left K-node labeled I contains the usual intrinsic stacking fault. The right P-node labeled E has expanded, containing a triangular region of extrinsic fault. Only one of the three bounding dislocations is visible in the (111) reflection operating.

on the stacking-fault width and on certain mechanical properties determined by the width, (3) the relation between the stacking-fault energy and the occurrence of phase boundaries in f.c.c. alloys. A paper has been prepared and has been accepted (Dewit and Howard 1965).

3.7 Oxidation of Iron at Low Pressures

Jerome Kruger
H. T. Yolken

Corrosion Section

Preliminary studies of the oxidation at 300°K of high purity polycrystalline iron surfaces prepared under ultra-high-vacuum conditions was studied using ellipsometry to measure film thickness. By working at low oxygen pressures (between 10^{-7} and 10^{-4} torr) it was found that the early stages of the oxidation process followed a linear growth law (see Fig. 14) with rate being proportional to the pressure. This behavior is in agreement with a picture proposed by Cabrera. The sticking probability of oxygen in the pressure range studied was of the order of 5×10^{-3}. Traces of water vapor lowered the limiting film thickness approached in the latter, nonlinear, oxidation stage to 18 Å from the 26 Å found at all pressures for dry oxygen. This work has been published (Kruger and Yolken 1964).

Studies are now underway on iron single crystal surfaces with special attention being paid to thermal effects on the properties of the oxide film on the iron.

3.8 Defects in Thin Oxide Films

Jerome Kruger
Carol Lee Foley

Corrosion Section

The work described in Technical Note 251, Section 3.7 was extended to films formed on iron by anodic polarization in 0.1 N H_2SO_4. The films formed had the same spinel structures as those found for films formed in the slightly alkaline borate solutions indicating that the nature of the passive film on iron may be independent of the pH, in the range studied (1-9), at which it is formed. Further analysis of the electron diffraction data by C. J. Bechtoldt of the Lattice Defects and Microstructures Section have found that the super lattice lines reported earlier were probably not due to the oxide film on the iron but to impurities.

3.9 Order in Ag_3Sn

C. J. Bechtoldt

Lattice Defects and Microstructures Section

Single crystals of Ag_3Sn were grown in dilute solutions of silver in tin by slowly cooling. Single crystals of Ag_3Sn were separated by dissolving away the tin phase in concentrated HCl. Examination of processing patterns disclosed extra weak spots indicating that the "a" parameter of the orthorhombic cell is 5.99 A or twice that as given in the literature and the structure is that of the Ni_3Ta prototype. The intensity of the extra reflections resulting from ordering is probably enhanced by the additional freedom in atomic positions provided by this structure. Atomic parameters have not been determined.

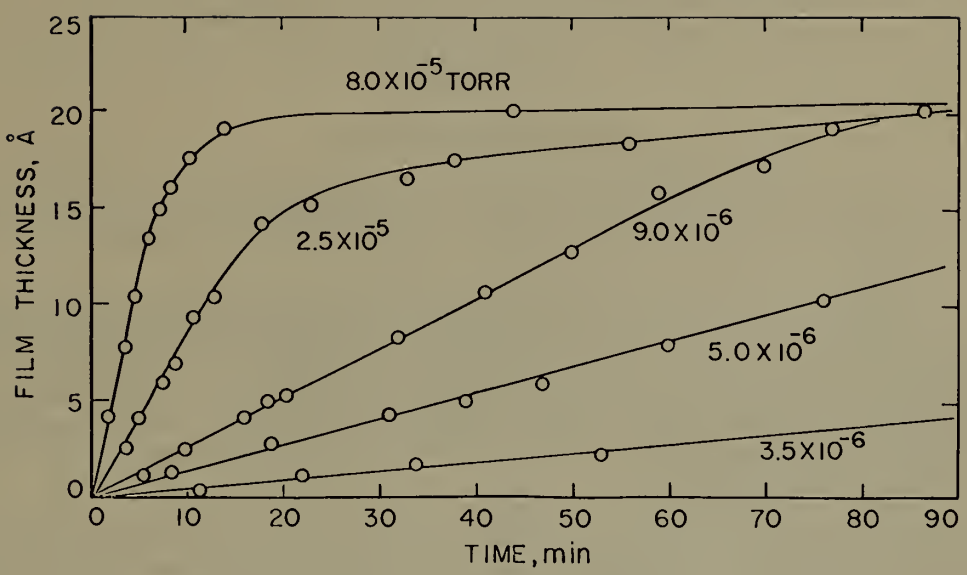

Figure 14. Change of oxide film thickness on iron with time at different oxygen pressures and at 300°K. All curves eventually approach the same limiting film thickness of 26 Å.

3.10 Copper Surface Self-Diffusion

A. J. Melmed

Corrosion Section

Experiments were undertaken to determine the activation energy for surface self-diffusion of copper and the effect thereon of a strong electric field. For this work copper crystals were grown on tungsten field emitters mounted on temperature-resistance calibrated support loops. Surface diffusion was caused to occur at various temperatures in the presence of an electric field and the rate of material transport was measured as a function of temperature and average field strength. The crystal was then smoothed with no applied electric field and the rate of this process vs. temperature was measured.

These measurements are still in progress, but tentatively the results indicate that both processes follow an Arrhenius-type relationship, and the activation energy is about 12 ± 4 kcal/mole for the zero field case.

3.11 Theory of Point Defects in Crystals

R. E. Howard

Metal Physics Section

This work is on the statistical theory of point defects in crystals. Its object is to understand certain macroscopic properties of crystals which depend on matter transport in terms of the atomistic properties of point defects.

1) A review article "Matter Transport in Solids" prepared in collaboration with Dr. A. B. Lidiard of the Atomic Energy Research Establishment, Harwell, England has appeared (Howard and Lidiard 1964). This article reviews the transport of atoms through crystalline solids under the influence of external electric fields, chemical and isotropic concentration gradients and thermal gradients. The main emphasis is on the statistical and thermodynamic description of these phenomena via the theory of mobile lattice imperfections.

2) Some recent experiments on thermal diffusion in dilute alloys were analysed theoretically and values of impurity heats of transport were derived from the experimental data. (Heats of transport are basic atomistic parameters that describe the tendency of an atom to move up or down a temperature gradient). A paper on this has been accepted (Howard and Lidiard 1965).

3) A new method was developed for the calculation of correlation factors, quantities that relate measured diffusion coefficients to atomic jump frequencies. In particular, the so-called random-walk technique for calculating correlation factors was extended from cases of special symmetry to those of general symmetry. A paper on this will appear in the Proceedings of the Fifth Conference on the Reactivity of Solids Munich (Howard 1964). Work is in progress applying the method to several special cases involving diffusion by di-vacancy pair and impurity-vacancy pair mechanisms in metals and ionic salts.

3.12 Nuclear Magnetic Resonance

L. H. Bennett
R. W. Mebs
R. J. Snodgrass

Alloy Physics Section

a) Nuclear Magnetic Acoustic Resonance

The studies of nuclear magnetic resonance through acoustic excitation of single crystals in high magnetic fields were continued. Employing a potassium iodide crystal as a means for determining methods of improving the experimental technique, however, resulted in an actual degradation of the observed signal with time. Careful inspection indicated deterioration of the crystal probably occurred due to diffusion of its gold plateing beneath the surface. New crystals of this and other salts are being secured; these will be carefully processed to appropriate forms and finish for further tests.

Further effort was made to observe the Cu acoustic resonance, as reported by Barnes (Nature 200, 253 (1963)), without success. Theoretical analysis indicates serious errors in Barnes' explanation for the resonance frequency shifts and the two narrow differing excitation voltage ranges over which observable resonances were reported for Cu^{63} and Cu^{65} by Barnes. We conclude that the observation of actual copper resonances by Barnes is open to question.

Other experts in the field of nuclear acoustic magnetic resonance have indicated to us that they have also failed to observe the copper resonance.

b) Wide Line Nuclear Magnetic Resonance

Information about the electronic structure of alloys has been obtained by analyzing nuclear magnetic resonance linewidths, Knight shifts and quadrupole effects. Extensive measurements on lead base solid solutions have brought about a better understanding of the changes in internuclear and electron-nuclear interactions produced by the addition of impurities. In particular, the oscillations of electronic charge density screening impurity atoms have been shown to be ineffective in producing large changes in the local magnetic field at a nucleus in the polyvalent system. The fractional change in the Pb^{207} Knight shift expressed as a function of solute concentration, C, is only $\Delta k/k \approx 0.05C$, the slope being proportional to the difference in valence between the impurity atoms and the lead atoms. The absorption linewidths broaden rapidly upon addition of solute and depend linearly on the applied magnetic field. Indirect spin exchange and pseudo-dipolar coupling are largely responsible for the broadening, while the non-contact, ordinary magnetic dipolar interaction between the electron and nuclear spin plus a distribution of Knight shifts (charge oscillations) may explain the field dependence. Large amounts of p-character in the wave function at the Fermi surface are indicated from values of the near-neighbor exchange constant, in lead-indium alloys $h^{-1}|B_{Pb-In}| = 1.0$ kc/sec.

The nuclear resonances of In^{115}, Bi^{209}, Tl^{205}, Hg^{195}, and Sb^{121} as solutes in fcc lead solid solutions have also been measured. The unexpected observation at different solute concentrations of the quadrupolar nuclei In^{115}, Sb^{121} and Bi^{209} indicate that quadrupole interactions are screened to a high degree. Comparison of values of the solvent and solute shifts are also consistent with short range screening in these alloys, although no quantitative theory has yet been offered.

c) Nuclear Magnetic Resonance in Ferromagnetic Metals

Apparatus has been developed for measuring the nuclear magnetic resonance spectra in ferromagnetic metals under hydrostatic pressure of up to 7 kbars. With this apparatus, the changes in internal field at the position of the nucleus upon application of hydrostatic pressure have been measured for Ni^{61} in nickel and for Co^{59} as an impurity in nickel. This data was used to separate the implicit and explicit effects of temperature on the internal fields at these two nuclei. Although the effect of thermal expansion is rather large, the changes in the internal field due to implicit effects of temperature at the two nuclei remained as large after correction for thermal expansion as before. We have no satisfactory theoretical explanation for even the sign of the pressure effect.

3.13 Influence of Stacking Faults on Plastic Deformation at High Temperatures

J. A. Simmons

Metal Physics Section

H. C. Burnett

Metallurgy Division

and

W. D. Jenkins
W. A. Willard

Engineering Metallurgy Section

Research has been started on the role of stacking faults in plastic deformation in the particular area of high temperature creep. A Baldwin creep machine has been adapted for inert atmosphere tests of copper and copper-germanium alloys in the 500°C - 800°C range at stresses above 1200 psi, and on an experimental program worked out for the determination of activation energies for intragranular motion of dislocations using etch pit studies. Experiments will be run to determine the influence of stress and stacking faults in creep near subgrain boundaries.

3.14 Effect of Fast Neutron Irradiation on Plastic Deformation of the B.C.C. Refractory Metals

B. W. Christ

Engineering Metallurgy Section

This investigation was initiated at the National Bureau of Standards on November 2, 1964. The National Bureau of Standards' reactor at Gaithersburg, Maryland, currently in the final stages of construction, figures prominently in this research program.

A comprehensive review of the literature relating to radiation effects on the mechanical properties of the b.c.c. refractory metals has been completed. Laboratory facilities to permit treatment of these materials in the temperature range, 1000-2000°C, and at pressures of 10^{-5} - 10^{-7} mm Hg, are being developed. An experimental investigation of the effect of the interaction between radiation-induced defects and dislocation recovery structures (as revealed by optical and electron microscopy) on tensile deformation at various strain rates in polycrystals and monocrystals is currently being organized. The role of the aforementioned variables in the transition from dutile-to-brittle behavior will be examined. High purity vanadium has been selected as the most appropriate b.c.c. metal for this study.

3.15 Characterization of Electrodeposited Crystals

F. Ogburn
A. de Koranyi

Electrolysis and Metal Deposition Section

Two general shapes of copper crystals were grown electrolytically in acid solutions of cuprous chloride and sodium chloride. These two shapes may be designated as dendrites and approximately equiaxed. By appropriate control of the current, potential, and solution composition, we can grow dendrites of a centimeter or so in length at will or grow clusters of large equiaxed crystals, each such crystal being several millimeters across the shortest dimension. It appears that all the equiaxed crystals and dendrites are twinned, and growth is along the twin plane.

The difference between dendrite and equiaxed crystal growth appears to be one of rate of growth in the plane of the twin boundary. That is, the dendrites grow very much more rapidly than the equiaxed crystals, and this rapid growth is parallel to the twin boundary. Other factors were operating since the growth of an equiaxed crystal could not be changed to dendrite growth even though the reverse change was easily made by reducing the rate of growth for a short time.

Microscopic examination of cross sections of the copper deposits and x-ray diffraction patterns indicate significant amounts of foreign material and misalignment. We have also noted features of the mode of growth which might be explained by the presence of impurities that are absorbed on the copper surfaces.

The current work is directed at eliminating the organic impurities in our copper solutions and working out techniques for testing the purity of our solutions. This will permit comparison of copper crystals grown from ordinary and purified solutions.

The work with lead dendrites reported in Technical Notes 236 and 251 was reported to the Electrochemical Society in October and has been written up for publication (Ogburn, Bechtoldt, Morris and de Koranyi 1965).

3.16 Application of the Kossel Technique to Cubic Materials

H. Yakowitz
D. L. Vieth

Lattice Defects and Microstructures Section

The geometrical factors governing the reduction of a Kossel X-ray microdiffraction pattern to lattice spacing values have been considered in detail. In particular, the proper pattern geometry and orientation yielding the maximum precision and closest approach to accuracy in cubic materials was investigated. The results indicate that conic interactions yielding lens shaped figures on the pattern (Fig. 15) should be used to reduce lattice spacings.

It is found that such "lenses" could be expressed in terms of the wavelength used to excite the pattern, the indices of the conics responsible for the lens shaped figure, the unknown lattice spacing and the angular length of the lens, as (Gielen et al 1965)

$a = f \sec \gamma$ where:

a is the lattice parameter

f is a constant depending on the wavelength and indices

γ is the half-angle of the lens

The reduction of a measured length on the flat film to a true angular dimension has been deduced. It is found that three special cases of lens orientation can be rigorously solved for this gnomonic projection distortion and that obtaining these cases is not is not difficult (Yakowitz 1965). A ratio of lens lengths, $R = L_1/L_2$, is used to reduce the measurements to the final lattice spacing. Using one wavelength, the resultant equations are:

$$a = \frac{\lambda}{u}\left[\frac{vR^2 - w}{R^2 - 1}\right]^{\frac{1}{2}}$$ where:

u, v, and w are numerical constants depending only upon the indices of the conics forming the lines.

From this, one obtains the sensitivity as:

$$\left|\frac{\Delta a}{a}\right| = \left|\frac{R\Delta R\,(w - v)}{(R^2-1)(vR^2 - w)}\right|$$

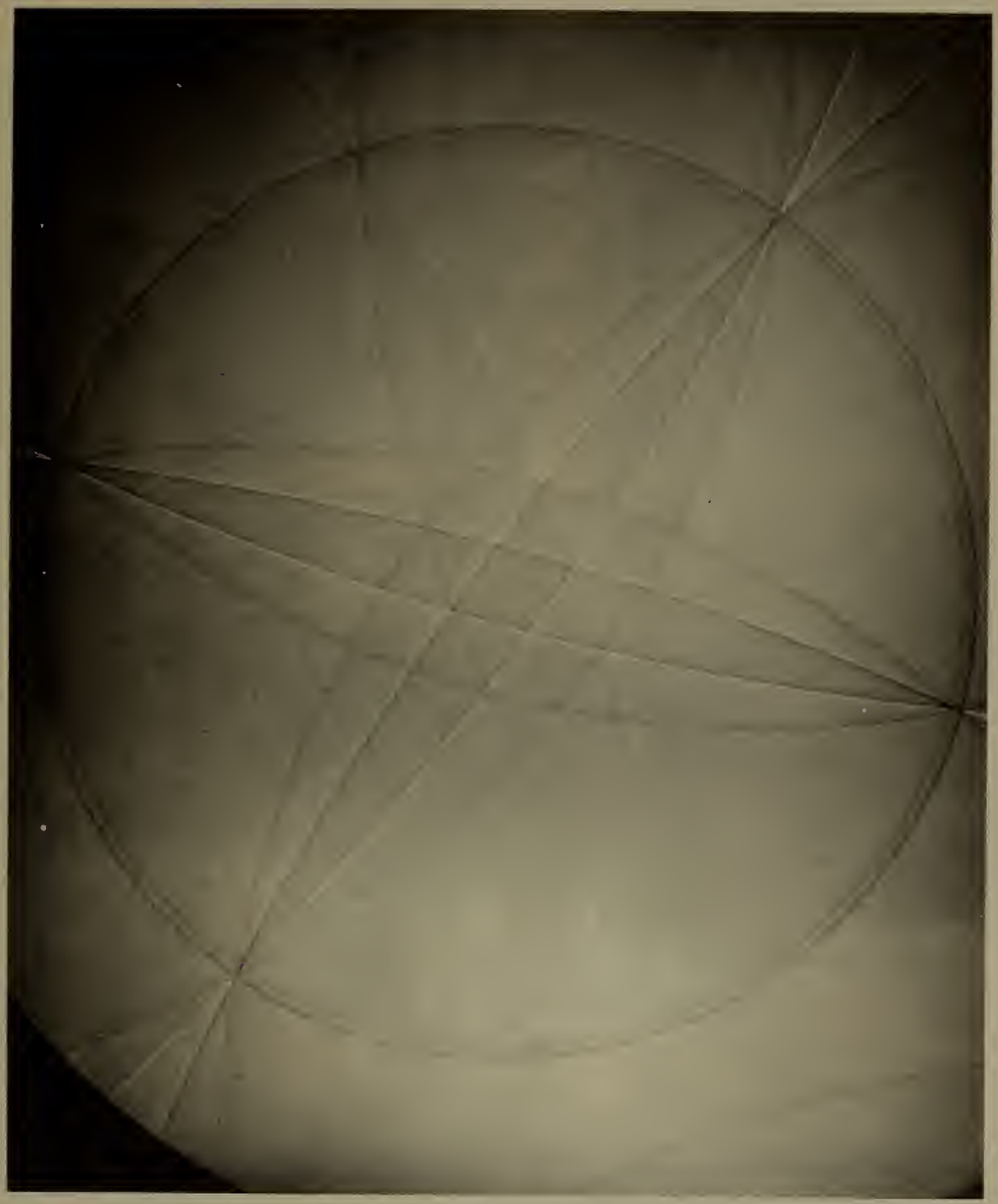

Figure 15. Transmission Kossel pattern of Fe-3w/o Si taken using Fe-K radiation. Sample oriented {110} : [001]. The source was an electron probe microanalyzer beam, ten micron diameter operating at 30 klV.

For LiF, the measured value of the lattice parameter is a = 4.02668A ± 0.000035A, a precision of better than 7 PPM.

In Fe-Si alloys, the {110} : [001] orientation is being studied with a view toward correlating magnetic domain structures with local strains as deduced by the Kossel method. Figure 14 is a transmission pattern of Fe-3%Si showing lenses capable of use for lattice parameter measurement. The value measured for the unstrained alloy is a = 2.86268 Å ± 0.00003 Å, a precision of 10 PPM.

3.17 Study of Crystal Defects

D. J. Barber and N. J. Tighe

Physical Properties Section

and

E. N. Farabaugh

Crystal Chemistry Section

Difficulty in specimen preparation has hitherto prevented the direct study of structural defects in bulk crystals of rutile by electron microscopy. In earlier work, Ashbee, Smallman and Williamson [Proc. Roy. Soc. A, 276, 542 (1964)] and van Landuyt, Gevers and Amelinckx [Phys. Stat. Solidi 7, 307 (1964)] have used TiO_2 samples produced by the oxidation of TiC or Ti metal. A method reported previously in NBS Technical Note 236 has now been used to prepare samples from bulk crystal, and these were examined directly at high temperatures. The results, which include the discovery of a previously unknown slip system <100> {001}, have been submitted for publication (Barber and Farabaugh 1965). Three slip systems are now known for TiO_2.

Optical and etching studies on magnesium fluoride, associated with electron microscope investigations reported in NBS Technical Note 236, have revealed that the slip behavior of MgF_2 closely parallels that of TiO_2. Selective etching of dislocations emerging on {100} and {110} surfaces is produced in hot concentrated sulfuric acid. Etch pits on matched {110} cleavage faces are shown in Figure 16a while Figure 16b shows the distribution of glide dislocations around a 10 gm hardness indentation. It is now known that MgF_2 has the following glide elements: {110} <001>, {001} <100> and $\{01\bar{1}\}$ <011>.

Some earlier work on sapphire crystals (Barber, 1964) has now been published.

3.18 High Voltage Laue X-Ray Photography

B. Paretzkin and H. S. Peiser

Crystal Chemistry Section

A more complete paper on our high-voltage x-ray photography technique (see NBS Technical Notes 174, Section 5.13, 197, Section 3.14, 236, Section 3.16) has now been published (Paretzkin and Peiser, 1964).

The advantage of using fine-focus x-ray tubes has now been demonstrated, but so far such x-ray tubes are not readily available for voltages above 150 kV. For crystals with a thickness-density product in excess of 10g cm^{-2} voltages above 150 kV are required.

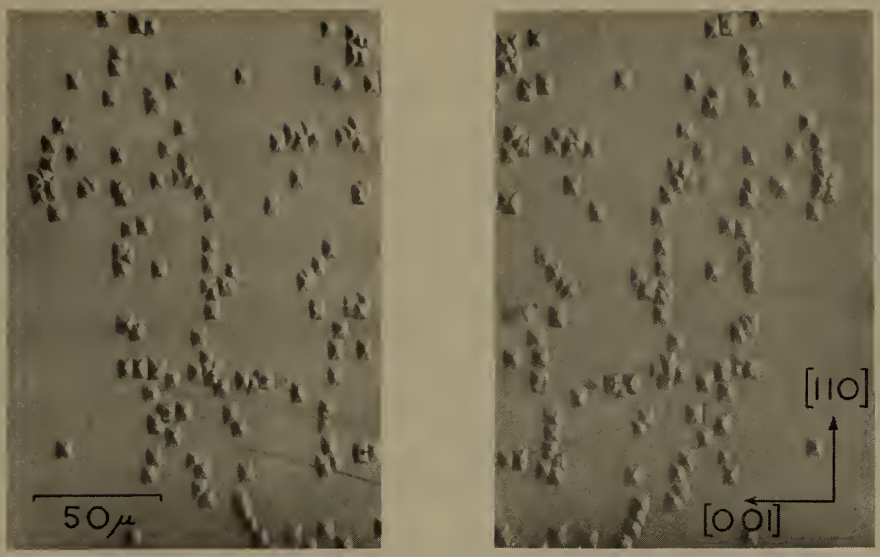

Figure 16a.

Figure 16b.

Figure 16. a). Matching {110} cleavage faces after etching for 12 seconds in sulfuric acid at 200°C.
b). Etch pits at the sites of glide dislocations produced by a 10 gm hardness indentation on a {100} surface.

3.19 Diffraction Topography

R. D. Deslattes and B. Paretzkin

Crystal Chemistry Section

Our work on the diffraction topographic characterization of ammonium dihydrogen phosphate (see NBS Technical Notes 236, Section 3.14, NBS Technical Note 251, Section 3.13) has reached a more or less satisfactory completion (see Section 2.13 of this report). The topographic features tentatively ascribed in previous reports to dislocations have been shown to be in approximate one to one correspondence with etch pits. The latter have been shown to occur at sites of emergent line defects which have in turn been shown to be mobile along preferred directions under stress at elevated temperatures. The association of defect images with edge dislocation is thus possible. When, however, an attempt is made to calculate the shape of the diffraction contours according to the schematic theory of Bonse [Z. Physik 153, 278 (1959)], the results strongly disagree with observations. While the significance of dynamical effects has been noted [U. Bonse, Z. Physic 177, 385, 543 (1964)] this seems to be a situation in which they must be assumed to be dominant. It is hoped to make some initial attempts during the next report period at a formulation of the dynamical theory applicable to defect-occasioned diffraction contrast.

3.20 Effect of Point Defects on the Dynamic Properties of Crystals

J. B. Wachtman, Jr., S. Spinner, S. Marzullo, R. W. Dickson

Physical Properties Section

and

A. D. Franklin

Institute for Materials Research

Mechanical and electrical properties are being studied as a function of temperature and frequency and the results interpreted in terms of chemical impurities and related point defects.

Measurements at frequencies near 2k Hz of internal friction in rutile doped with .1% Ni showed a peak at 40°C with tensile stress along [100] or [110] and a peak at 180°C which occurred with stress along [100] but not with stress along [110]. As mentioned in the last report, these two peaks can be attributed to single interstitial ions and pairs of interstitials respectively. The symmetry arguments supporting this conclusion have been given (Wachtman and Doyle, 1964). This conclusion was supported by the observation that the peak for pairs is still present after vacuum reduction but that the other peak was not. Recent observations show that upon reoxidization in stages the peak for isolated interstitials reappears and grows at the expense of the peak for pairs. It is thus reasonable to assume that Ni is predominantly in interstitial sites and forms pairs with interstitial titanium ions when these are introduced by vacuum reduction.

Recent measurements on TiO_2 doped with .05% Cr show very similar behavior. Two peaks are again seen in lightly reduced specimens; the peak for isolated interstitials grows with reoxidization and the peak for pairs can be made unobservably small by heating in one atmosphere O_2 at 800°C. In Ni doped rutile the same heat treatment does not completely remove the peak for pairs; this result suggests a tighter binding for Ni-Ti pairs than for Cr-Ti pairs.

This simple model of interstitial ions in rutile agrees with spin resonance evidence for Ni and Ti but is in conflict with the claim that Cr ions do not go into interstitial sites but substitute for Ti ions in normal structural sites. It may be that some defect model associated with substitutional Cr could give the observed orientation dependence of the internal friction but none has yet been devised. The close parallel with the behavior of Ni doped rutile supports the idea of interstitial Cr and suggests that the spin resonance evidence should be reexamined.

Work on the dielectric relaxation associated with small amounts of CaO in solid solution in ThO_2 was continued. Analysis of the dispersion of ϵ' and ϵ'' due to the point defect associated with Ca (presumably a dipole consisting of substitutional Ca paired with an oxygen vacancy) is complicated by the fact that the background contribution of these quantities does not have the simple frequency dependence associated with finite direct current conductivity. It was suspected that this effect might be associated with grain boundaries (single crystals of ThO_2 doped with CaO are not available). Measurements on undoped polycrystalline ThO_2 support this belief; a very broad dispersion was found which did not occur in undoped single crystals. This broad dispersion is itself superimposed upon a low frequency dispersion in ϵ' which is also seen in undoped single crystals and which may be a surface layer effect. The effect of specimen thickness and dc bias is being investigated.

These background effects are interesting in themselves, but better quantitative description is also desirable to permit improved analysis of the dipole relaxation effect. The latter is well described by a Debye function at 240°C but preliminary analysis based on fitting a Fuoss-Kirkwood function indicates a broadening of the relaxation as the temperature is increased to 309°C. This effect is surprising but might result from additional modes associated with second nearest and more distant sites as discussed for the rock salt structure (Franklin, Shorb, and Wachtman, 1964).

The relaxation mode analysis mentioned above has been applied to the calculation of correlation coefficients for diffusion of impurity ions by a point-defect mechanism in crystals. Tracer diffusion can be handled readily and neatly with results in precise agreement with those obtained earlier by Compaan and Haven [Trans. Faraday Soc. 52, 786 (1956)]. For impurity diffusion, the formalism is the same, but the computer problem is more difficult. Work on solving this problem is proceeding in collaboration with R. C. F. McLatchie, at Harwell.

The intensity of the relaxation associated with coupled point defects is usually treated by simple Debye theory, with no internal field effects. However, recent experimental results ascribed to vacancy pairs in KCl by Sastry and Scrinivasan [Phys. Rev. 132, 2445 (1963)] and Economou [Phys. Rev. 135, A1020 (1964)] have cast doubt upon this treatment. It has been shown (Boswarva and Franklin, 1965) that indeed internal field effects should be included. For impurity-vacancy pairs they may not be significant, but for vacancy pairs they can introduce a factor of 2 or 3 in the intensity.

3.21 Formation Energies of Point Defects in CaF_2

A. D. Franklin

Institute for Materials Research

The Born model of the ionic solid is being used to calculate the formation energies of various point defects in CaF_2.

Repulsive parameters were chosen that successfully reproduced the interatomic spacing, elastic constants, and static dielectric constant of CaF_2. Using these constants, preliminary calculations were made of the energy of insertion of an F^- ion

from infinity into an interstitial site, and the energy of removal of an F^- ion from a lattice site to infinity, leaving an F^- vacancy. The resulting numbers (Franklin, 1965) are

Interstitial Energy	-1.6 ev
Vacancy Energy	4.3 ev
	2.7 ev

The sum is satisfactorily close to the experimental value of 2.8 ev of Ure [J. Chem. Phys. 26, 1363 (1957)].

In this preliminary calculation, the relaxation of only the ions immediately adjacent to the defect was considered explicitly, that of the second shell being handled by an approximation. Work has proceeded on writing expressions for the energy including explicit relaxation of two shells of neighbors, and incorporating other refinements. A computer program to find the minimum energy will be written, and used to find the energy of insertion of F^-, Na^+, and Ca^{2+} interstitials, Na^+ and Y^{3+} substitutionals, and creation of F^- and Ca^{2+} vacancies.

3.22 Laser Probe for Micro-analysis

B. F. Scribner
M. Margoshes

and

S. D. Rasberry

Spectrochemical Analysis Section

A description of a laser probe for analysis of small samples was given in NBS Technical Note 197, Section 3.10; and a discussion of single-spike output operation of the laser was presented in NBS Technical Note 251, Section 3.9. In the past six months the factors which govern the precision of quantitative chemical analysis with the laser probe have been under investigation.

The reproducibility of the peak power output of the laser in single spike operation was investigated. A coefficient of variation of 9% was observed, on the basis of two groups of observations, each containing 12 successive laser bursts. Single-spike operation is obtained only with a sacrifice in total energy output, consequently a smaller amount of material is vaporized than if multiple-spike operation were employed. Single-spike operation produces spectra having lower intensity; however, due to the consistency in output the spectra are more reproducible. The reproducibilities of intensity ratios of spectral line pairs were measured. Lines having well matched excitation potentials gave ratios with coefficients of variation as low as 4 to 6% in one set of 14 measurements and four sets of 11 measurements. Currently, improvements are being made in the recording and photometry of the laser probe spectra in order to improve the precision of the overall method. The precision and accuracy of analysis for a variety of matrices are currently being examined using the laser probe in multiple-spike as well as single-spike operation.

In addition to studies of the aspects of quantitative analysis with the laser probe and application of it to several qualitative analysis problems, the laser probe has been used to melt small regions on a single-crystal silicon wafer in a controlled manner. This work was undertaken at the request of H. A. Schafft and N. Winogradoff, of the Electron Devices Section in an effort to simulate the strains produced in single-crystal semiconductors during second breakdown. (See NBS Technical Note 251, Section 3.10). A melt zone of 5μ diameter was achieved on a single-crystal silicon wafer by attenuation of the single-spike laser beam with a Schott BG-3 filter, which transmits 10^{-5} of incident 6943Å light, coupled with a 50%T filter. These filters reduced the peak power incident at the wafer from 3×10^{13} watts/cm^2 to 15×10^7 watts/cm^2, and the effect on the wafer was to reduce the affected zone. nominally a crater 40μ diameter by 20μ deep, to a melt zone 5μ in diameter.

3.23 Diffusion in Solids

J. R. Manning

Metal Physics Section

When diffusion occurs by a vacancy mechanism, the individual atoms do not follow a random walk. As a result, a "correlation factor" must be introduced into the diffusion equations. In recent work under this project, the correlation factors for dilute impurities in body-centered cubic, face-centered cubic and diamond structures were calculated in terms of the vacancy jump frequencies near an impurity. Jump frequencies for both association and dissociation of bound vacancy-impurity complexes were explicitly included. It was found that the re-association jumps considerably affect the expressions for the correlation factor.

Because of correlation effects, accurate kinetic equations for diffusion in a driving force have been difficult to obtain. This difficulty was overcome by considering planar diffusion along particular crystallographic directions and using the idea of effective jump frequencies. With this approach, accurate kinetic equations having the same form as those for a one-dimensional random walk were obtained. These equations can easily be modified to treat diffusion in a driving force. Final results, including effects from a driving force, are accurate to first order in small quantities. (Manning, 1964).

3.24 Evidence for Inclusion of Perfluoromethyl Groups In the Lattice of Copolymers of Tetrafluoroethylene and Hexafluoropropylene

R. K. Eby

Polymer Physics Section

L. H. Bolz

Physical Properties Section

Earlier measurements of the lattice parameters of tetrafluoroethylene-hexafluoropropylene copolymers (Eby and Bolz, Technical Note 236, Section 5.13) have been extended. Results obtained at room temperature with samples of very nearly the same lamella thickness but different concentrations of perfluoromethyl groups show a

significant increase of lattice size with increasing concentration of perfluoromethyl groups. On the other hand, results for samples with the same concentration of perfluoromethyl groups but different lamella thicknesses show no significant variation of lattice with thickness (i.e., the variation is zero within our experimental limits). These results indicate that the larger lattice in the copolymers is not an artifact associated with lamella thickness but is the consequence of inclusion of perfluoromethyl group in the lattice. Such a conclusion is supported by the diffuseness of (h 0 l) and (0 0 l) reflections in the copolymer. These reflections, which are relatively sharp for polytetrafluoroethylene below 300°K, remain much more diffuse for the copolymer even at 78°K. This result is consistent with the presence of small rotational and longitudinal disordering of the molecules in the copolymer [E. S. Clark and L. T. Muus, Z. f. Kristallographie 117, 213, 109 (1962)]. This effect would be expected from inclusion of perfluoromethyl groups in the lattice.

3.25 Magnetic Resonance Studies

T. Chang, R. A. Forman, and R. C. Frisch

Solid State Physics Section

The work of the group can be divided into two major categories, electron paramagnetic resonance and nuclear magnetic resonance.

(a) Electron Paramagnetic Resonance

The work on the EPR spectrum of Mo^{5+} in rutile was concluded. An article about this was published (T. Chang, 1964). The study of line shape and the measurement of relaxation time are in progress.

The EPR spectrum of W^{5+} in rutile has been observed. The characteristic appearance of the W^{5+} spectrum is analogous to that of the Mo^{5+} spectrum. This indicates that the electronic configuration ($5d^1$) and the crystalline environment are similar (c.f. NBS Technical Note No. 251, p. 38). The crystal had been carefully oxidized and was used as its own cavity. Because of the high dielectric constant and the high resistivity, the cavity has a very high Q (~ 200,000 at 20°K). Much finer details were observed. The spectrum shows resonance lines due to the interaction of the electron wave function not only with nuclear spin of I = 0, I = ±1/2, and with neighboring Ti nuclei, but also with some unidentified centers. So a number of weak lines cannot be explained. Forbidden transitions, or clusters of W^{5+} ions, or modulation interference were suspected, but no conclusion could be drawn.

(b) Nuclear Resonance

Measurements have been made on the N^{14} NMR in $NaNO_3$ at room temperature. Preliminary results yield a quadrupole coupling constant of 775 kHz. A study of the temperature dependence of the quadrupole coupling constant in this material as a function of temperature is in preparation. The purpose is to study the λ-transition at 275°C.

As the quadrupole interactions of titanium are presently unknown, a large number of titanium samples are being investigated. To date we have been unable to observe the titanium NMR in Ti (metal), TiO, Ti_2O_3, TiN. The Knight-shifted titanium NMR has been observed in TiH_2 and a study of it is currently in progress. In addition, the Knight-shifted N^{14} resonance in TiN has been observed and is being studied.

3.26 Magnetic Resonance Studies

L. M. Matarrese, J. S. Wells,
R. L. Peterson, and A. R. Cook

Radio and Microwave Materials Section

The zero-field splittings of the $^6S_{5/2}$ level of ferric ion in quartz have been measured directly, in order to check the values derived from the spin Hamiltonian (which was deduced from high-field measurements). The measured values are 7113 and 8812 MHz and the theoretical values are 7117 and 8764 MHz, respectively. This is very good agreement and confirms our analysis of the spectrum.

The technique used was very simple. A regular X-band spectrometer with tunable cavity and klystron was used, but the field was swept through zero. The frequency of the cavity was adjusted until the two resonances occurring at $-H_{res}$ and $+H_{res}$ came together at the center of the trace, and this frequency was recorded as the zero-field resonance frequency, i.e., the zero-field splitting in frequency units.

In the course of these measurements, two interesting effects were discovered. The intensity of the zero-field resonance, particular the one at 8812 MHz, depended strongly on the direction of the rf field (maintained perpendicular to the sweeping field) relative to the crystal. A theoretical analysis of the transition probabilities shows that such behavior is indeed expected, and that the direction of the crystal field axes can be unequivocally determined from such an experiment. The second effect was the absence of certain of the $\Delta M = c$ low-field transitions. A tentative explanation for this depends on the lower level involved in the transition lying very close in energy to the other level of the same Kramers doublet, from which a transition to the upper level is strictly forbidden. Spin-phonon interaction may cause relaxation into this latter level, from which transitions can no longer be excited, thus causing disappearance of the line. There is such a closely spaced pair of levels in the energy level diagram for ferric ion in quartz, and the requirement that it lie lowest forces the conclusion that the sign of D is positive. If the theory is correct, this appears to be a method of determining the sign of D without going to very low temperatures.

Low temperature and ENDOR experiments are still being planned on iron-doped quartz. We have also begun experiments on cobalt-doped quartz.

The AFMR experiments on $CuSO_4$ and $NiBr_2$ are being delayed by the necessity of constructing a cryogenic system that will precisely maintain sample temperatures in the range 4 to 60°K.

Measurements of spin-lattice relaxation times of dilute potassium ferricyanide, $K_3[(Co,Fe)CN_6]$, are in progress in order to check the effect of finite lattice heat capacity.

3.27 Use of Single Crystals of Disodium Pentacyanonitrosoferrate Dihydrate (Sodium Nitroprusside) as a Standard Reference Material for Mössbauer Spectroscopy

J. J. Spijkerman, F. C. Ruegg and J. R. DeVoe

Radiochemical Analysis Section

The recent advances in the application of the Mössbauer Effect in analytical and structural chemistry, as well as in solid state physics necessitates standardization to provide a uniform basis for comparison of data from various laboratories and to provide reference tables of Mössbauer Spectra.

Since the energy state of an atomic nucleus is altered by its chemical or crystal environment, and since these energy changes (chemical shifts) can only be compared, rather than measured absolutely, NBS will provide single crystals of nitroprusside for standardization of the differential chemical shift.

The sodium nitroprusside crystallizes [P. W. Cooke, Nature 157, 518 (1946)] in the bipyramidal class D2h, or mmm of the orthorhombic system. The forms exhibited are the [110] primary rhombic prism, the [010] brachydomal prism. The crystals are needles along the C-axis, with a =11.8A, b = 15.52A, c = 6.22A. There are two n glides of components (a/2)+(b/2)+(c/2). The space group is D_{2h}^{12} or Pnmn, with 4 molecules per unit cell

Due to molecular assymmetry, the Mössbauer Effect shows quadrupole splitting. The center of the doublet (shown in Fig. 17) is defined as the zero differential chemical shift for Fe^{57}.

4. PHYSICAL PROPERTIES OF CRYSTALLINE MATERIAL

This chapter is concerned with the physical properties of crystalline material where crystal perfection is not a primary consideration.

4.1 Crystal Orientation Methods*

E. N. Farabaugh and P. R. Miller

Crystal Chemistry Section

Modifications of the standard Laue back-reflection technique and the psuedo-Kossel method are being studied to determine which of these diffraction techniques is most suitable for quick and precise orientation of large single crystals.

A pseudo-Kossel line back-reflection pattern of TiO_2 is shown in Figure 18. The TiO_2 specimen was orientated with (100) planes parallel to the film.

In this laboratory the development of competence in the pseudo-Kossel technique has the attraction arising from the applicability of this technique to measurement of:·(1) lattice parameters in large crystals to high accuracy, (2) elastic or plastic strain within small subgrain, (3) the range of misorientations within a crystal.

---

* This work is partially supported by the Atomic Energy Commission.

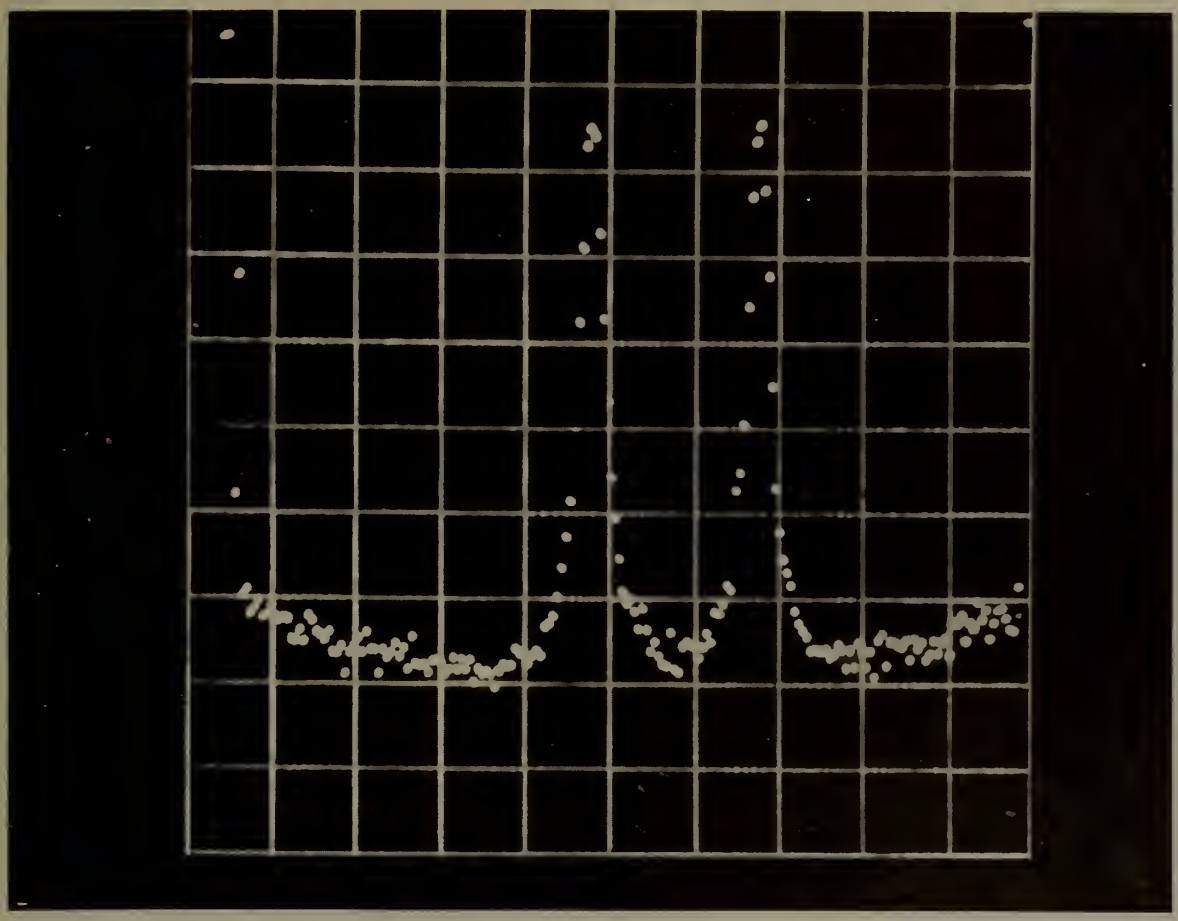

Figure 17. Mossbauer Effect Spectrum of Disodium Pentacyanonitrosoferrate Dihydrate. The number of 14.4 Kev photons vs. the energy difference (4.25×10^{-8} eV/division), with zero at the center of the doublet.

Figure 18. Back-reflection pseudo-Kossel line pattern from TiO_2.

4.2 Crystal Symmetry and Crystal Properties

J. B. Wachtman, Jr.

Physical Properties Section

and

H. S. Peiser

Crystal Chemistry Section

The application of homogeneous stress to a crystal causes a lowering of symmetry in general with the result that atoms which originally had the same energy levels may become non-equivalent and have different energy levels. Every such transformation from an initial group to a final group can be expressed as a succession of minimum steps each of which leads to a group which is a subgroup of the initial group, a super-group of the final group and is distinct from both the initial and final groups. There are 12 such minimum steps for centrosymmetric point groups and 25 for noncentrosymmetric point groups. The results for loss of equivalence of sites in space groups can thus be collected into 37 tables according to the point group associated with each of the space groups. These tables can be simplified by listing only the behavior of the general position (see NBS Technical Note 251, Section 4.2). The resulting tables for all centrosymmetric space groups have been given (Wachtman and Peiser, 1965) together with a discussion of the method of using these results to determine the behavior of special positions. Results have also been derived for all the noncentrosymmetric space groups and are being compiled for publication. A set of stereograms which are useful in visualizing the results for general positions and in carrying out the process of specialization has been prepared.

4.3 Studies in Solid-State Theory

A. H. Kahn

Solid State Physics Section

The investigation of the electronic energy-bands of cuprous oxide by the tight binding approximation is in progress.

4.4 Seebeck Effect and Thermal Conductivity of Semiconductors*

W. R. Thurber and A. J. H. Mante†

Solid State Physics Section

The thermal conductivity K and the thermoelectric power Q of single crystal samples of rutile (TiO_2) were measured from 2 to 300°K. Pure, niobium-doped, vacuum-reduced, and hydrogen-reduced specimens were investigated. The thermal conductivity of the pure crystals is similar to that usually found for insulators with a maximum at about 15°K. Boundary scattering determines K below the maximum and in the range 25 to 100°K the conductivity varies exponentially with temperature which is characteristic of Umklapp scattering. The Callaway expression for K was used to fit the data over the entire temperature range. From measurements in both the c and an a direction, it was found that the anisotropy ratio $K_c/K_a = 1.5 \pm .1$ above 25°K. The ratio decreases

---

* This work was supported in part by the U. S. Office of Naval Research.

† NATO Fellow, 1964; (present address: Department of Physics, University of Utrecht, Netherlands).

below 25°K to a limiting value of 1.05 ± .1. A sample doped with 0.1% Nb has thermal conductivity quite similar to the pure TiO_2. The K of the reduced samples is strongly depressed at low temperatures and not well understood at present. On oxidation of a reduced sample it was discovered that the thermal conductivity did not recover completely to the original values measured on the same specimen before reduction. For one crystal a comparison of K in the reduced and reoxidized states yields values for the extra thermal resistance which are compatible with the number of point defects introduced by the reduction. The thermoelectric power of the semiconducting samples (Nb doped and reduced) increases rapidly below 100°K indicating a large phonon drag contribution.

4.5 Photoconductivity of Semiconductors*

L. H. Grabner

Solid State Physics Section

The investigation of the quenching of photoconductivity in CdS near the band-edge is completed and has been written up for publication. (Grabner, 1965). Photoemission and photoconductivity studies as a function of temperature showed that the quenching sets in at approximately 70°K. This coupled with coincidence of an emission line with the quenching band has led to the following interpretation: irradiation with "quenching" radiation at the energy of a bound exciton leads to the creation of an exciton complex, at sufficiently high temperatures the hole of the exciton complex thermally ionizes into the valence band. The free hole then recombines with a trapped electron. The emptied trap is then able to capture a free electron leading to a decrease of photocurrent. The exciton complex responsible has not been reported previously. It has a binding energy of 0.040 eV.

---

* This work was supported in part by the U. S. Office of Naval Research.

4.6 Research on Superconducting Semi-conductors

J. F. Schooley and E. Ambler
Cryogenic Physics Section

and

W. R. Hosler and H. P. R. Frederikse
Solid State Physics Section

The work discussed in Article 4.21 of Technical Note 251 was continued. The dependence of transition temperature on charge carrier concentration, n_c, has been examined over the range of $n_c = 10^{18}$ cm^{-3} to 10^{21} cm^{-3} and for temperatures as low as 0.05°K. A strong maximum occurs at $n_c \sim 10^{20}$ and $T_c \sim 0.4$°K. In other experiments, the dependence of transition temperature on uniaxial pressures up to 200 atm. has been briefly examined. Shifts in T_c of approximately $-0.1T_c$ have been observed for specimens in which uniaxial stress was applied along the 100 or the 110 crystallographic directions, whereas no shift was observed in specimens stressed in the 111 direction. Interpretation of these results is in progress, and it follows the theoretical treatments of A. H. Kahn and A. J. Leyendecker (Phys. Rev. 135, A1321 (1964)

and M. L. Cohen (Phys. Rev. 134, A511 (1964). Another experiment, in which the resistive transition was observed in magnetic fields up to 3 koe, indicates a gradual return of normal specimen resistivity over a substantial region of magnetic field. This effect will be investigated further in the coming year.

Finally, preliminary measurements have been made of the magnetic field dependence of the magnetic moment. The specimen examined was found to have a first critical field of about 1 oersted and a second critical field in excess of 100 oersted at $T \sim 0.3T_c$, and magnetic hysteresis was shown to be present. A sensitive magnetometer is under construction so that precise data of this type can be obtained.

4.7 Resistivity and Hall Effect of Semiconductors

H. P. R. Frederikse
W. R. Hosler
J. H. Becker
R. C. Keezer
R. A. Forman

Solid State Physics Section

During this period a considerable effort was spent on the reconstruction and modification of an apparatus for measuring the piezoresistance of $SrTiO_3$. The original equipment had been designed for experiments on InSb using small stresses (10^7 dynes/cm^2); the present investigation requires stresses about 20 to 40 times larger.

In order to check the pressure exerted on the specimens, a number of commercial strain gauges (including some designed for very low temperatures) were tested. It appeared that these gauges did not measure up to expectations. Recent experiments indicate that Sb-doped germanium (concentration of impurities $\sim 10^{16}$ - 10^{17}/cc) will be very useful as a stress indicator in the liquid helium range of temperatures [Fritzsche, H., Phys. Rev. 125, 1552 (1962)].

A large number of $SrTiO_3$, $BaTiO_3$ and MoO_3 samples (both bulk and powder) with different electron concentrations were prepared to be tested for superconductivity below 1°K (see Section 4.6).

Electrical characteristics of bulk samples of these materials were measured between 1 and 300°K. In spite of concentrated efforts no Hall effect has been measured on MoO_3 or $BaTiO_3$ samples (except for one reading on the latter substance, which indicates an electron mobility of 0.1 cm^2/volt-sec at room temperature.).

$SrTiO_3$ samples were prepared with donor concentrations between 10^{17} and 10^{21}/cc; this wide range appeared to be essential for the study of the superconducting transition temperature as a function of carrier concentration.

The analysis of conductivity and Hall effect data obtained from measurements on semiconducting TiO_2 (rutile) has been completed and the existence of multiple conduction bands has been proven. This work has been accepted for publication, (Becker and Hosler 1965).

4.8 Optical Constants of Iron Single Crystal Surfaces in the Visible Region

H. T. Yolken
J. Kruger

Corrosion Section

The optical constants of clean iron single crystal surfaces maintained in an ultra-high vacuum were determined. An ellipsometric technique was used to determine values of the optical constants as a function of wavelength in the region of 3600 Å to 7000 Å.

In Fig. a and b, in the real part of the dielectric constant $n^2(1 - \kappa^2)$, ϵ_1, and the imaginary part $2n^2\kappa$, ϵ_2, from both our data and from that of previous workers are plotted on a logarithmic scale as a function of wavelength. In Figure 19 where ϵ_1 is plotted it can be clearly seen that the iron surface prepared by ultra-high vacuum techniques shows the most marked minimum. A maximum at 4900 Å in the conductivity versus wavelength (Fig. 20) curve indicates the presence of an interband transmtion.

A paper describing this work has been prepared (Yolken and Kruger, 1965).

4.9 Enthalpy Measurements to 2800°K

E. D. West
S. Ishihara

Heat Measurements Section

A new apparatus is now in operation for enthalpy measurements on condensed phases in the temperature range 1200-2800°K. Measurements have been completed on a very pure graphite, (Grade CCH). Measurements are planned on pure specimens of Mo, W, MgO, ThO, Al_2O_3, and B. The work on the enthalpy of graphite has been published (West and Ishihara, 1965)

4.10 Soft X-Ray Spectroscopy

R. D. Deslattes

Crystal Chemistry Section

Owing to the continued lack of good crystals of potassium acid phthalate either from outside sources or from in-house activities (cf. Section 2.13 of this report) we have again had to postpone any attack on the main present objectives of this program. These objectives are to obtain precise measurements of the profiles of the absorption spectra and valence emission bands of metallic sodium, gaseous and solid neon, and of sodium and fluorine in NaF.

In the meanwhile the high (though short-lived) resolving power of ammonium dihydrogen phosphate crystals out to 10 Å has been exploited in a careful restudy of the L absorption fine structure of krypton and in preliminary reexamination of the K absorption spectra of aluminum and alumina. The latter seems particularly interesting, since in anodically prepared specimens the fine-structure amplitude is rather less than that of aluminum metal. This is in sharp contrast to the usual situation. Our hypothesis is that this anomaly is due to the "amorphous" character of anodically

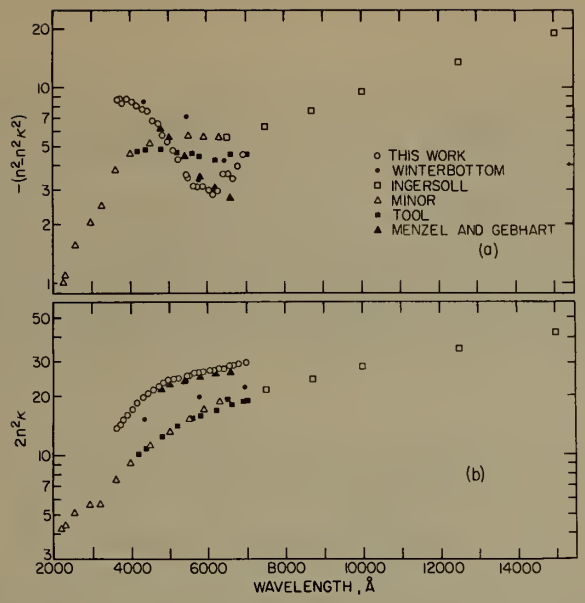

Figure 19. a. The real part of the dielectric constant, $n^2(1-\kappa^2)$ on a logarithmic scale versus wavelength for iron.

b. The imaginary part of the dielectric constant, $2n^2\kappa$ on a logarithmic scale versus wavelength for iron.

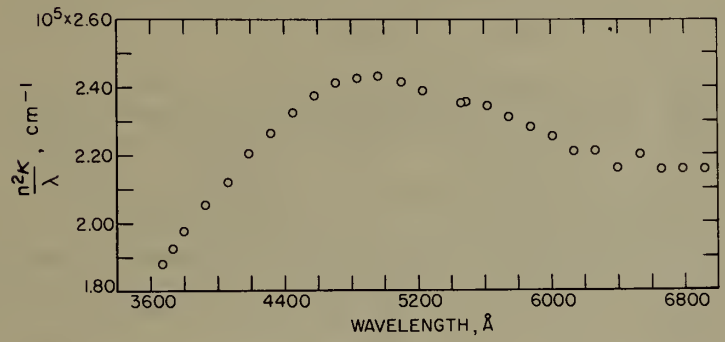

Figure 20. The frequency dependent conductivity, $n^2\kappa/\lambda$, versus wavelength for iron.

prepared films. Accordingly, the spectra effects of recrystallization of prolonged exposure to elevated temperatures will be studied during the next report period.

In addition, it is planned to devote some time to investigation of the revelance of short-range order theories of the long range fine structure in absorption spectra. To this end careful measurements of the K absorption fine structure of sulphur in SF_6 are planned (cf. Section 4.11 of this report). These will offer a much more definitive comparison with the theory of Hartree, Kronig and Petersen [D. R. Hartree, R. De L. Kronig and H. Petersen, Physica I, 895 (1934)] than has been previously possible.

4.11 Optical Constants of Materials from 1 to 1000 Rydbergs

R. E. LaVilla and R. D. Deslattes

Crystal Chemistry Section

The objectives of this new project have been set forth in the previous report (see NBS Technical Note 251, Section 4.5). Various designs for different components of the single-crystal vacuum spectrometer for absorption measurements in the 20-200 Å range on ultra-pure materials have been developed and assessed.

A further investigation of errors in the analysis of available optical data up to about 3 Rydbergs has been conducted for germanium, silicon, and beryllium.

4.12 Silicon Density and the Scale of X-Ray Wavelengths

Horace A. Bowman

Mass and Volume Section

Richard D. Deslattes and Boris Paretzkin

Crystal Chemistry Section

We have undertaken to repeat independently the recent work of Henins and Bearden [Phys. Rev. 135, A890 (1964)] in which the x-ray wavelength scale was successfully related to the density of silicon and thus established with a probable error of 5 ppm. Our motivations are: (1) an experiment of such fundamental importance is well served by an independent repetition, (2) silicon of higher perfection than that used in the above experiment has become available, (3) a density comparator of considerably increased precision has been made operative [H. A. Bowman, to be published], (4) it has become possible to eliminate the uncertainties associated with assigning a density to water and to relate the density of silicon directly to that of N.P.L. mercury, which was determined by volumetry and weighing [A. H. Cook and N. W. B. Stone, Phil. Trans. Roy. Soc., London, 250A, 279 (1957)].

In anticipation of this work, and for subsequently planned investigation of absolute lattice parameters and x-ray wavelengths, the double crystal diffraction apparatus (see Section 4.10 of this report) has been equipped with an absolute angle generator of high accuracy. This generator as received from its manufacturer (and unmounted) had a claimed accuracy of ± 1/4 arc second. It has been calibrated in its required mounting many times over the past six months by the NBS Metrology Division*.

---

* We are extremely grateful to D. B. Spangenberg for this very special calibration.

An error curve has been obtained such that any point on the angle generator can be corrected to a true angular reading within 0.3 arc second (3 σ limit).

Two principal problems have been encountered toward the end of the report period, one or both of which are likely to persist as dominant concern over the next period. The first and most fundamental is: With what precision can this material which we call silicon be assigned a density? The problems here are manifold: isotopic abundance, chemical purity, perfection, wetting by the comparator water, and so forth. Not the least of these is the recent discovery of a strong diffraction contrast image in a topograph of a "dislocation-free" specimen.

The second question is one of alignment of the double crystal diffraction apparatus with a precision which will not degrade the precision required of the angular measurements. Bearden, J. A., et al, [Phys. Rev. 135, A890 (1964)] have described a procedure which depends on two things (a 1 second tilting level and an instrument whose axis can be made parallel to local gravity with the same precision) which are not readily available to us. We are therefore trying to formulate an alignment procedure of comparable precision which can be entirely carried out with the existing instrument and without involving the direction of local gravity. One such procedure has been devised and its evaluation will be reported on in future NBS Technical Notes.

4.13. Hall-Effect Measurements*

S. Rubin

Engineering Electronics Section

The objective of this project, as indicated in NBS Technical Note 251, Section 4.6, is the establishment of standardized terminology and measuring methods for galvanomagnetic (Hall effect and magnetoresistive) devices.

The first international standard on Hall effect device terminology was issued in the form of a Secretariat document by TC 47 of the International Electrotechnical Commission in September of 1964. S. Rubin represented the United States on the special task group which drew up the document and which is continuing work in ratings, characteristics, and measuring methods. The proposed military standard on Hall effect devices (originally Hall generators) was revised to conform with the TC 47 document.

A transistorized magnetic flux density meter using electron spin resonance was built, but its operation was marginal. An improved version, modified to allow determination of the effect of sample orientation on meter reading, is in the process of construction. The unit is designed for tunable operation, using plug-in heads, in the range from 1 to 25 millitesla (10 to 250 gauss). Initial operation was in the 17 to 20 millitesla range.

---

* This work was supported by the Bureau of Naval Weapons.

4.14 Reference Data on Single-Crystal Elastic Constants

J. B. Wachtman, Jr., S. Spinner, and R. W. Dickson

Physical Properties Section

Elastic constants of inorganic single crystals are being determined as a basic physical property when suitable single crystals become available. Four elastic compliances of rutile have been measured from room temperature to 1000°C (Spinner and Wachtman, 1964) to augment the complete set of six compliances previously determined at room temperature [J. B. Wachtman, Jr., W. E. Tefft, and D. G. Lam, Jr., J. Research NBS 66A, 465 (1962)]. Rutile has point group 4/mmm and so belongs to the higher symmetry division of the tetragonal crystal system. The complete set of six compliances for several other crystals of this division have been determined by other workers, but the complete set of seven elastic compliances for a crystal of the lower symmetry division apparently has never been determined. The existence of a nonvanishing s_{16} complicates the measurements and analysis for this case. The equations for a thin-rod resonance technique have been worked out; this method offers an advantage over the ultrasonic method in that all equations are linear and no sign ambiguities arise. A set of specimens of $CaMoO_4$ (point group 4/m, lower symmetry tetragonal) has been obtained from W. S. Brower, of the Crystal Chemistry Section, and measurements are underway.

4.15 Deformation and Fracture of Ionic Crystals

S. M. Wiederhorn and R. L. Moses

Physical Properties Section

The fracture surface energy of soda-lime glass is being studied as a preliminary step to making such measurements on non-cleavable ionic crystals. The double-cantilever cleavage technique, first developed by Gilman [J. Appl. Phys., 31, 2208 (1960)] and by Westwood and Hitch [J. Appl. Phys., 34, 3085 (1963)], was modified and used to measure the fracture surface energy of soda-lime glass at temperatures of 77°K, 195°K and 300°K in various media. Values obtained for the fracture surface energy were 3.20 joules/meter^2 in $N_2(\ell)$, 3.10 joules/meter^2 in toluene (ℓ)-CO_2(s) and 2.83 joules/meter^2 in dry N_2(g). Although these values are reasonable, they are greater than theoretically predicted. The difference may be due to irreversible effects at the crack tip during fracture. A theoretical estimate of the strength of glass, 5.6×10^6 psi, was obtained by substituting the measured value of the fracture surface energy into the Griffith equation ["Theory of Rupture," Proc. First Intern. Cong. Appl. Mechanics, Delft., pp 55-63 (1924)]. This value is high and may mark an upper limit for the strength of glass.

Fracture was observed to occur in two stages, an initial stage during which velocities were less than 10^{-4} meters/sec and a catastrophic stage during which the velocity increased very rapidly. The initial stage of fracture was attributed to stress corrosion or statistical fluctuations at the crack tip, depending on the environment. The catastrophic stage was believed to be dynamically controlled. The double-cantilever cleavage technique was found to be an excellent method for studying stress-corrosion in soda-lime glass and it is felt that the technique could be applied to study stress-corrosion in other materials. A complete description of the above work is to be published, (Wiederhorn, 1964).

Further experiments are planned on glass. We are presently measuring the activation energy for crack motion in soda-lime glass in an aqueous environment. Preliminary measurements yield a value for the activation energy of approximately 20 kcal/mole. This value is close to the activation energy for Na^+ diffusion in soda-lime glass, 18.7 kcal [J. R. Johnson, R. H. Bristow and H. H. Blau, J. Am. Ceram. Soc. 34, 165 (1951)], and suggests the diffusion of Na^+ as the limiting rate process for the fracture of glass, proposed by Charles [Prog. in Ceram. Sci., 1, edt. J. E. Burke, Pergamon Press, New York (1961)]. We also plan to measure the fracture surface energy of several different types of glasses to determine the effect of composition and elastic modulus on the fracture surface energy of glass.

4.16 Velocity of Sound in Ice Single Crystals*

T. M. Proctor

Sound Section

Since the last report the first ice data have been obtained. The longitudinal velocity of sound V_3 in an ice single crystal has been measured from -30 to -240°C. V_3 is the velocity associated with propagation along the Z axis of the hexagonal ice structure and is related to the elastic constant C_{33} as follows:

$$C_{33} = V_3^2 \rho$$

where ρ is the density.

Figure 21 shows the values of C_{33} versus temperature and is compared to recently published data by A. Zarembovitch and A. Kahane, C. R. Acad. Sci. Paris t.258 (2 Mar. 1965) Group 6, p. 2529, and V. V. Bogorodskii, Soviet Phys. Acoustic, Vol. 10 (2), Oct.-Dec. 1964, p. 124; F. Jona and P. Scherrer, Helv. Phys. Acta, 25, 35 (1951); R. Bass, D. Ross Berg and G. Ziegler, Z. Phys., 149, 199 (1957); R. E. Green and L. Machinnon, J. Acoust. Soc. Amer., 28, 6, 1631 (1956). Discrepancies among the data are presently unexplained. However, it appears that the data reported here agree with Zarembovitch and Kahane better than the various "near 0°C" measurements do.

Two problems with this experiment at low temperatures are presently being studied. First there exists a problem of thermometry in the region of 40°K and below. Due to the complexity of the velocity measurement it is advantageous to obtain a fast readout thermometer of fairly good accuracy. Investigation of carbon resistance controlled RC oscillators is underway. There is a related problem which concerns temperature calibration of such a device. A sinple calibration standard is needed which will work in a small evacuated space. The helium vapor pressure method cannot be used because the helium region is isolated from the sample container.

The second problem has to do with low temperature (less than 40°K) acoustic coupling. The large expansion coefficient of ice makes bonding of transducers a problem. Presently isopentane is being studied as an acoustical bonding material.

---

* This work is partially supported by the Office of Naval Research.

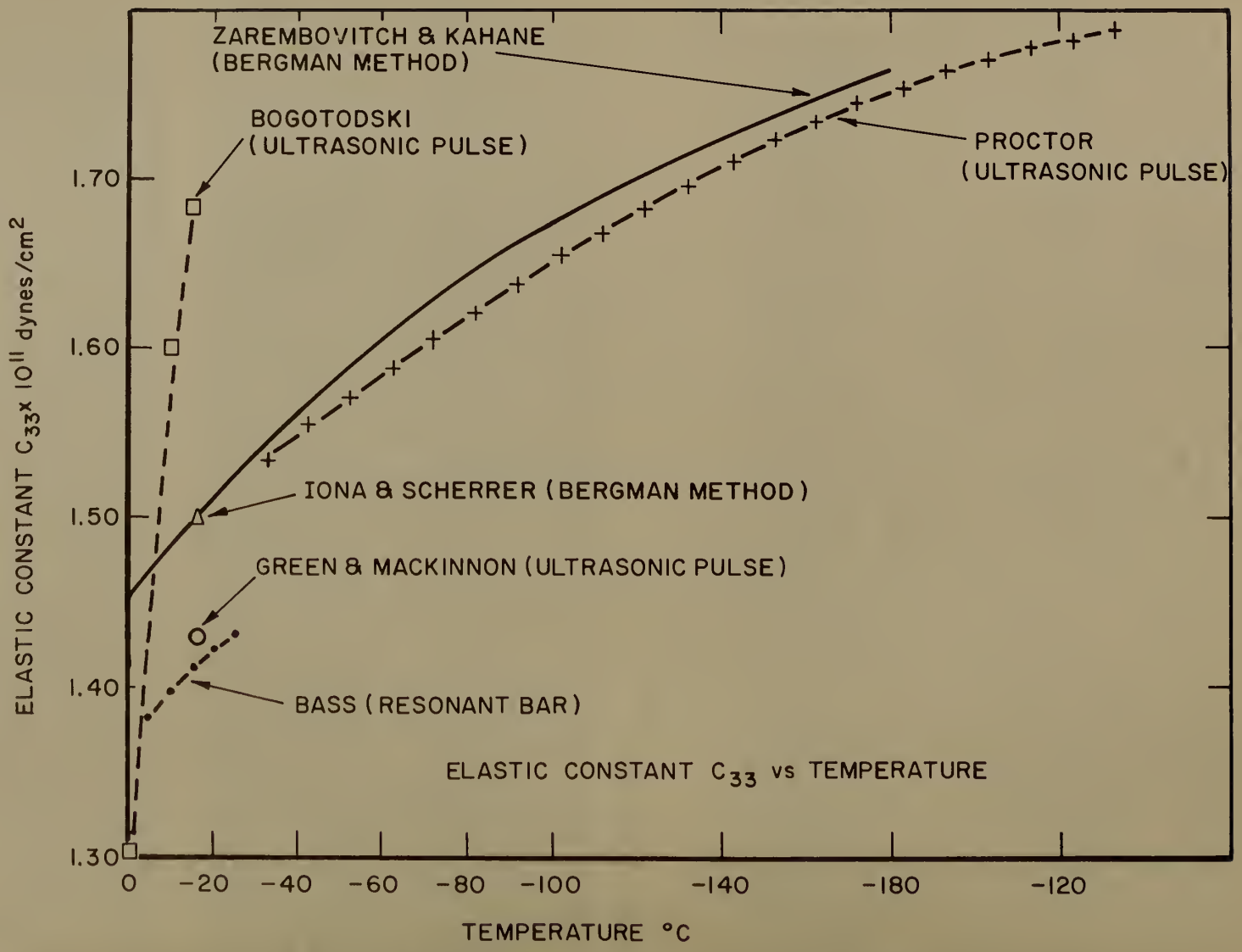

Figure 21. Elastic constant $C_{33} \times 10^{11}$ dynes/cm^2

4.17 Accurate Measurement of the Fundamental Electrical Properties of Semiconductor Crystals

J. C. French, L. J. Swartzendruber, G. G. Harman, H. A. Schafft
N. Winogradoff and J. A. Coleman

Electron Devices Section

As indicated in NBS Technical Note 251, Section 3.10, the variation in resistivity throughout a single crystal of silicon appears to be one of the limiting factors in the establishment of standard samples for bulk resistivity or in the correlation of measurements of this property among various laboratories. A cooperative program being carried out with industry with the aim of producing more uniform material for this purpose has resulted in a substantial increase in radial uniformity, but so far at the cost of an increased longitudinal gradient. Samples with radial variations of less than ± 1% over a diameter of 2.5 cm and a longitudinal gradient of 12% per cm have been measured. These results may be compared with values of about ± 3% and 2%, respectively, observed in the best commercial sample previously received for evaluation. The nominal values of resistivity in these cases were 0.2 ohm cm and 14 Ohm cm, respectively. Despite the higher longitudinal gradient, the characteristics of the new material are considerably more suitable for the purposes of this work and its homogeneity is believed to be reproducible while that of the single commercial sample was largely fortuitous.

Measurements are underway on the temperature coefficient of resistivity of silicon, at temperatures near room temperature and as a function of impurity concentration and conductivity type. Because of its magnitude (roughly 0.2 to 0.9% per degree celsius), it is necessary to know this coefficient accurately in order to evaluate measurement errors and to compare resistivity measurements made at slightly different temperatures to the accuracy desirable in this work.

A bibliography on the measurement of bulk resistivity of semiconductor materials for electron devices has been published (French, 1964), and the last of the current series of papers concerned with electrical potential problems and correction factors having application to resistivity measurements has also been published (Reber, 1964).

Studies* mentioned in NBS Technical Note 251, Section 3.10 showed that the effect of crystal defects revealed by x-ray diffraction microscopy on the susceptibility of transistors to the development of second breakdown was either not significant or overshadowed by surface related effects that appeared to have been present. As part of an effort to evaluate a theory [A. C. English, Solid State Electronics 6, 511 (1963)] of the second breakdown mechanism, it was determined that the extent of strain fields about microscopic melts in silicon was negligible as observed using x-ray diffraction apparatus. A ruby laser was used to produce melts as small as 2.5 μm on the surface of a defect-free silicon crystal. The melts were made with the aid and equipment of the Spectrochemical Analysis Section (See Section 3.22).

With respect to the program in which the recombination properties of hot carriers in silicon crystals are to be measured, some further refinements in measurement equipment have been made. However, because of delays in obtaining good samples for recombination studies, emphasis has been temporarily shifted to studies of optical absorption.

The extent of the effort devoted to silicon single crystal nuclear particle detectors has been considerably increased with the start, during this period, of the establishment of facilities necessary to (a) measure the physical properties of the crystalline material (such as resistivity, minority carrier lifetimes, and mobilities),** (b) evaluate and improve the fabrication procedures for lithium-drifted detectors with the aim of producing reliable devices with extended shelf and operating lifetimes,** (c) assist in device measurements standardization,** and (d) in cooperation with the National laboratories, measure the properties of these and other solid state nuclear particle detectors and correlate anomalies in operating characteristics with defects in crystal structure or fabrication procedures.***

Successful epitaxial gallium-arsenide injection lasers have been produced in selected material. Initial failures to achieve lasing were traced, by a combination of electrical optical measurements and of metallurgical and electron probe data supplied through the Analysis and Purification Section, in inadequate doping of the tellurium doped epitaxial layer in the wafers supplied. This defect may be characteristic of the gaseous deposition utilized, suggesting the need for deposition from a melt to achieve n-type doping in excess of 1×10^{19} cm^{-3}.

---

* The work was supported in part by the Rome Air Development Center.

** This work was supported in part by the National Aeronautics and Space Administration.

*** This work was supported in part by the Atomic Energy Commission.

4.18 Dielectric and Mechanical Properties of Crystals*

J. H. Wasilik

Solid State Physics Section

I. Simple Lattice Dynamics of Zinc Blende Structures

In our previous report (NBS Technical Note 251, page 42), in applying the Nath, Born-Smith, de Launay theory for the elastic constants of diamond lattices to zinc blende structures, we assumed a Born-Mayer interaction between the ions. Using this interatomic potential, we showed that the next-nearest-neighbor central-force-type force constant, de Launay's α_2 = the nearest-neighbor central-force force constant, de Launay's α_1, x (the nearest-neighbor distance/next-nearest-neighbor distance)^2. This resulted in a relationship among the elastic constants which fitted reasonably well to the experimental values. Further investigation using a Lennard-Jones type interaction $V = -A/r_{ij}^n$, gave α_2/α_1 = (nn distance/nnn distance)^3. The ensuing relationship among the elastic constants was also in good agreement with the experimental results. The next step is to express $\alpha_2 = \beta\,\alpha_1$, and solve for β using the relations given by de Launay (NBS Technical Note 251, page 42) between α_1, α_2, α and the elastic constants. The result is a quadratic equation in β, $a\beta^2 + b\beta + c = 0$, wher a, b, and c are functions of the elastic constants. When a and b are evaluated, they are found to be quite small compared to their positive or negative components a_+, a_-, b_+, b_-, i.e.: $a = a_+ - a_-$, $a \ll a_+$ or a_-, and $b \ll b_+$ or b_-. This situation makes it impossible to calculate β in view of inaccuracies of the elastic constants, $\simeq .2\%$. However, we seem to have found an empirical relationship among the elastic constants.

$$a = 24\,C_{11}\,C_{12} + 20\,C_{11}\,C_{44} - (11\,C_{11}^2 + 4\,C_{12}^2 + 40\,C_{12}\,C_{44}) = 0$$

which in most instances is obeyed to within the accuracies of the experimental data.

For example, $a/a_+ < 4 \times 10^{-3}$ for InSb, GaSb, GaAs, AlSb, InAs, Ge and diamond. For CdTe $a/a_+ = 3.4 \times 10^{-2}$, and for Si $a/a_+ = 7.6 \times 10^{-3}$. Possible theoretical foundations for this relationship are being investigated. A report (Wasilik and Wheat,1965) has been written.

[The b = 0 relation fits to ~ 4% for the zinc blende structures, but only to ~20% for Si and diamond; for Ge, $b/b_+ = 7\%$.]

II. Exciton Contribution to the Dielectric Constant

A search for an exciton contribution to the low frequency dielectric constant has been performed. The Stark splitting of exciton levels in Cu_2O reported by Gross indicates polarizabilities per exciton ~ 10^{-18} cm^3, ~ 10^5 times the electronic polarizabilities of ions in common lattices. Using a Q-spoiled ruby laser to populate the exciton levels in CdSe, we searched for an exciton contribution to the dielectric constant. The results to date are negative, possibly due to the masking effects of photoconductive and photovoltaic currents.

---

* This work was supported by the Atomic Energy Commission.

4.19 Metal-Oxide Melting Point Standards

S. J. Schneider and C. L. McDaniel

Crystallography Section

The investigation of phase relations between container materials and metal oxides in varous environments (NBS Technical Note 251, Section 4.14) has been continued. Work has been completed on the reactions that occur in air between Ir and a number of the sesquioxides (Schneider, Waring and Tressler, 1965). These data show that Ir is suitable as a container even though it oxidizes to IrO_2 and usually forms binary compounds with the admixture oxide. Significantly, IrO_2 (and Ir) did not react even partially with In_2O_3, Sc_2O_3, and Al_2O_3 in the solid state. Similar studies utilizing an environment of inert gas or vacuum have been initiated on systems involving Al_2O_3 and either Ir or W. Preliminary information indicates that no significant reaction (compound or solid solution formation) occur in the solid state. However, the presence of Ir causes an apparent lowering of the melting point of Al_2O_3. In addition, research is also being conducted on the polymorphism and stability of Rh_2O_3 in air.

4.20 Experimental Determination of Atomic Scattering Factors

G. Burley

Crystallography Section

A redetermination with improved equipment of the experimental atomic scattering factors for magnesium oxide reported earlier (NBS Technical Note 251, Section 4.17) gave substantially the same results. The revised values are tabulated below

sin θ/λ	Mg^{+2}	O^{-2}
.20	8.45	5.90
.25	7.80	4.84
.30	7.14	4.01
.35	6.60	3.36
.40	6.04	2.89
.45	5.47	2.48
.50	4.99	2.26
.55	4.88	2.08
.60	4.04	1.95

Preliminary measurements on the atomic scattering factor for copper metal are now in progress. This material has been tentatively chosen as an interlaboratory comparison, but results to date indicate that reproducible accuracy of the order of one percent may be difficult to attain with it.

A study of the relation of the effect of ultraviolet radiation with the x-ray characteristic temperature in the alkali halides has been begun. Powder diffraction data for sodium chloride indicate both an increase in structural disorder and an apparent increase in the characteristic temperature. Both effects decrease after cessation of irradiation.

4.21 Visco-Elastic Properties

P. B. Macedo and W. Capps

Glass Section

The elastic constants of thorium dioxide, ThO_2, at 25°C were determined in collaboration with J. B. Wachtman, Jr. of the Physical Properties Section (Macedo, Capps, and Wachtman, 1964). The constants in units of 10^{11} n/m^2 (10^{12} dynes/cm^2) were found to be: $c_{11} = 3.67 \pm .04$, $c_{12} = 1.06 \pm .02$, and $c_{44} = 0.797 \pm .008$. The above measurements were made as part of the calibration of the high temperature ultrasonic interferometer now being built. This apparatus will make ultrasonic measurements up to 1700°C under neutral or reducing atmospheres, and will be used initially to study viscous relaxation in molten glasses. The interferometer will be an improved and more flexible version of that reported (Macedo and Litovitz, 1965) in that higher temperatures, a greater accuracy and a wider frequency range will be obtained.

4.22 Electron Spin Resonance of Transition Metal Complexes

H. C. Allen, Jr., and G. F. Kokoszka

Inorganic Materials Division

E. P. R. and optical studies have been completed on copper-doped bis 8-hydroxyquinolate zinc (II). The magnetic parameters were obtained from polycrystalline samples at both X-band and K-band. The magnetic parameters at liquid nitrogen temperature are $g = 2.287 \pm 0.004$, $g_{\perp} = 2.066 \pm 0.066$, $A_{\parallel} = 0.0171 \pm 0.0005$ cm^{-1}, $A_{\perp} = 0.003 \pm .001_{\parallel}$ cm^{-1}, and $A_N = .0090 \pm 0.0001$ cm^{-1}. In the spectral range from 10,000 cm^{-1} to 30,000 cm^{-1} three optical transitions were observed, one at 15,400 cm^{-1}, one at 23,000 cm^{-1}, and one at 28,500 cm^{-1}. Bonding parameters were calculted from these data. The in-plane sigma and pi bonding parameters were found to be $\alpha^2 = .86$ and $\beta^2 = .84$, which indicates relatively strong in-plane bonding, while the out-of-plane bonding was found to be relatively weak, $\delta = 1$. These results are quite

different from the results obtained by Gersmann and Swallen for bis 8-hydroxyquinolate copper (II) in a frozen solution of 60% chloroform and 40% toluene. [J. Chem. Phys. 36, 322 (1962)]. A paper reporting our data and discussing the implications of the differences found for the two cases has been submitted for publication.

An interpretation of the electron spin resonance results on zinc-doped copper acetate monohydrate suggested the existence of an additional optical transition in copper acetate monohydrate. This has been observed as a shoulder on a previously reported band and its polarization properties have been determined. A consistent explanation for the magnetic and optical properties of copper acetate monohydrate and the magnetic properties of zinc-doped copper acetate monohydrate has been proposed and submitted for publication.

Single crystals of the tris coordination compound of Zn^{+2} with 1-10 phenanthroline containing a small amount of the corresponding cobaltous compound are presently being investigated. Preliminary results indicate that the ligand field has rhombic symmetry and the orbital reduction factor is estimated to be .84. The results of this study will be compared with the results obtained in the cupric complex in the same host lattice. The latter complex showed a pseudo-Jahn-Teller effect. These studies should be completed early in 1965.

Magnetic studies are also underway on a recently-synthesized tetrahedral complex of V^{+4}. Preliminary results indicate that the g values are quite similar to those found in various VO^{++} complexes but that the A values are somewhat smaller.

4.23 Mössbauer Line Broadening in SnO_2 Due to Twinning Effects

R. H. Herber (Rutgers University) and J. J. Spijkerman

Radiochemical Analysis Section

Stannic oxide (cassiterite, SnO_2) crystallizes in the tetragonal system, class 4/m 2/m 2/m. The space group is $P4_2/mnm$, with two SnO_2 molecules per unit cell. The most detailed investigation of the structure of a single crystal SnO_2 [J. A. Marley and T. C. MacAvoy, "Investigation of the Mechanism of Single Crystal Growth in High Temperature Systems", J. Appl. Phys. 32, 2504 (1961)] showed a single Sn-O bond distance of 2.055A, with six oxygen atoms occupying the corners of an octahedron. This should lead to a vanishing field gradient tensor at the tin atom lattice point, and zero quadrupole splitting, if all of the O-Sn-O bond angles are either π or $\pi/2$. Mossbauer spectra of SnO_2 with $Mg_2 Sn^{119m}$ source (23.8 KeV, $3/2 \rightarrow 1/2$ transition) showed definite, though not completely resolved, quadrupole splitting. This splitting is attributed to twinning, which was observed even in the best single crystals grown by the vapor transport method. This twinning occurs primarily in the (031) plane, so that the oxygen octahedron around the tin atom in the twin plane is slightly deformed with a resulting non-vanishing electric field gradient tensor.

5. CHEMICAL PROPERTIES OF CRYSTALLINE MATERIAL

This chapter is concerned with studies of crystal structure, phase relations, and other chemical properties not sensitive to crystal perfection.

5.1 Automation of Single-Crystal X-ray Diffraction Intensity Measurements

F. A. Mauer

Crystallography Section

Modification of an existing single crystal diffractometer by the addition of programming and positioning modules has been completed. The three shafts required to orient the crystal and position the counter are controlled from a console. Shaft settings and scaler counts are recorded on a printer and on punched paper tape. Provisions have been made for adding a tape reader and circuit modules at a later time to permit the system to follow a complete program punched on a control tape.

Measurements are now being made on a crystal of $Na_2O{\cdot}4B_2O_3$ and a computer program to edit and process the output tape is being written.

5.2 Radial Distribution Studies of Glasses

G. J. Piermarini, A. Hyman, and S. Block

Crystallography Section

Radial distribution studies on vitreous and polycrystalline barium and strontium borates [$BaO{\cdot}2B_2O_3$, $SrO{\cdot}4B_2O_3$, $SrO{\cdot}1.5\ B_2O_3$] have been completed (Block and Piermarini, 1964). The conclusion drawn from these studies is that the heavy cations in the vitreous systems occupy characteristic positions in the overall glass structure which are governed to a certain extent by crystal chemical restraints. This is demonstrated by a correlation between distribution curves obtained from both the glass and corresponding polycrystalline material, and is further supported by an analysis of these distribution curves based on the random packing of hard spheres.

An investigation of the general nature of x-ray scattering techniques, as applied to studies of vitreous matter, is being undertaken. The purpose is twofold:

1) To minimize the errors inherent in present procedures.

2) To determine just how sensitive the intensity distribution in reciprocal space is to the electron distribution in real space, and thus to setup criteria for how far one may extend the interpretation of x-ray data obtained from non-crystalline matter.

5.3 Infrared Studies of Inorganic Materials

C. E. Weir

Crystallography Section

With completion of studies of infrared spectra of anhydrous inorganic borates (NBS Technical Note 251, Section 5.9), work has been initiated on a similar study of the hydrated borates. The hydrated borates studied are naturally occurring minerals because of the difficulties involved in synthesizing and identifying the hydrated compounds. Therefore, it is not possible to utilize isotope substitution to assist in interpreting the spectra and there is a possibility that impurities may influence the data obtained. Interpretations will necssarily be based on the previous data on the anhydrous borates and known structure types of the hydrates. Most of the spectra have been obtained but the analysis is not complete. Preliminary results show that hydrates with similar cationic structure give spectra which are quite analogous. Because of the complexity of the cations and the corresponding spectra, it seems that conclusions concerning coordination of boron and cation structure must be made with considerably more restraint than in the case of the anhydrous materials.

5.4 X-Ray Diffraction Studies at High Pressures

C. Weir, S. Block, and G. Piermarini

Crystallography Section

X-ray diffraction data are being obtained for ice VI and ice VII by means of powder and single crystal techniques. An existing high pressure powder diffraction camera has been modified to permit examination of materials of low scattering power such as ice, and at the same time to permit observation of lines at higher scattering angles. A new single crystal high pressure cell has been designed, constructed, and tested. This instrument uses a diamond high pressure cell mounted on a modified precession camera. Both the powder and single crystal devices are undergoing further modifications.

By using metal gaskets both single and polycrystalline specimens of ices VI and VII have been obtained. The hk0, hk1, c-cone-axis and other single crystal precession photographs show that ice VI has an orthorhombic unit cell ($a = 8.38$ Å, $b = 6.17$ Å, and $c = 8.75$ Å), which is consistent with published powder diffraction data. The systematic absences indicate a space group P**a and from the known density of ice VI it is calculated that $z = 20$. Insufficient data have been obtained on ice VII to permit reaching any conclusions.

5.5 Phase Equilibria Determination with the Aid of Crystal Structure Analysis

R. S. Roth and J. L. Waring

Crystallography Section

The phase equilibrium relations in the system Nb_2O_5-WO_3 have been carefully studied. The thermal stability of the four compounds whose compositions have been fully substantiated by crystal structure analyses (0-50 mol percent WO_3) has been found to be dependent on the size of the "building-block" which is the basis of the structure of each phase. The compound containing the smallest building block (highest in Nb_2O_5 content) melts congruently whereas the other three melt incongruently at

decreasing temperatures with increasing WO_3 content and size of the building block. The last two phases also have minimum stability temperatures increasing with increasing WO_3 content, and size of block.

The compositions of the phases containing more than 50 mol percent WO_3 have been reduced from experimental phase equilibria data, based on hypotheses as to the crystal structures involved. Unfortunately, single crystal structure analyses is not yet available to confirm these compositions.

The phase equilibrium relations in the Al_2O_3-WO_3 system have also been examined. At least one new compound (and possibly several structurally related phases) has been found. Its x-ray diffraction powder pattern is apparently unrelated to any known phase. No single crystals are yet available for determining the unit cell dimensions of the phase or phases. The compositions cannot even be approximated without such data, as the powder patterns over a rather wide range of compositions show no recognizable systematic change and no evidence of free Al_2O_3 or WO_3.

Some experiments have been begun to determine the type of phases which are formed in the TiO_2-Ta_2O_5 and Ta_2O_5-WO_3 systems. It is expected that phases structurally related to the two polymorphs of Ta_2O_5 will be formed in this system and that these will be different from the compounds structurally related to Nb_2O_5 which are formed in the corresponding niobate systems.

Various aspects of these studies have been reported, (Roth and Wadsley, 1965); (Roth, Wadsley and Anderson, 1965); (Waring and Roth, 1965); and (Waring and Schneider, 1965).

5.6 Standard X-ray Diffraction Powder Patterns

H. E. Swanson

Crystallography Section

Diffraction patterns are produced for the Powder Data File, a reference compilation used in laboratories throughout the world for identification of crystalline materials. The patterns have been published in ten volumes of NBS Circular 539 and in three sections of NBS Monograph 25. The fourth section is being prepared for release in 1965 and will be the first to include powder patterns calculated from single crystal data. Fifty calculated patterns are included. Much of the best published crystallographic data is for single crystals and the technique of calculating powder patterns from this data provides an economical means of extending the coverage of the Powder Data File, particularly in the case of materials that are difficult to obtain or to handle.

5.7 Crystal Chemistry of Silver Iodide*

G. Burley

Crystallography Section

A discussion of the role of strain in the hexagonal to low-cubic phase transformation of silver iodide (Burley, 1964a) and the analysis of the ice nucleation by photolyzed silver iodide (Burley, 1964b) have been published.

---

* This work was supported by the National Science Foundation, Atmospheric Sciences Program.

A radial distribution study of the powder diffraction data from different samples of the high-cubic structure, derived from the low-cubic and hexagonal phases, respectively and taken just above the transition temperature of 147°C indicates that there is a difference in the average silver-iodine distance of about 0.04 Å, suggesting a non-random distribution of silver atoms over all available sites at this temperature. An occupation site analysis using the available intensity data is now in progress.

5.8 Crystal Structure Analysis

S. Block, H. M. Ondik, A. Perloff, L. H. Hall, and A. D. Mighell

Crystallography Section

The crystal structure of bis-dodecacarborane, $B_{20}C_4H_{22}$, has been determined by the relatively new symbolic addition technique for direct phase determination. The molecule consists of two slightly distorted icosahedra joined by a c-c bond across a center of symmetry. In each icosahedron, a second carbon atom and four boron atoms are distributed over the five sites adjacent to the linking carbon.

In a second investigation, the crystal structure of the low temperature form of Li_3PO_4 was shown to be related to that of the high temperature form, but with a disordering of phosphate tetrahedra.

Work in progress includes determination of the structures of YBO_3, BaB_2O_4, $Na_2B_8O_{13}$, and $BeGe_4O_9$.

Work reported earlier (NBS Technical Note 251, Section 5.4) and since published or accepted for publication includes descriptions of the structure of sodium tetrametaphosphate (Ondik, 1964), and the structures of $Na_3P_3O_9$ and $Na_3P_3O_9 \cdot H_2O$ (Ondik, 1965).

5.9 Phase Equilibria

E. M. Levin and R. S. Roth

Crystallography Section

A revised edition of "Phase Diagrams for Ceramists" has been published (Levin, Robbins, and McMurdie, 1964). It contains phase diagrams from the literature for 1002 oxide systems, 912 salt systems and combinations, and 142 water-containing systems. Many of these systems have potential applications in crystal growing problems.

Work on the heat of transition and heat of fusion of Bi_2O_3 (NBS Technical Note 251, Section 5.6) has been completed and the results have been accepted for publication (Levin and McDaniel, 1965).

Phase equilibria in rare earth oxide-boric oxide systems are being investigated as part of a long range study of immiscibility in borate systems. Partial phase diagrams between B_2O_3 and the 1:1 compounds were established for the following oxides: Nd_2O_3, Sm_2O_3, Eu_2O_3, Gd_2O_3, Dy_2O_3, Y_2O_3, and Ho_2O_3.

5.10 Subliquidus Phase Separation in Inorganic Oxides

W. Haller

Glass Section

Melts of certain inorganic oxide systems which solidify without apparent crystallization, have the tendency to segregate into two immiscible glasses upon cooling. This segregation occurs at such low temperatures, that the involved phase is too rigid to flow and coalesce in the way low viscosity liquids do. The result is a solid composed of two continuous microdisperse networks.

Probability calculations were performed, which showed that the continuous nature of the two networks may be due to the high degree of intersection within a population of spheres, grown from randomly placed nuclei. A theory was proposed whereby the thermal rearrangements within such microheterogeneous systems is caused by a diffusive transport, facilitated by interface curvatures of opposite signs. Equations for a number of transport models were derived. To prove this theory, phases separation in Na_2O-B_2O_3-SiO_2 melts was initiated by cooling. The resulting glasses received different heat treatment schedules and the degree of microdispersity was measured by N_2 adsorption on one of the isolated phases.

The experimentally determined law follows the theoretically derived equation for an interface-controlled bulk diffusion process. The process was found to be arrhenian with an apparent activation energy of 40 kcal/mole.

Some aspects of this work have been accepted for publication (Haller, 1965).

5.11 Ultrasonic Measurements at Pressure-Induced Polymorphic Phase Changes

P. Heydemann

Pressure Measurements Section

The aim of this work is to establish transition pressures of various crystalline materials for use as fixed points on the pressure scale. To achieve this, a study will be made of the elastic constants and internal friction at ultrasonic frequencies, combined with various electrical and PVT-measurements.

The ultrasonic apparatus has now been assembled and velocity measurements with polycrystalline and single crystal bismuth have been made at atmospheric pressure. Measurements under pressure will be undertaken shortly, using a rotating-piston gage which has been assembled and checked up to 18 kilobars, using the polymorphic phase transition of $AgNO_3$. This range will be extended to 25 kilobars using the transition pressures of KBr and Bi I-II.

5.12 Heats of Formation of Refractory Crystalline Substances from the Elements

G. T. Armstrong, K. L. Churney, E. S. Domalski, and R. C. King

Heat Measurements Section

As this is the first report of the work of this group, we briefly review recent tasks finished prior to the current period, as well as current activity.

In a study of the heats of formation of fluorine compounds by fluorine bomb calorimetry, a study has been completed of the heat of formation of $AlF_3(c)$ and currently under way and nearly completed is a study of glassy BeF_2 which will ultimately be related to the crystal phase. The technique consists of mixing the powdered metal with an easily combustible material, in these experiments Teflon, and burning the pelleted mixture in an atmosphere of pressurized fluorine. The Teflon sustains and moderates the combustion, assures a high degree of completeness of reaction, and thus simplifies the problem of determining how much reaction occurs. The reactions are carried out in an advanced version of the Dickinson calorimeter, with which a measurement of the heat evolved is made with an accuracy approaching 0.01%. The overall uncertainty of the heat of reaction is much greater, however, because the amount of reaction cannot be determined so exactly, and because the combustions are not reproducible with this precision.

In a series of experiments employing the same general techniques, the heats of formation of AlB_2 and α-AlB_{12} have also been determined and measurements of the heat of formation of B_4C are under way. In these cases, calculation of the heat of formation of the crystalline substance depends upon knowledge of the heats of formation of the products of combustion, $AlF_3(c)$, $BF_3(g)$ and $CF_4(g)$. The samples for these studies were prepared by the Carborundum Company in a special task under which they developed techniques and prepared very high quality samples.

The heat of formation of Al_4C_3 was determined by a somewhat different technique, in which the carbide was burned in atmosphere of oxygen. Calculation of the heat of formation of the carbide in this case requires knowledge of the heats of formation of the combustion products $Al_2O_3(c)$ and $CO_2(g)$. The samples used in the combustion measurements were from the same material used by Furukawa and Saba for heat capacity measurements at low temperatures and by Douglas and Victor for enthalpy measurements at high temperatures. The combustion in the calorimetric bomb led to the little known phase, δ-Al_2O_3, in amounts of 40-75% of the total product. The remainder of the product was α-Al_2O_3. In order to interpret the heat measurements in terms of the heats of formation of the starting material and products, a separate determination was needed of the difference in heats of formation of α-Al_2O_3 and δ-Al_2O_3. This difference was determined for us by Kleppa and Yokohawa to be 2.7 ± 0.4 kcal mole^{-1}.

5.13 Microcomposition and Structure Characterization by Electronprobe Methods

H. Yakowitz and D. L. Vieth

Lattice Defects and Microstructures Section

and

J. R. Cuthill

Alloy Physics Section

The analytical capabilities of the NBS electron probe microanalyzer were improved by the addition of a new light optical system and a new magnetic objective lens. The new lens permits an X-ray emergence angle of 51°. A new fully-focussing spectrometer was designed and built. Provisions for light element analysis are also being made. A Kossel camera was built and is being used to prepare patterns in the study of cubic materials by the Kossel method (See Section 3.16).

In collaboration with the electron probe microanalysis group under Dr. Heinrich in Division 310, investigation and characterization of standards for use in quantitative electron probe studies has continued. In particular NBS low alloy steel standard 463 has been characterized analytically.

5.14 Crystal Structure of Phases in Nb-Sn System

C. J. Bechtoldt

Lattice Defects and Microstructures Section

Studies were made on single crystals of $NbSn_2$ grown and extracted from dilute solutions of niobium in tin. They are orthorhombic, crystallizing in the space group, Fddd, and structure of the $CuMg_2$ prototype. Using the setting as shown in the literature for the prototype the parameters are a = 9.853 Å, b = 19.07 Å, and c = 5.64 Å. Measurements were made on the intensities of reflections of the type 0k0 and 0k2 up to k = 52 and on the type h00 and h02 up to h = 24. In addition to the absences fixed by the space group and that of the special positions, accidental absences occurred in such a sequence which fixed the position of Sn in 16(f) at y = 0.4125 and Nb in 16(f) at y = 0.1250. Final determination of the Sn atoms at 16(e) have not been made but appear to be close to x = 0.161.

5.15 Low-Temperature Calorimetry of Crystalline Substances

G. T. Furukawa, M. L. Reilly, and W. G. Saba

Heat Measurements Section

The heat capacity of a variety of substances is investigated in the range 10 to 400°K by means of adiabatic calorimetry. The construction of a calorimeter for extending the measurements down to 2°K is in progress.

Measurements on KBH_4 revealed a λ-type solid-phase transition at 77.16 ± 0.02°K with an entropy change of 2.92 J/deg-mole plus a broad transition extending from about 200 to 450°K (Furukawa, Reilly, and Piccirelli, 1964). A similar λ-type transition

found in $NaBH_4$ with an entropy change of 5.10 J/deg-mole, which is close to the theoretical value of $R\ell n2$, has been interpreted as an order-disorder transition involving two possible orientations of the BH_4^- tetrahedrons similar to the NH_4^- tetrahedrons in ammonium halides [W. H. Stockmayer and C. C. Stephenson, J. Chem. Phys. 21, 1311 (1953)]. The entropy change of the λ-type transition observed in KBH_4 is approximately one-half of $R\ell n2$. The broad transition at the higher temperatures is interpreted as a continuation of the order-disorder transition still incomplete at 77.16°K.

An examination of the "additivity" of the heat capacity of mixed metal oxides showed that the additivity is followed within a few percent around room temperature, but below about 200°K the compound deviates positively, increasingly with decrease in temperature (Furukawa and Saba, 1965). The correlation of additivity with structure is in progress.

5.16 Apparatus for High-Temperature Preparation of Pure Crystalline Polymorphs

A. R. Glasgow, Jr.

Analysis and Purification Section

A cross-sectional drawing of the special cell (discussed in Section 5.2, NBS Technical Note 251) for use to 1000°C in phase purifications and thermal analysis for the preparation of pure polymorphic forms of BeF_2 is shown in figure 22. The numbers in the figure refer to the disassembly parts, the lower case letters to welds, and the capital letters to details of other parts; these are described in the legend to the figure. Photographs of the assembled and disassembled cell are shown in figures 23 and 24. Figure 22 also shows two heat-exchange probes that are used for removal of heat at re-entrant coolant well, B, and at protrusion, M, of cell for crystal nucleation. Figure 24 shows the tool for removing vessel 6 by locking into grooves, J.

Provisions for placing this cell into operation were completed and have entailed the following: mounting in three-zone furnace; design and fabrication of two heat-exchange probes; installation in hood of coolant lines to probes and of a system for evacuation and pressure-control of nickel-Inconel spaces of body (F in figure) and well (C in figure); easily removable thermocouples; and placement of a well in a dry box to house the closed cell in a vertical position during disassembly for filling and product removal.

Anhydrous conditions have been achieved in the dry box and work is in progress using these developed facilities to start processing 50-gram amounts of BeF_2 by the different phase-purification processes (Thermal decomposition of $(NH_4)_2\ BeF_4$, crystallization, distillation, and sublimation). The process that yields a pure polymorph will be continued until sufficient material is obtained for NBS needs before attempts will be made to prepare a different polymorph.

Legend

Phase Purification and Thermal Analysis Cell

1 - 7; Disassembly parts:

1 - Unit containing vapor condenser for liquid reflux or solid deposit.
2 - Removable nickel support for Dewar.
3 - Nickel Dewar
4 - Soft nickel gasket
5 - Nickel tube with tapered Monel Flange at top.
6 - Removable nickel vessel
7 - Inconel-nickel shell welded to Monel high-vacuum coupling and cavity portion for vessel 6.

a - h; Welds: a, e - Monel to Inconel; f, g - Nickel to nickel
b, c, d - Monel to nickel; h - Inconel to Inconel

A - Monel, "Cajon gland", ultra-high vacuum coupling for attachment to manifold through high-temperature valve.
B - Re-entrant cooling well

C, F - Monel, "Cajon body", ultra high-vacuum coupling for pressure control of space between nickel-Inconel walls.
D - Monel, "Cajon-type gland", ultra-high vacuum coupling for cell.
E - Monel, "Cajon-type body", ultra-high vacuum coupling for cell.
G - Nickel baffles
H, K, L - Thermocouple port
I - Knob used as lock-device for part 2.
J - Grooves for cell-insertion or removal tool for vessel 6.
M - Protrusion for crystal nucleation in vessel 6.
N - Small portion of contents of vessel 6 supercooled for crystal nucleation.

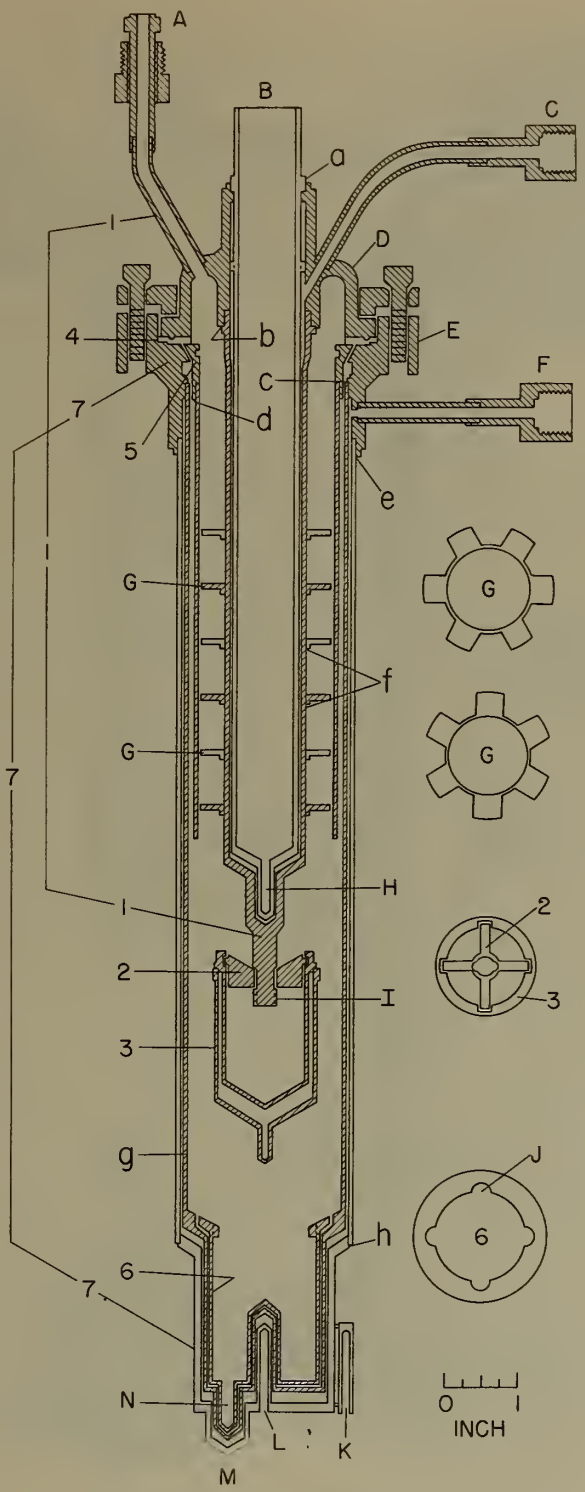

Figure 22. Phase Purification and Thermal Analysis Cell.

Figure 23. Assembled cell for use at 1000°C in phase purification.

Figure 24. Disassembled cell for use at 1000°C for phase purification

6. PARTIAL LIST OF PARTICIPANTS

There follows a partial list of scientists engaged in activities described in this note, with indications of their research fields and organizational location within the National Bureau of Standards. The latter may be helpful in making contact with individuals for the purpose of obtaining reprints or further technical information.

Participants at the Washington Laboratories

Abramowitz, Stanley: Ph.D. Polytechnic Inst. of Brookly, 1963; infra-red molecular spectra; Heat Division

Allen, Harry C., Jr.: Ph.D. University of Washington 1951; electron-spin-resonance studies; Chief, Inorganic Materials Division
Author: 4.22

Ambler, Ernest: Ph.D. Oxford University, 1953; nuclear reactions, low-temperature magnetism; Chief, Cryogenic Physics Section, Heat Division
Author: 4.6

Armstrong, G. T.: Ph.D. John Hopkins University, 1948; thermochemistry of inorganic materials; Heat Division Author: 5.12

Barber, David J.: Ph.D. Univ. of Bristol, England, 1959; growth perfection of crystals; Physical Properties Section, Inorganic Materials Division
Author: 3.17

Barnes, J. D.: Optical and electron microscopy of polymers; Polymer Physics Section, Polymer Division Author: 2.19

Bass, Arnold M.: Ph.D. Duke University, 1949; molecular spectroscopy; Heat Division

Bechtoldt, C. J.: X-ray studies; Lattice Defect and Microstructures Section Metallurgy Division Author: 3.9, 5.14

Becker, J. H.: Ph.D. Cornell University, 1957; optical and transport properties of semiconductors; now at Xerox Corporation, Rochester, New York
Author: 4.7

Bennett, Lawrence H.: Ph.D. Rutgers University, 1958; nuclear resonance studies; Chief Alloy Physics Section, Metallurgy Division Author: 3.12

Block, Stanley: Ph.D. Johns Hopkins University, 1955; x-ray crystallography; Crystallography Section, Inorganic Materials Division Author: 5.2, 5.4, 5.8

Blunt, Robert F.: Ph.D. Rice University, 1949; optical properties of solids; Solid State Physics Section, Inorganic Materials Division Author: 3.1

Bolz, Leonard H.: Crystal perfection by electron microscopy; Physical Properties Section, Inorganic Materials Division Author: 3.24

Bowman, Horace A.: Cartesian diver; Mass and Volume Section, Metrology Division.
Author: 4.12

Breen, David E.: Inter- and intra molecular properties of organic molecules, crystals, and rigid glasses; Physical Chemistry Division

Brower, William S.: Crystal growth by Verneuil process and floating-zone technique; Crystal Chemistry Section, Inorganic Materials Division
Author: 2.13

Brown, Walter E.: Ph.D. Harvard University, 1949; solubility and crystallography of calcium phosphate; Dental Research Section, Polymers Division

Burley, Gordon: Ph.D. Georgetown University, 1962; crystallography; Crystallography Section, Inorganic Materials Division Author: 4.20, 5.7

Burnett, H. C.: Physical metallurgist, mechanical properties, etc.; Metallurgy Division Author: 3.13

Calvert, Joan P.: Growth of oxide films; Corrosion Section, Metallurgy Division
Author: 2.8

Capps, Webster: Physics and chemistry of glass; Glass Section, Inorganic Materials Division Author: 4.21

Cataland, George: Low-temperature thermometry; Cryogenic Physics Section, Heat Division

Chang, Te-Tse: Ph.D. Univ. of Colorado, 1962; magnetic resonance; Solid State Physics Section, Inorganic Materials Division Author: 3.25

Christ, B. W.: Ph.D. Cornell Univ., 1965, radiation effects in metals, Engineering Metallurgy Section, Metallurgy Division Author: 3.14

Churney, K. L.: Ph.D. Mass. Inst. of Technology, 1961; heats of formation by bomb calorimetry; Heat Division Author: 5.12

Cohen, Martin L.: X-ray diffraction studies of crystals grown at high temperatures; Solid State Physics Section, Inorganic Materials Division Author: 3.2

Coleman, J. H.: Ph.D. Univ. of Washington, 1962; nuclear physics, semiconductors, nuclear radiation detector and radiation damage; Electron Device Section, Instrumentation Division Author: 4.17

Colson, J. P.: Polymer morphology; Polymer Physics Section, Polymer Division Author: 2.18

Comeford, J. J.: Molecular spectroscopy; Molecular Spectroscopy Section, Physical Chemistry Division

Cook, Richard K.: Ph.D. Univ. of Illinois, 1935; acoustics and solid state physics; Chief, Sound Section, Mechanics Division

Cooter, Irvin L.: Nuclear magnetic resonance in garnets; Chief, Magnetic Measurements Section, Electricity Division

Coriell, Sam. R.: Ph.D. Ohio State Univ., 1961; mathematical physics; Crystallization of Metals Section, Metallurgy Division Author: 2.3

Crissman, J. M.: Ph.D. Pennsylvanis State Univ., 1963; polymer mechanical properties, Polymer Physics Section, Polymer Division Author: 2.21

Cuthill, J. R.: Ph.D. Purdue Univ., 1952; soft x-ray spectroscopy, electro-probe electron analysis; Alloy Physics Section, Metallurgy Division Author: 5.13

de Koranyi, Alexandra: Crystal growth by electrodeposition; Electrolysis and Metal Deposition Section, Metallurgy Division Author: 3.15

Deslattes, Richard D.: Ph.D. Johns Hopkins Univ., 1959; x-ray spectroscopy; Crystal Chemistry Section, Inorganic Materials Division Author: 3.19, 4.10, 4.11, 4.12

deWit, Roland: Ph.D. Univ. of Illinois, 1959; dislocation theory; Lattice Defects and Microstructures Section, Metallurgy Division Author: 3.6

Diamond, J. J.: Vaporization of refractories; High Temperature Chemistry Section, Inorganic Materials Division Author: 2.15

Dickson, Robert W.: Homogeneous stress on oxide structures; dislocation studies by x-ray methods; Physical Properties Section, Inorganic Materials Division Author: 3.20, 4.14

DiMarzio, E. A.: Statistical mechanics; Polymer Physics Section, Polymer Division Author: 2.22

Dragoo, A. L.: Vaporization of refractories; High Temperature Chemistry Section, Inorganic Materials Division Author: 2.15

Domalski, E. S.: Ph.D. Univ. of Buffalo, 1959; heats of formation of bomb calorimetry; Heat Division Author: 5.12

Dove, Robert B.: Nuclear magnetism; Cryogenic Physics Section, Heat Division

Duecker, H. C.: Ph.D. Univ. of Maryland, 1964; physical effects of pressure; Pressure Group, Inorganic Materials Division

Early, James G.: Ph.D. Rennsalaer Polytechnic Inst., 1963; kinetics of crystallization; Crystallization of metals section, Metallurgy Division Author: 2.2

Eby, Ronald K.: Ph.D. Brown Univ., 1958; acoustics, polymer physics; Polymer Physics Section, Polymers Division Author: 2.18, 3.24

Edlow, Martin E.: Low-temperature thermometry; Cryogenic Physics Section, Heat Division

Eisenstein, Julian C.: Ph.D. Harvard Univ., 1948; low-temperature magnetism; Cryogenic Physics Section, Heat Division

Escalante, Edward: Field emission; Corrosion, Metallurgy Division

Evans, Eloise H.: Physical chemistry, x-ray diffraction; Crystallography Section, Inorganic Materials Division, A.S.T.M. Fellowship supported.

Farabaugh, Edward N.: Etch-pits crystal orientation; Crystal Chemistry Section, Inorganic Materials Division Author: 2.11, 3.17, 4.1

Frisch, R. C.: Structure of materials and the imperfection of solids; Solid State Physics Section, Inorganic Materials Division Author: 3.25

Foley, Carol L.: Growth of oxide films; Corrosion Section, Metallurgy Division Author: 3.8

Forman, Richard A.: Nuclear and quadrupole resonance; Solid State Physics Section, Inorganic Materials Division. Author: 3.25, 4.7

Franklin, Alan D.: Ph.D. Princeton Univ., 1949; properties of point defects in crystal; Institute of Material Research Author: 3.20, 3.21

Frederickse, Hans P. R.: Ph.D. Leiden University, 1950; semiconductors at low temperatures; Chief, Solid State Physics Section, Inorganic Materials Division Author: 4.6, 4.7

French, Judson C.: Solid state devices and materials; Electron Devices Section, Instrumentation Division Author: 4.17

Frolen, Lois J.: Ph.D. Pennsylvania State Univ., 1963; spectroscopy, crystallography, microscopy; Polymers Division Author: 2.23

Furakawa, G.: Ph.D. Univ. of Wisconsin; low temperature calorimetry; Heat Division Author: 5.15

Glasgow, Augustus R.: D.Sc., Univ. of Brussels, 1957; preparation and purification of polymeric forms, phase equilibria, purity determinations at high pressures; Analytical and Purification Section, Analytical Chemistry Division Author: 2.16, 2.25, 5.16

Gornick, Fred: Ph.D. Univ. of Pennsylvania, 1959; physical chemistry of high polymers; Polymers Division Author: 2.23

Grabner, Ludwig H.: Ph.D. Columbia Univ. 1950; semiconductors, photoconductivity; Solid State Physics Section, Inorganic Materials Division Author: 4.5

Greenspan, Martin: Ultrasonics, mechanics; Sound Section, Mechanics Division

Hall, L. H.: Ph.D. Johns Hopkins Univ., 1963; crystal structure; now at Florida Atlantic University Author: 5.8

Haller, Wolfgang K.: Ph.D. Univ. of Vienna, 1950; physical chemistry of glasses; Glass Section, Inorganic Materials Division Author: 5.10

Hardy, Stephen C.: Vapor growth of metal crystals; Crystallization of Metals Section, Metallurgy Division Author: 2.4

Harmon, George G.: Solid state physics, surface phenomena and electroluminescence; Electron Devices Section, Instrumentation Division Author: 4.17

Heydemann, Peter: Ph.D. Univ. of Gottingen, 1958; Physical acoustics; mechanical and electrical properties of polymers; Pressure Measurements Section, Mechanics Division Author: 5.11

Hoffman, John D.: Ph.D. Princeton Univ., 1949; dielectrics, nucleation rate of polymer crystals; Chief, Polymers Division Author: 2.20

Holly, Sylvanus: Crystal growth; Crystal Chemistry Section, Inorganic Material Division

Horton, Avery T.: Crystal growth, impurity retention; Crystal Chemistry Section, Inorganic Materials Division Author: 2.14, 2.16

Horton, W. S.: Ph.D. Ohio State University, 1945; chemical kinetics and thermodynamics; High Temperature Chemistry Section, Inorganic Materials Division

Hosler, William R.: Electronic transport phenomena; Solid State Physics Section, Atomic Physics Division Author: 4.6, 4.7

Howard, Robert E.: Ph.D. Oxford Univ., 1959; theoretical physics; Metal Physics Section, Metallurgy Division Author: 2.7, 3.6, 3.11

Hudson, Ralph P.: Ph.D. Oxford Univ., 1949; low-temperature magnetism, Chief, Heat Division

Hyman, A.: Ph.D. Rutgers, 1964; physical chemistry; Crystallography Section, Inorganic Materials Division Author: 5.2

Ishihara, S.: Calorimetry, high temperature heat measurements; Heat Measurement Section, Heat Division Author: 4.9

Ives, Lewis K.: Electron microscopy; Lattice Defects and Microstructures Section, Metallurgy Division Author: 3.3, 3.5

Jackson, Ronald W.: Ph.D. Univ. of Bristol, 1950; thermodynamics of sucrose solutions, kinetics of growth of sucrose crystals; Crystal Chemistry Section, Inorganic Materials Division Author: 2.10

Kaeser, Robert S.: Low temperature magnetism, cryogenics; Cryogenic Physics Section, Heat Division

Kahn, Arnold H.: Ph.D. University of California, 1955; electronic energy levels of solids; Solid State Physics Section, Inorganic Materials Division Author: 4.3

Keezer, Richard C.: Optical properties and physical chemistry of semiconductors; now at Xerox Corporation, Rochester, New York Author: 4.7

Keller, Richard A.: Ph.D. Univ. of California, 1961; inter- and intramolecular properties of organic molecules, crystals, and rigid glasses; Physical Chemistry Division

Khoury, Fred: Ph.D. Leeds Univ., 1956; morphology and crystallization of polymers; Polymer Physics Section, Polymers Division Author: 2.19

Jenkins, W. D.: High temperature mechanical properties of metals; creep, tensile and stress-rupture; Engineering Metallurgy Section, Metrology Division Author: 3.13

King, R. C.: Ph.D. Univ. of Chicago, 1962; fluorine flame calorimetry; Heat Division Author: 5.12

Klein, Ralph: Ph.D. Univ. of Pittsburgh, 1950; field-emission and low-temperature chemistry; Chief, Surface Chemistry Section, Physical Chemistry Division

Kokoszka, Gerald F.: Electron-spin resonance studies; Inorganic Materials Division Author: 4.22

Kruger, Jerome: Ph.D. Univ. of Virginia, 1953; corrosion reactions at metal surfaces; Corrosion Section, Metallurgy Division Author: 2.8, 3.7, 3.8, 4.8

Lauritzen, J. I., Jr.,: Ph.D. California Inst. of Techn., 1955; theoretical physics; Polymer Division Author: 2.22

LaVilla, Robert E.: Ph.D. Cornell University, 1960; study of transient phenomena by diffraction techniques; Crystal Chemistry Section, Inorganic Materials Division Author: 4.11

Levin, Ernest M.: Phase equilibria of oxide systems; Crystallography Section, Inorganic Materials Division Author: 5.9

Lippincott, Ellis R.: Ph.D. Johns Hopkins University, 1947; infrared spectroscopy; Pressure Group, Inorganic Materials Division

Macedo, P. B.: Ph.D. Catholic University, 1963; viscoelastic properties; Glass Section, Inorganic Materials Division Author: 4.21

Mangum, Billy W.: Ph.D. University of Chicago, 1961; low-temperature magnetism; Cryogenic Physics Section, Heat Division

Mann, David E.: Ph.D. University of Chicago, 1948; spectroscopy; Chief, Molecular Spectroscopy Section, Physical Chemistry Division

Manning, J. R.: Ph.D. University of Illinois, 1958; diffusion in solids; Chief, Metal Physics Section, Metallurgy Division Author: 3.23

Mante, Alexander J. H.: NATO Fellow (1963-54); thermoelectricity, Solid State Physics Section, Inorganic Materials Division Author: 4.4

Margoshes, Marvin; Ph.D. Iowa State University, 1953; spectrographic analysis; Spectrochemical Analysis Section, Analytical Chemistry Division Author: 3.22

Marshak, Harvey: Ph.D. Duke University, 1955; nuclear reactions, cryogenics; Cryogenic Physics Section, Heat Division

Martin, G. M.: Polymer Physics; Polymer Physics Section, Polymer Division

Marvin, Robert S.: Ph.D. University of Wisconsin, 1949; rheology and polymer physics; Chief, Rheology Section, Mechanics Division

Marzullo, Sam: Dielectric properties; Physical Properties Section, Inorganic Materials Division Author: 3.20

Mauer, Floyd A.: Instrumentation for Crystallography; Crystallography Section, Inorganic Materials Division Author: 5.1

McDaniel, C. L.: Phase equilibria of oxide systems; Crystallographic Section, Inorganic Materials Division Author: 4.19

McMurdie, Howard F.: Crystallography and chemical phase studies; Chief, Crystallography Section, Inorganic Materials Division

McNish, Alvin G.: Precise density determinations for solid materials; Chief, Metrology Division

Mebs, Russell W.: Ph.D. Ohio State Univ., 1940; nuclear acoustic resonance; Alloy Physics Section, Metallurgy Division Author: 3.12

Melmed, Allen J.: Ph.D. Univ. of Pennsylvania, 1958; surface studies by field emission; Corrosion Section, Metallurgy Division Author: 2.5, 3.10

Mighell, Alan D.: Ph.D. Princeton Univ., 1963; crystal structure; Crystallography Section, Inorganic Materials Division Author: 5.8

Miller, Paul R.: High-temperature crystal growth, crystal orientation; Crystal Chemistry Section, Inorganic Materials Division Author: 4.1

Milligan, Dolphus E.: Ph.D. Univ. of California, 1958; molecular spectroscopy; Molecular Spectroscopy Section, Physical Chemistry Division

Moreno, E. C.: Ph.D. Univ. of California, 1957; physical chemistry of calcium phosphates Dental Research Section, Polymer Division

Morris, Marlene C.: Physical chemistry, x-ray diffraction; Crystallography Section, Inorganic Materials Division; A.S.T.M. Fellowship supported.

Moses, R. L.: Optical properties of high pressure, fracture of solids; Physical Properties Section, Inorganic Materials Division Author: 4.15

Newton, Clarence J.: Ph.D. Univ. of Texas, 1952; x-ray crystallography of metals; Lattice Defects and Microstructure Section, Metallurgy Division Author: 3.4

Ogburn, Fielding: Electrochemistry, electrodeposition; Electrolysis and Metal Deposition Section, Metallurgy Division Author: 2.6, 3.15

Ondik, Helen M.: Ph.D. Johns Hopkins Univ., 1957; Crystallography, inorganic chemistry; Crystallography Section, Inorganic Materials Division Author: 5.8

Orem, Theodore H.: X-ray studies of crystal perfection; Corrosion Section, Metallurgy Division Author: 2.1

Oser, Hans J.: Ph.D. Univ. of Freiburg, 1957; boundary value problems; Applied Mathematics Division Author: 2.7

Paretzkin, Boris: Study of perfection of single crystals by x-ray diffraction; Crystal Chemistry Section, Inorganic Materials Division Author: 3.18, 3.19, 4.12

Parker, Harry S.: Ceramic engineering; Crystal Chemistry Section, Inorganic Materials Division Author: 2.9

Parker, Robert L.: Ph.D. Univ. of Maryland, 1960; growth of crystals; Chief, Crystallization of Metals Section, Metallurgy Division Author: 2.1, 2.2, 2.3, 2.4, 2.7

Passaglia, Elio: Ph.D. Univ. of Pennsylvania, 1955; mechanical relaxation processes in polymers; Polymer Physics Section, Polymer Division Author: 2.21, 2.22

Payne, Richard E.: Nuclear resonance; Solid State Physics Section; Inorganic Materials Division

Peiser, H. Steffen: Crystallography and crystal chemistry; Chief, Crystal Chemistry Section, Inorganic Materials Division Author: 3.18, 4.2

Perloff, Alvin: Structure analysis; Crystallography Section, Inorganic Materials Division Author: 5.8

Pfeiffer, Earl R.: Crystal growth from solution; Cryogenic Physics Section, Heat Division

Piermarini, Gasper J.: Radial-distribution studies, high-pressure x-ray diffraction studies; Crystallography Section, Inorganic Materials Division Author: 5.2, 5.4

Plumb, Harmon H.: Ph.D. Northwestern University, 1954; low-temperature thermometry; Cryogenic Physics Section, Heat Division

Poland, Duncan E.: Ph.D. University of Wisconsin, 1963; physical chemistry and transport properties of solids; Solid State Section, Inorganic Materials Division

Pollack, Gerald L.: Ph.D. California Institute of Technology, 1962; low-temperature physics; Crystal Chemistry Section, Inorganic Materials Division Author: 2.11

Pontius, Paul E.: Accurate measurements of mass volume and density; Chief, Mass and Volume Section, Metrology Division

Proctor, Thomas M.: Solid state physics; Sound Section, Mechanics Division Author: 4.16

Rasberry, Stanley D.: Spectrographic analysis; Spectrochemical Analysis Section, Analytical Chemistry Division Author: 3.22

Read, Susan F.J.: Ph.D. Oxford Univ., 1963; solid state physics; Temperature Physics Section, Heat Division

Reilly, M. L.: Low-temperature calorimetry, Heat Division Author: 5.15

Robbins, Carl R.: Phase-rule equilibria of inorganic systems; Crystallography Section, Inorganic Materials Division

Roberts, D. Ellis: Crystal growth; Solid State Physics Section, Inorganic Materials Division Author: 2.17

Robinson, Henry E.: Thermal conductivity, measurements on solids at high and low temperatures; Chief, Heat Transfer Section, Building Research Division

Ross, Gaylon S.: Nucleation, crystal growth; Polymers Division Author: 2.23

Roth, Robert S.: Ph.D. Univ. of Illinois, 1951; x-ray diffraction studies, phase equilibria; Crystallography Section, Inorganic Materials Division Author: 5.5, 5.9

Rubin, Robert J.: Ph.D. Cornell Univ., 1951; theoretical chemical physics; Heat Division

Rubin, Sherwin: Electronic engineering; Eningeering Electronics Section, Instrumentation Division Author: 4.13

Reugg, F. C.: Mossbauer Spectroscopy; Radiochemical Analysis Section, Analytical Chemistry Division Author: 3.27

Ruff, Arthur W., Jr.: Ph.D. University of Maryland, 1963; dislocations and etch pits; Chief, Lattice Defects and Microstructures Section, Metallurgy Division Author: 3.3, 3.4, 3.5

Saba, W. G.: Ph.D. University of Pittsburgh, 1961; low temperature calorimetry; Heat Division Author: 5.15

Saylor, Charles P.: Ph.D. Cornell University, 1928; precise characteristics of compounds, accurate microscopic measurements of optical properties; Analytical Chemistry Division

Schafft, Harry A.: Semiconductor devices and breakdown phenomena; Electron Devices Section, Instrumentation Division Author: 4.17

Schneider, Samuel J.: Phase equilibria of oxide systems and melting-point standards; Crystallography Section, Inorganic Materials Division Author: 4.19

Schooley, James F.: Ph.D. University of California, 1961; super-conductivity, low temperature electrical and magnetic measurements; Cryogenic Physics Section, Heat Division Author: 4.6

Schoonover, Irl C.: Ph.D. Princeton University, 1933; research administration; N.B.S. Deputy Director

Schoonover, R. M.: Density determination; Mass and Volume Section, Metrology Division

Schribner, Bourdon F.: Analytical applications of optical and x-ray spectroscopy; Chief, Spectrochemical Analysis Section, Analytical Chemistry Division Author: 3.22

Simmons, John A.: Ph.D. University of California, 1961; mathematical physics; Metal Physics Section, Metallurgy Division Author: 2.7, 3.13

Snodgrass, R. J.: Ph.D. University of Maryland, 1963; nuclear magnetic resonance in alloys, electron structure of alloys; Alloy Physics Section, Metallurgy Division Author: 3.12

Spijkerman, J. J.: Ph.D. Johns Hopkins University, 1962; Mössbauer spectroscopy; Radiochemical Analysis Section, Analytical Chemistry Division Author: 3.27, 4.23

Spinner, Sam: Elastic properties of inorganic solids; Physical Properties Section, Inorganic Materials Division Author: 3.20, 4.14

Sober, A. J.: Inorganic chemistry; Crystal Chemistry Section, Inorganic Materials Division Author: 2.12

Streever, Ralph L.: Ph.D. Rutgers University, 1960; nuclear magnetic resonance; Magnetic Measurements Section, Electricity Division

Swanson, Howard E.: Physical chemistry, x-ray diffraction; Crystallography Section, Inorganic Materials Division Author: 5.6

Swartzendruber, Lydon J.: Solid state physics; Electron Devices Section, Instrumentation Division Author: 4.17

Termini, Dominic J.: Nucleation and crystal growth; Analytical Chemistry Division

Thurber, Willis R.: Thermoelectricity; Solid State Physics Section, Inorganic Material Division Author: 4.4

Tighe, Nancy J.: Defect studies by electron microscopy of non-metallic crystals; Physical Properties Section, Inorganic Materials Division.Author: 3.17

Torgensen, John L.: Ph.D. Columbia University, 1942; crystal growth from solutions, impurity retentions, crystal properties; Crystal Chemistry Section, Inorganic Materials Division Author: 2.10, 2.12, 2.14

Vieth, D.: Electronprobe microanalysis; Lattice Defects and Microstructures Section, Metallurgy Division Author: 3.16, 5.13

Wachtman, John B., Jr.: Ph.D. University of Maryland, 1961; mechanical properties of crystals; Chief, Physical Properties Section, Inorganic Materials Division Author: 3.20, 4.2, 4.14

Wagman, Donald D.: Thermochemistry and chemical thermodynamics; Chief, Thermochemistry Section, Physical Chemistry Division

Waring, J. L.: Phase equilibria studies; Crystallography Section, Inorganic Materials Division Author: 5.5

Wasilik, John H.: Ph.D. Catholic University, 1956; dielectric constant and losses, ultrasonics; Solid State Physics Section, Inorganic Materials Division Author: 4.18

Weeks, James J.: Measurements of dielectric properties of polymers, crystallization and melting of polymers; Dielectric Section, Electricity Division Author: 2.20

Weir, Charles E.: Infrared spectroscopy and high-pressure physics; Pressure Group, Inorganic Materials Division Author: 5.3, 5.4

West, E. D.: Calorimetry, high temperature heat measurements; Heat Measurements Section, Heat Division Author: 4.9

Wiederhorn, Sheldon M.: Ph.D. University of Illinois, 1960; optical properties of high pressure, fracture of solids; Physical Properties Section, Inorganic Materials Division Author: 4.15

Will, Richard S.: Electron-field emission; Electron Physics Section, Atomic Physics Division

Williams, Robert S.: Solid state; Crystal Chemistry Section, Inorganic Materials Division

Willard, W. A.: High temperature mechanical properties of metals; creep, tensile and stress-rupture; Engineering Metallurgy Section, Metallurgy Division Author: 3.13

Winogradoff, N.: Ph.D. University of Edinburgh, 1945; interaction of radiation with matter; Electron Devices Section, Instrumentation Division Author: 4.17

Yakowitz, H.: X-ray microdiffraction, electronprobe microanalysis; Lattice Defects and Microstructures Section, Metallurgy Division Author: 3.16, 5.13

Yolken, Howard T.: Growth of oxide films; Corrosion Section, Metallurgy Division Author: 3.7, 4.8

Young, J. P.: Electro crystallization, growing single crystals by electrodeposition; Electrolysis and Metal Deposition Section, Metallurgy Division Author: 2.6

Participants at the Boulder Laboratories

Arp, Vincent D.: Ph.D. University of California, 1959; super-conductivity; Cryogenic Properties of Solids Section, Cryogenic Engineering Laboratories

Bamberger, Edwin C.: Dielectric measurements; Radio and Microwave Materials Section, Radio Standards Physics Division

Bussey, Howard E.: Ph.D. Univ. of Colorado, 1964; magnetism and ferrites; Radio and Microwave Materials Section, Radio Standards Physics Division

Cook, Alan R.: Physical instrumentation; Radio and Microwave Materials Section, Radio Standards Physics Division Author: 3.26

Dalke, John L.: Characterization of materials at radio frequencies; Chief, Radio and Microwave Materials Section, Radio Standards Physics Division

Gruzensky, Paul M.: Ph.D. Oregon State University, 1960; ultra pure materials and crystal growth; Radio and Microwave Materials Section, Radio Standards Physics Division Author: 2.24

Guntner, Charles S.: Imperfections, flow and fracture, phase transformations; Properties of Materials Section, Cryogenic Engineering Laboratories

Jefferson, Clinton F.: Ph.D. University of Michigan, 1959; solid solution for ferrimagnetic characteristics; Radio and Microwave Materials Section, Radio Standards Physics Division

Mahler, Robert J.: Ph.D. Univ. of Colorado, 1963; solid state physics relating to NMR and phonon interactions; Radio and Microwave Materials Section, Radio Standards Physics Division

Matarrese, Lawrence M.: Ph.D. University of Chicago, 1954; solid state physics, EPR resonance spectroscopy related to solid state mechanisms; Radio and Microwave Materials Section, Radio Standards Physics Division Author: 3.26

Peterson, Robert L.: Ph.D. Lehigh University, 1959; theoretical physics; Radio and Microwave Materials Section, Radio Standards Physics Division
Author: 3.26

Powell, Robert L.: Thermal and electrical conduction of metals at low temperatures; Properties of Materials Section, Cryogenic Engineering Laboratory.

Reed, Richard P.: Imperfections, flow and fracture, phase transformations; Properties of Materials Section, Cryogenic Engineering Laboratory

Risley, Allan S.: Magnetism and ferrites; Radio and Microwave Materials Section, Radio Standard Physics Division

Wells, Joseph S.: Ph.D. Univ. of Colorado, 1964; microwave physics, solid state physics relating to EPR and AFMR, Radio and Microwave Materials Section, Radio Standards Physics Division
Author: 3.26

Winder, Dale, R.: Ph.D. Case Institute of Technology, 1957; solid state physics; Radio and Microwave Materials Section, Radio Standards Physics Division

7. LITERATURE REFERENCES

Barber, D. J., (1964); Electron Microscopy and Diffraction of Aluminum Oxide Whiskers; Phil. Mag. 10, 75.

Barber, D. J. and Farabaugh, E. N., (1965); Dislocation and Stacking Faults in Rutile Crystals Grown by Flame-Fusion Method; J. Appl. Phy., (accepted).

Barber, D. J. and Tighe, N. J., (1965); Electron Microscopy and Diffraction of Corundum Crystals Grown by the Verneuil Process. I. Pure Aluminum Oxide; Phil. Mag., March.

Becker, J. H. and Hosler, W. R., (1965); Multiple-Band Conduction in n-Type Rutile (TiO_2); Phys. Rev., 137, A1872.

Block, S. and Piermarini, G. J., (1964); Alkaline-earth Cation Distributions in Vitreous Borates; Physics and Chemistry of Glasses, 5, 138.

Blunt, R. F. and Cohen, M. I., (1964a); Irradiation Induced Color Centers in Magnesium Fluoride; Bull. Am. Phys. Soc. 9, 643.

Blunt, R. F. and Cohen, M. I., (1964b); Irradiation Induced Color Centers in Magnesium Fluoride; NBS Report 8614.

Boswarva, M. and Franklin, A. D., (1965); Orientation Polarization of Defect Pairs in Crystals; Phil. Mag., 11, 335.

Brower, W. S. and Farabaugh, E. N., (1965); Etch Pits in Chromic Oxide; J. Appl. Phys., April.

Burley, G., (1964a); X-ray Investigation of Strain in Cold-Worked Silver Iodide; J. Res. NBS 68A, 4 355-8.

Burley, G.,(1964b); Ice Nucleation by Photolyzed Silver Iodide; Phil. Mag. 10, 527-534.

Chang, T., (1964); Electron Spin Resonsance of Mo^{+5} in Rutile; Phys. Rev. 136, 1413.

Coriell, S. R. and Parker, R. L., (1965); Stability of the Shape of a Solid Cylinder Growing in a Diffusion Field; J. Appl. Phys. 36, 2 632-37.

Deslattes, R. D., Torgesen, J. L., Partezkin, B., and Horton, A. T., (1964); Preliminary Studies on the Characterization of Solution-Grown ADP Crystals; presented at the 13th Annual Conf. on Applications of X-Ray Analysis; Denver, Colorado, August, 1964; in press in Advances in X-Ray Analysis, Vol. 9, Plenium Press, New York.

deWit, R. and Howard, H. E., (1965); Relation of the Stacking Fault Energy to Segregation at Stacking Faults and to the Occurrence of Phase Boundaries in FCC Binary Alloys; Acta Met., (accepted).

Eby, R. K., (1964); An Example of a Lamellar Copolymer; J. Res. Nat. Bur. Stds. 68A, (3).

Eby, R. K., (1963); First Order Transition Temperatures in Crystalline Polymers; J. Appl. Phys. 34, 2442.

Franklin, A. D., (1965); Energy of Formation of the Anion Frenkel Pair in Calcium Fluoride; J. Phys. Chem. Solids, (accepted).

Franklin, A. D., Shorb, A., and Wachtman, J. B., Jr., (1964); Relaxation Modes of Trapped Crystal Point Defects: the Three-Neighbor Shells Model in NaCl; J. Res. NBS 68A, 425.

French, J. C., (1964); Bibliography on the Measurement of Bulk Resistivity of Semiconductor Materials for Electron Devices; Natl. Bur. Std. Technical Note 232.

Furukawa, G. T. and Saba, W. G., (1965); Heat Capacity and Thermodynamic Properties of Beryllium Aluminate (Chrysoberyl), $BeO \cdot Al_2O_3$, from 16 to 380°K; J. Res. NBS 69A, (1), 13-18.

Furukawa, G. T., Reilly, M. L., and Piccirelli, J. H., (1964); Heat Capacity of Potassium Borohydride (KBH_4) from 15 to 375°K. Thermodynamic Properties from 0 to 700°K; J. Res. NBS 68A, (6) 651-649.

Grabner, L. H., (1965); Optical Quenching of Photoconductivity near the Band Edge in CdS; Phys. Res. Ltr., (submitted).

Haller, W., (1965); Rearrangement Kinetics of the Liquid/Liquid Immiscible Microphases in Alkaliborosilicate Melts; J. Chem. Phys. 42, 2 686-93.

Howard, R. E., (1964); Random Walk Calculations of Diffusion Coefficients; Proc. Fifth International Symposium on the Reactivity of Solids, Munich, (in press).

Howard, R. E. and Lidiard, A. B., (1965); Thermal Diffusion of Substitutional Impurities in Metals; Acta Met., (in press).

Howard, R. E. and Lidiard, A. B., (1964); Reports on Progress in Physics, 27, 161.

Kruger, Jerome and Calvert, Joan P., (1964); The Oxide Films Formed on Copper Single Crystal Surfaces in Water. III. Effect of Light; J. Electrochem. Soc. 111, 1038.

Kruger, Jerome and Yolken, H. T., (1964); Room Temperature Oxidation of Iron at Low Pressures; Corrosion 20, 29t.

Levin, E. M. and McDaniel, C. L., (1965); Heats of Transformation in Bismuth Oxide by Differential Thermal Analysis; J. Res. NBS 69A, (accepted).

Levin, E. M., Robbins, C. R., and McMurdie, H. F., (1964); Phase Diagrams for Ceramists; The Amer. Ceram. Soc., Columbus, Ohio.

Macedo, P. B., Capps, W., and Wachtman, J. B., Jr., (1964); Elastic Constants of Single Crystal ThO_2 at 25°C; J. Am. Ceram. Soc. 47, 651.

Macedo, P. B. and Litowitz, T. A., (1965); Ultrasonic Relaxation in Molten Boron Trioxide; Physics and Chemistry of Glasses, Vol. 6, (accepted).

Manning, J. R., (1964); Correlation Factors for Impurity Diffusion, bcc, Diamond, and fcc Structures; Phys. Rev., 136, A1758.

Ogburn, F., Bechtoldt, C., Morris, J. B., and deKoranyi, A., (1965); Structure of Electrodeposited Lead Dendrites; J. Electrochem. Soc.,(accepted).

Ondik, H. M., (1965); The Structures of Anhydrous Sodium Trimetaphosphate, $Na_3P_3O_9$, and the Monohydrate, $Na_3P_3O_9 \cdot H_2O$; Acta Cryst. 18, 226.

Ondik, H. M., (1964); The Structure of the Triclinic Form of Sodium Tetrametaphosphate Tetrahydrate; Acta Cryst. 17, 1139.

Paretzkin, B. and Peiser, H. Steffen, (1964); High-Voltage Laue X-ray Photography of Large Single Crystals; Science 146, 260-261.

Pollack, G. L. and Farabaugh, E. N., (1965); Crystal Growth and Thermal Etching of Argon; J. Appl. Phys., 36,513.

Reber, J. M., (1964); Potential Distribution in a Rectangular Semiconductor Bar for use with Four-Point Probe Measurments; Solid-State Electron. 7, 525. (See also Erratum, Solid-State Electron. 7, 945.).

Roth, R. S. and Wadsley, A. D. (1965); Mixed Oxides of Titanium and Niobium; The Crystal Structure of $TiNb_{24}O_{62}$ ($TiO_2 \cdot 12Nb_2O_5$); Acta Cryst., (accepted).

Roth, R. S., Wadsley, A. D., and Anderson, S. (1965); The Crystal Structure of PNb_9O_{25}($P_2O_5 \cdot 9Nb_2O_5$); Acta Cryst., (accepted).

Schneider, S. J., Waring, J. L., and Tressler, R. E., (1965); Phase Relations between Iridium and the Sesquioxides in Air; J. Res. NBS 69A, (accepted).

Spinner, S. and Wachtman, J. B., Jr., (1964); Some Elastic Compliances of Single Crystal Rutile from 25° to 1000°C; J. Res. NBS 68A, 669.

Tergesen, J. L. and Strassburger, J., (1964); Growth of Oxalic Acid Single Crystals from Solution; Solvent Effects on Crystal Habit; Science 146, 53-55.

Wachtman, J. B., Jr., and Doyle, L. R., (1964); Internal Friction in Rutile Containing Point Defects, Phys. Rev. 135, A276.

Wachtman, J. B., Jr. and Peiser, H. S., (1965); Splitting of a Set of Equivalent Sites in Centrosymmetric Space Groups into Subsets under Homogeneous Stress; J. Res. NBS 69A.

Waring, J. L. and Roth, R. S., (1965); Phase Equilibria in the System Vanadium Oxide-Niobium Oxide; J. Res. NBS 69A, 2, March-April.

Waring, J. L. and Schneider, S. J., (1965); Phase Equilibrium Relationships in the System Gd_2O_3 - TiO_2; J. Res. NBS 69A, (accepted).

Wasilik, J. H. and Wheat, M. L., (1965); Elastic Constants of Lead Fluoride at Room Temperature; J. Appl. Phys., March.

Weeks, J. J. and Hoffman, J. D., (1965); X-Ray Study of Isothermal Thickening of Lamellae in Bulk Polyethylene of the Crystallization Temperature; J. Chem. Phys., (accepted).

Wiederhorn, S. M., (1964); Fracture Surface Energy of Soda-Lime Glass; to be published in Proc. of the Conf. on Role of Grain Boundaries and Surfaces in Ceramics, held at North Carolina State of the Univ. of North Carolina, Raleigh , Nov. 16-18.

West, E. D. and Ishihara, S., (1965); A Calorimetric Determination of the Enthalpy of Graphite from 1200 to 2600°K, Third Symposium on Thermophysical Properties; Am. Soc. Mech. Engrs.

Yakowitz, H., (1965); Precision of Cubic Lattice Parameter Measurements by the Kossel Technique; Proc. Symposium Electron Probe Microanal., Wash., D. C., J. Wiley and Sons, Publishers (In press).

Yakowitz, G. P., Ganow, H., Oglivie, R. E., (1965): Evaluation of Kossel Microdiffraction Procedures: The Cubic Case; J. Appl. Phys. 36, (3), (in press).

Yolken, H. T. and Kruger, J., (1965); Optical Constants of Iron in the Visible Region; J. of Opt. Soc. of Amer., (accepted).

U S DEPARTMENT OF COMMERCE
WASHINGTON D C 20230

OFFICIAL BUSINESS